UNIVERSITY OF MANITOBA

HYDRAULICS OF OVERFALLS IN BEDROCK RIVERS

by

RONALD ALLAN BOTHE

A THESIS

SUBMITTED TO THE FACULTY OF GRADUATE STUDIES

IN PARTIAL FULFILMENT OF THE REQUIREMENTS FOR THE DEGREE OF

MASTER OF SCIENCE

DEPARTMENT OF CIVIL ENGINEERING

WINNIPEG, MANITOBA

OCTOBER, 1974

HYDRAULICS OF OVERFALLS IN BEDROCK RIVERS

by

RONALD ALLAN BOTHE

A dissertation submitted to the Faculty of Graduate Studies of the University of Manitoba in partial fulfillment of the requirements of the degree of

MASTER OF SCIENCE

ABSTRACT

A synthetic means for developing rating curves at overfalls in bedrock rivers is important for it enables the derivation of water level relations in regions with limited streamflow records. In the proposed technique, derived from a dimensionless analysis of V-notched and trapezoidal weir data, a cross-section of the overfall and the anticipated degree of submergence at the overfall are the only necessary input data. Overfalls with submergence conditions in excess of 80 percent cannot be analyzed due to problems encountered in the dimensionless relations.

ACKNOWLEDGEMENTS

The author gratefully thanks his supervisor:

Professor V.J. Galay, Ph.D., P.Eng.

for his valuable assistance, guidance and constructive criticism made throughout the term of this study.

The author is also much indebted to:

Mr. G.D. Fonstad and Mr. D.G. Gibson

for their extensive and willing assistance during the initial phases of the model study.

Finally, the author expresses his thanks to Manitoba Hydro for supplying helpful data and for their financial assistance throughout the study.

TABLE OF CONTENTS

LIST OF TABLES

LIST OF FIGURES

LIST OF PHOTOGRAPHS

LIST OF SYMBOLS

Symbol	Description	Dimensions
b	bottom width of channel section	L
b_{ave}	average width; function of b, H and Z*	L
c	discharge coefficient	varies
g	gravitational acceleration	L/T^2
H	total head above overfall crest	L
h_s	downstream height of water above overfall crest	L
k	number of fundamental dimensions used in dimensionless analysis	-
L	length of overfall crest in direction of flow	L
n	number of fundamental and controlled variables used in dimensionless analysis	-
P	height of the overfall crest above the upstream channel bed	L
Q	total discharge	L^3/T
R_e	Reynold's Number	-
Z	overfall section side-slope	-
Z_A	adverse approach slope	-

Symbol	Description	Dimensions
$\bar{Z}^*$	horizontal component of average side-slope resulting when the vertical component is equal to 1	-
μ	dynamic viscosity	FT/L^2
ν	kinematic viscosity	L^2/T
e	mass density	FT^2/L^4
ϕ	angle at apex of V-notch	-

subscripts

L	refers to the left bank of a channel when viewed in a downstream direction
R	refers to the right bank of a channel when viewed in a downstream direction

CHAPTER I

INTRODUCTION

(a) Introduction

An overfall is defined as an anomaly in the bed profile of a river which produces over its reach a marked drop in the hydraulic grade line. In bedrock regions, an overfall is generally associated with an adverse approaching bed slope which rises to a crest at the overfall; the downstream bed slope being more or less parallel to the surface water level. Overfalls may operate under free flow or submerged flow conditions, or a combination thereof, depending upon the downstream water level situation in relation to the magnitude of the drop in the hydraulic grade line.

Knowledge of overfalls in terms of stage-discharge relationships is important in that overfalls generally act as control points for upstream water levels. Rating curve development of these overfalls is often necessary for accuracy in planning of hydro installations; for example, calculations of head. To date, rating curve development at overfalls has dealt mainly with observing known stage-discharge relationships for a particular site and extrapolating to the desired situation. In most cases, the results are acceptable, however, deviations from the derived rating curve could occur if significant submergence conditions were reached at the overfall. In many instances, no significant streamflow records occur at the site in question, making the above mentioned rating-curve development technique impossible. Rating curve development

from broad-crested weir formulae is also practised, although, since river channels tend more toward trapezoidal configurations, the results from this method are again questionable.

(b) Statement of problem

The problem dealt with in this study is to improve the techniques for developing rating curves of overfalls in bedrock rivers. The study is aimed at obtaining dimensionless curves and equations which would enable the calculation of rating curves, with a cross-section at the overfall in question and the possible degree of submergence anticipated being the only prerequisite.

(c) Previous work

Previous work on a dimensionless, mathematical approach to rating curve development utilizing trapezoidal broad-crested weir characteristics is, to the author's knowledge, non-existant. In terms of weir studies themselves, a complete analysis of 90° V-notched, broad-crested weirs was presented by C.D. Smith of the University of Saskatchewan, Saskatoon, Canada in 1969.

(d) Justification of topic

Northern streamflow records are sparse and often non-existant. If additional knowledge of extreme flow events is to be obtained, an understanding of the behavior of overfalls is important in that they are generally control points for upstream water levels. This condition justifies the study of techniques for developing rating curves at overfalls.

A comparison of the weir studies to an actual field site justifies the model of the Burntwood River at Thompson, Manitoba.

(e) Preview

In this thesis, the development of a synthetic rating curve technique for overfalls in bedrock rivers will be presented. Characteristics of an overfall are analyzed to assess the possibilities of obtaining reasonable theoretical formulae for this procedure. Weir studies, utilizing the theoretical analysis and the overfall characteristics, are discussed and from the resulting data a design procedure, involving dimensionless plots relating overfall channel characteristics to a stage-discharge relationship, is formulated. For a comparison of weir studies to an actual field site, a reach of the Burntwood River near Thompson, Manitoba, is modelled. The model is analyzed for stage-discharge relationships, and for the effects that varying water levels downstream of the overfall have on the stage-discharge relationship. To complete the analysis of the model, surface velocity patterns and parameters downstream of the Thompson Overfall are presented.

CHAPTER II

THEORY

(a) Rating curves at overfalls

(i) Problems of extrapolation

Extrapolation of known low-flow rating curves to regions of high flow events presents several problems. Changes in channel geometry and increased submergence effects during high flows could cause deviations from the existing low-flow stage-discharge relationship. With a mathematical extrapolation, these factors are often not accounted for. In many instances, there is a limited amount of data on which to base the extrapolation. Accuracy of the known data in terms of stage-discharge relations is a factor in that generally the scatter of the individual discharge measurements should be less than 5 per cent. Even with the limited degree of allowable scatter, a regression curve which conforms to known flow events could be in error in the extrapolated region.

(ii) Typical rating curves

Typical rating curves of bedrock overfalls and their locations are shown in FIGURE II-1 and listed as Thompson, Station 1, and Station 15. Station 26 is located downstream of an overfall zone and should therefore not be considered. The rating curves for Station 1 and Station 15 have recorded data to a maximum of approximately 13,000 cfs. Extrapolating to 35,000 cfs involves discharge values almost 3 times the recorded maximum leaving the accuracy of these extrapolations in question.

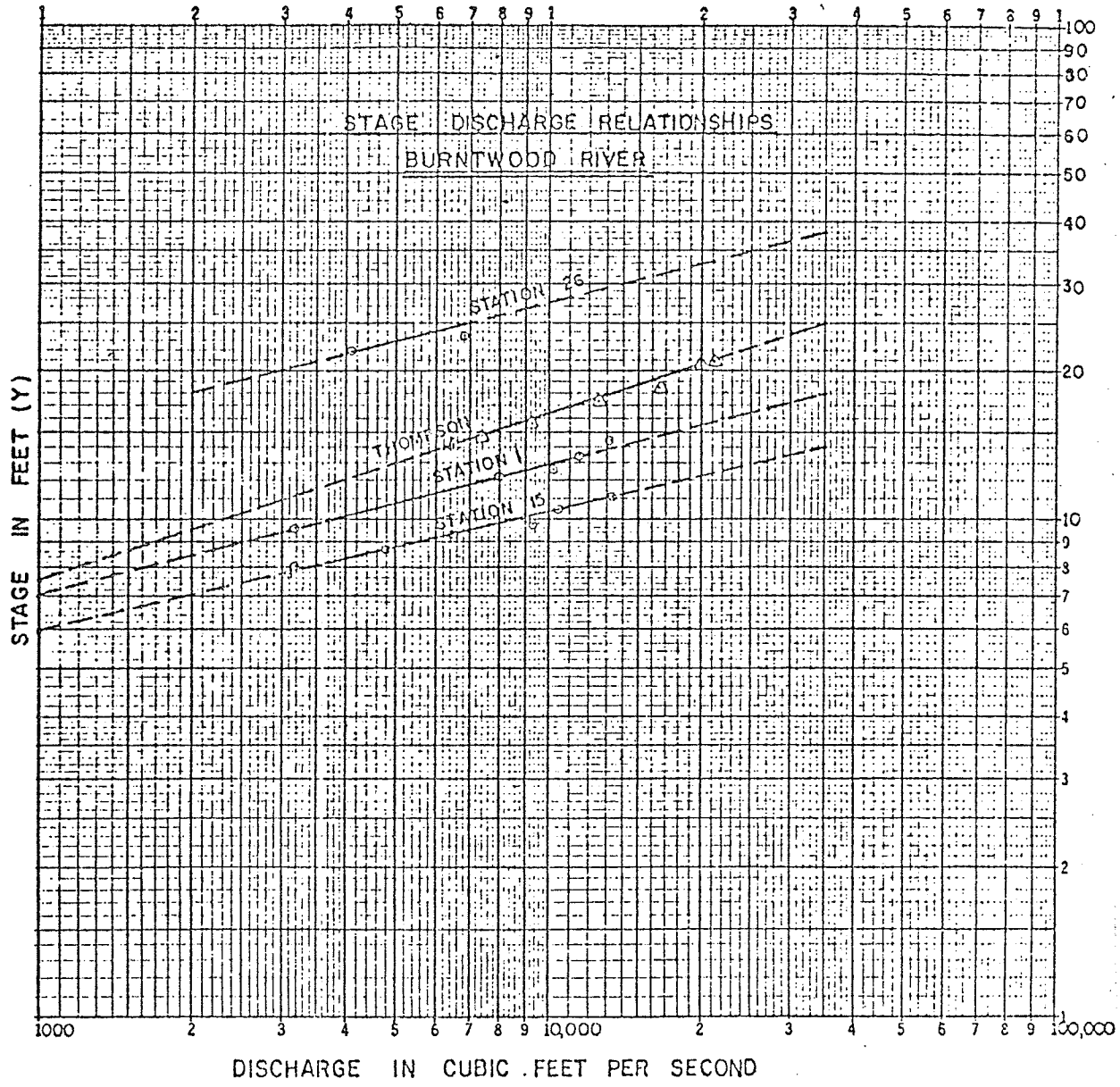

FIGURE II-1a - Typical Rating Curves of Bedrock Overfalls

Photographs II-1, -2 and -3 show two of these overfall sections, which are located on FIGURE II-1b

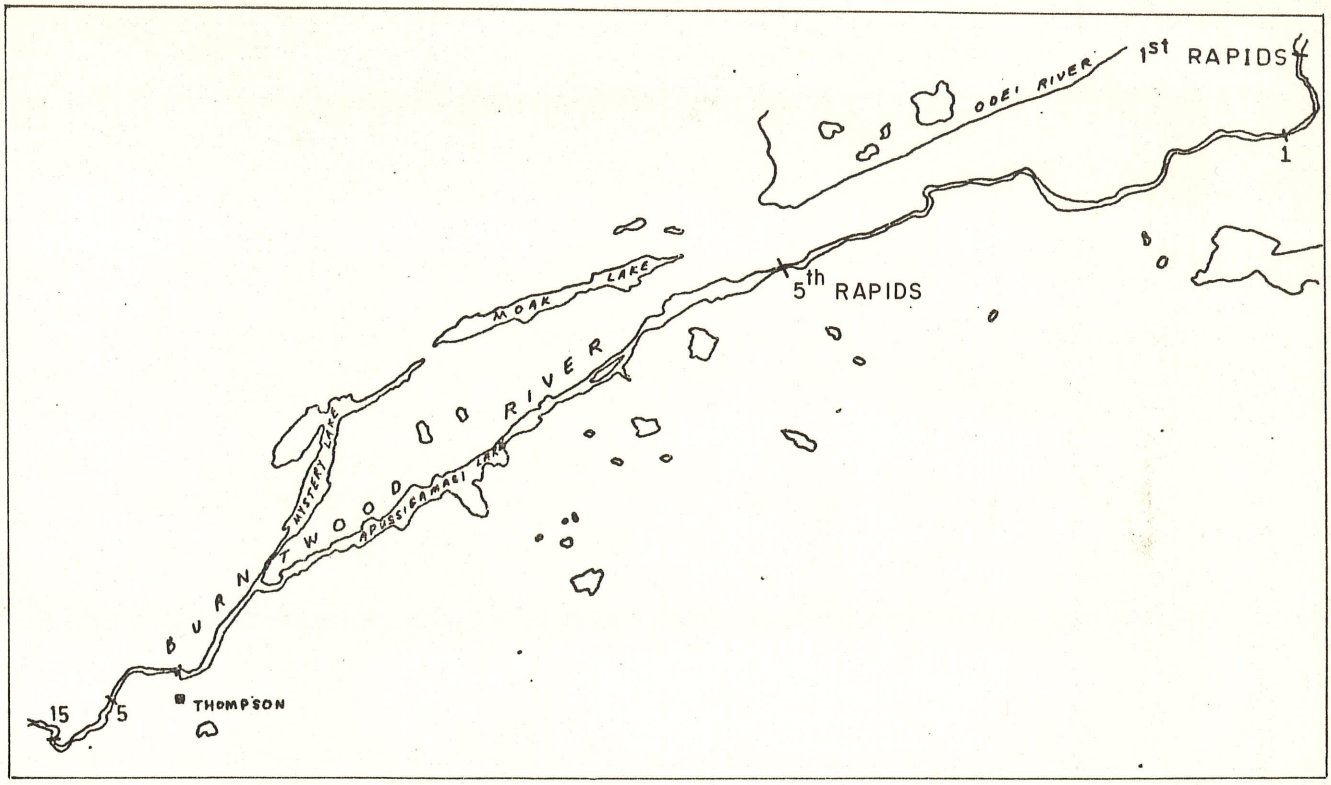

FIGURE II-1b Location Map

PHOTOGRAPH II-1 Thompson Bridge Overfall

PHOTOGRAPH II-2 Manasan Falls, Station 15

PHOTOGRAPH II-3 Aerial View of Manasan Falls

(b) Development of synthetic rating curve technique

In a modelled form, a bedrock overfall is similar to a broad-crested trapezoidal weir. Thus to further understand overfalls, weir tests could be undertaken. Since the geometry of the overfall sections vary from one site to another, a variety of weirs with varying trapezoidal and V-notched shapes could be studied. With the typical characteristics of overfalls simulated, relationships for rating-curve development at overfalls could be formulated. In dimensionless form, these relationships could then be applied to actual overfalls with similar parameters, from which actual stage-discharge relations could be calculated.

(c) Overfall parameters

The following is a list of parameters which are factors governing rating curves of bedrock overfalls:

(1) bottom width of overfall cross-section, b

(2) side slopes of overfall cross-section, Z

(3) upstream head above the overfall, H

(4) total discharge over the overfall, Q

(5) height of the overfall crest above the upstream channel bed, P

(6) length of the crest in the direction of flow, L

(7) adverse approach slope, Z_A

(8) downstream height of water above the overfall crest, h_s

(9) mass density of water, e

(10) gravitational acceleration, g

(11) dynamic viscosity of water, μ

All of the above mentioned parameters are considered in the design of the weirs. The geometric properties and the water level parameters are shown in FIGURE II-2.

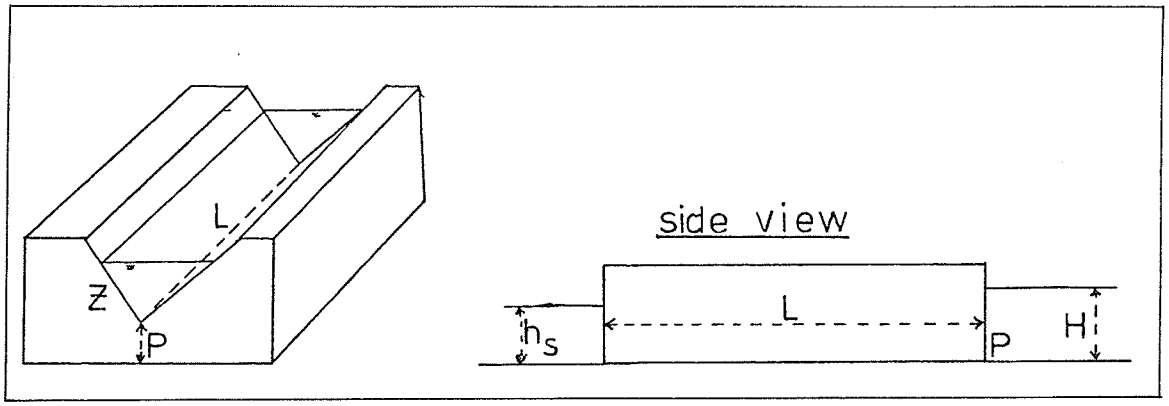

FIGURE II-2 Weir Properties

(d) The broad-crested weir

(i) definition

A weir is defined as broad crested if the crest has a horizontal portion in the direction of flow which is long enough to maintain essentially parallel stream lines. The significance is that this ensures a hydrostatic pressure distribution in a cross-section over the weir. Whether or not this condition is met depends not only on the length of the horizontal portion of the crest but also on the depth of flow over the weir.

(ii) the discharge formula

The discharge formula of a broad-crested weir for free flow conditions is:

$$q = 2/3(2/3)g\ H^{3/2}$$

or: $$q = 3.089\ H^{3/2} \qquad \ldots\ (II\text{-}1)$$

where: q = discharge/foot of weir crest

H = total upstream head above the crest

FIGURE II-3 shows a number of water surface profiles over a broad-crested weir as measured by Prentice.

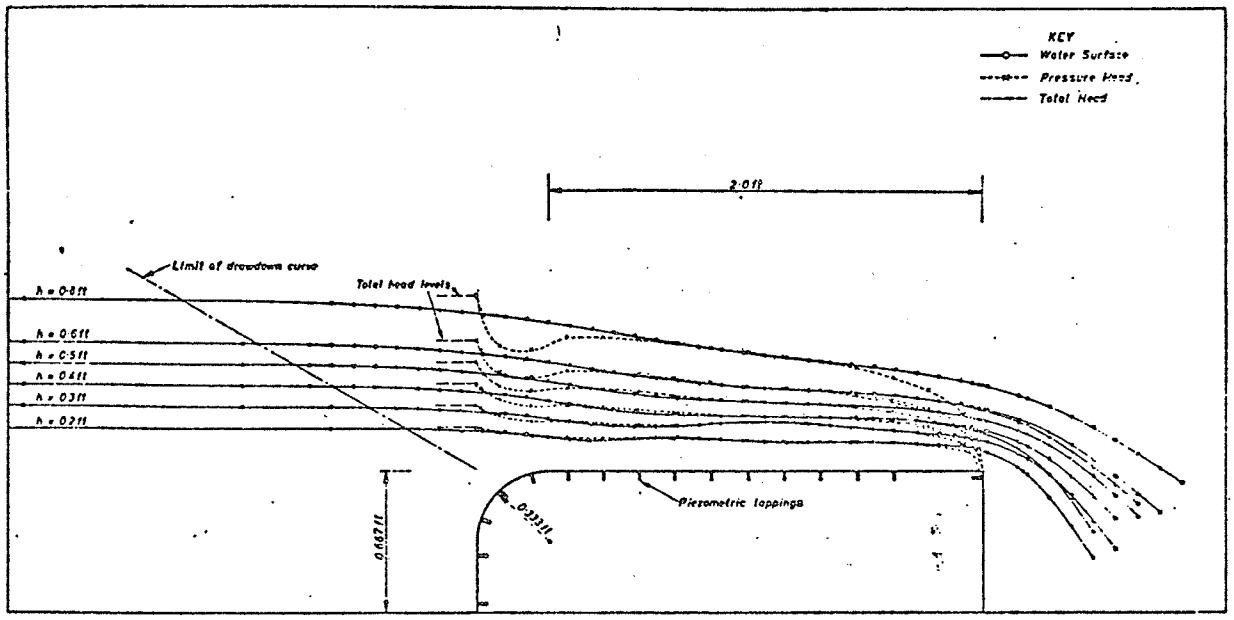

FIGURE II-3 Water Surface Profiles (Prentice)

EQUATION (II-1) is a theoretical formula. To make it applicable for practical problems, friction along the weir crest should be allowed for. This friction results in the formation of a boundary layer in which the velocity is retarded. The smaller the H/L ratio, where H is the head and

L the length of the weir, the greater will be the effect of the friction. On the other hand, with large H/L ratios the curvature of the streamlines may affect the discharge somewhat. TABLE II-1 shows classifications of weirs from H/L values.

TABLE II-1 CLASSIFICATION OF WEIRS *

Value of H/L	Nature of Water Surface	Classification of Weir
$0 < H/L \leq 0.1$	consists of series of standing waves	long-crested
$0.1 < H/L \leq 0.4$	parallel to the weir crest for considerable portion	broad-crested
$0.4 < H/L \leq$ 1.5 to 1.9 (upper limit depends on H/P)	wholly curvilinear	narrow-crested
$H/L \geq$ 1.5 to 1.9 (lower limit depends on H/P)	flow separates at the upstream corner and springs clear off the weir crest	sharp-crested

* Rao and Shukla (1971)

FIGURE II-4 is taken from C.D. Smith, Hydraulic Structures, University of Saskatchewan Publication. It shows the variation of the coefficient C in the formula

$$q = CH^{3/2} \qquad \ldots\ldots(II\text{-}2)$$

with the ratio H/L. EQUATION (II-2) applies only for the free flow condition.

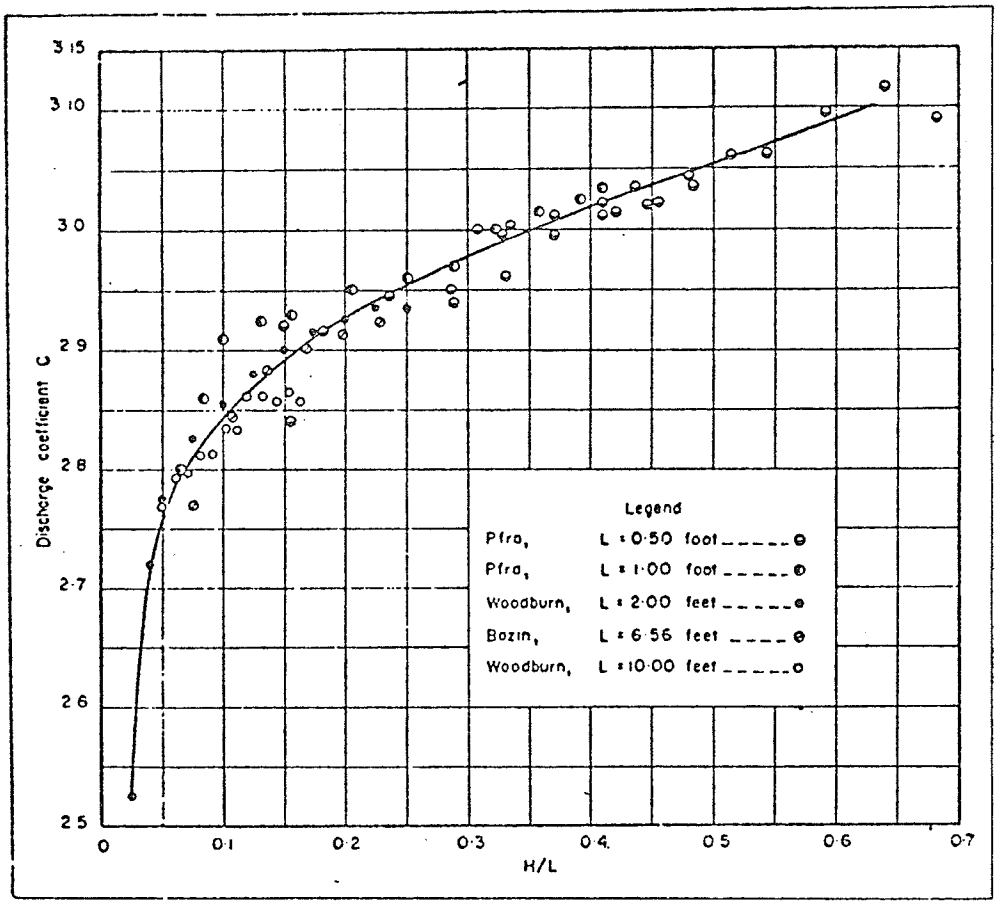

FIGURE II-4 Weir Coefficient vs H/L

(iii) submergence conditions

When the tailwater is high enough to influence the depth of flow on the weir, EQUATION (II-2) cannot be used. Instead, the relation used is:

$$q = h\sqrt{2g\ (H-h)} \qquad \text{.....(II-3)}$$

where h is the water depth on the weir in a cross-section with essentially parallel streamlines. Since flow is sub-critical throughout, this depth can only be determined by starting from downstream boundary conditions and by proceeding with the analysis in an upstream direction.

(e) Triangular broad-crested weir

(i) discharge formula

Studies on 90° V-notched broad-crested weirs were performed by C.D. Smith. It was found that the theoretical discharge becomes

$$Q = 2.30\ H^{5/2} \tan(\phi/2) \qquad .....(II-4)$$

where ϕ is the angle at the apex of the V-notch. This is comparable to the general equation for any triangular weir

$$Q = CH^{5/2} \qquad .....(II-5)$$

in which C is the weir coefficient, a coefficient which includes the effect on the discharge of all the variables.

Weir coefficient C verses H/L is given in FIGURE II-5d. A single curve is drawn through the results from all weirs. Theoretically, at the same H/L value, the value of C should not be exactly the same for each weir. Practically, the difference is small so a single curve is still representative. The coefficient is less than the theoretical value of 2.30 for the range of heads used in the tests.

Smith speculated that the weir coefficient for any angle will be the value given in FIGURE II-5d multiplied by tan ($\phi/2$). This remains to be confirmed experimentally.

(ii) submergence conditions

The experimental head-discharge relationship obtained for various submergence ratios and crest lengths is given in FIGURES II-5a, b, c. In each case the area to the right of the dashed line represents the area where tailwater submergence results in an increase in the upstream head

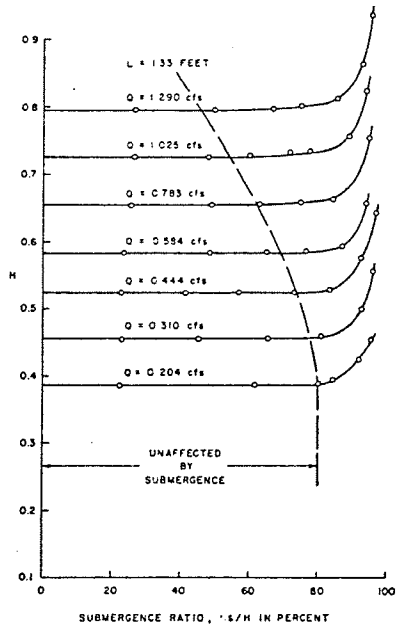

—DISCHARGE CAPACITY CURVES, L = 1.33 FT

-a-

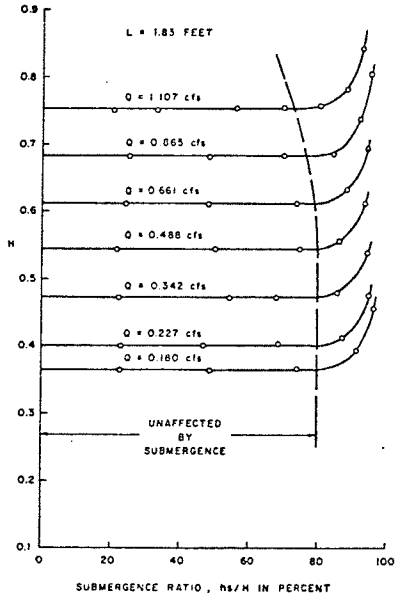

—DISCHARGE CAPACITY CURVES, L = 1.83 FT

-b-

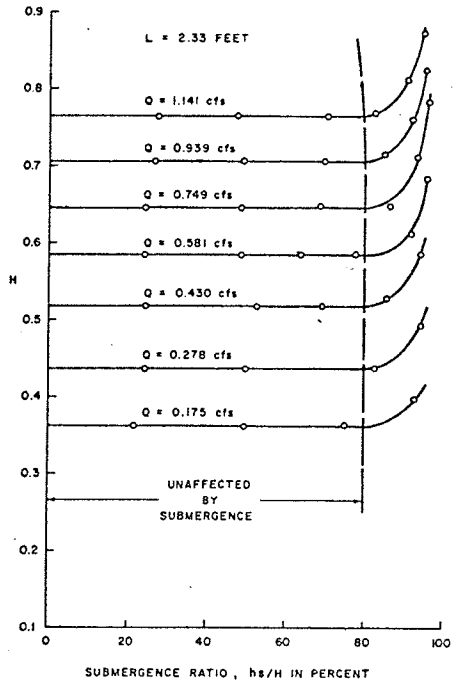

.—DISCHARGE CAPACITY CURVES, L = 2.33 FT

-c-

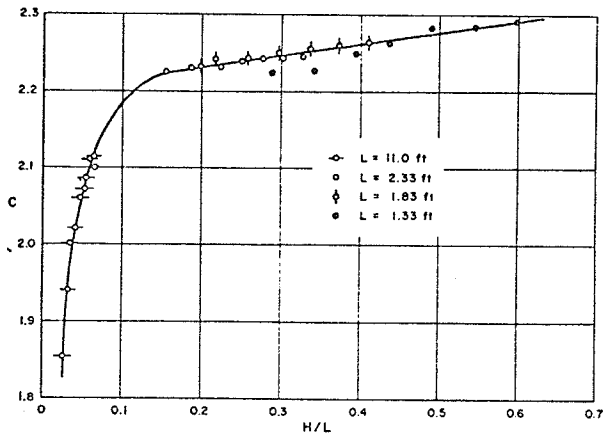

.—WEIR COEFFICIENT VERSUS H/L

-d-

FIGURE II-5 Triangular Broad-Crested Weir Studies by C.D. Smith

for a given discharge. It is significant that the submergence effect will occur for $h_s/H < 0.80$ if the H/L ratio is too large. The dashed line breaks away from $h_s/H = 0.80$ at an H/L value of approximately 1/3, which indicates that the pressure distribution on the crest becomes non-hydrostatic when H/L exceeds this value. Although the weir coefficient is shown for H/L values exceeding 0.333, the coefficient in this region will be affected before the submergence reaches 80 per cent.

The effect of submergence on the discharge is summarized in TABLE II-2. The percent reduction in weir coefficient C applies only to the case in which $H/L \leq 0.333$.

TABLE II-2 Effect of Submergence on Discharge

h_s/H	Coefficient Reduction in C, as a percentage
0.80	0.0
0.84	2.5
0.88	7.5
0.92	18.0
0.96	40.0
1.00	100.0

(f) Dimensional analysis of trapezoidal weirs

Since no mathematical formulation of broad-crested trapezoidal weirs could be obtained, a dimensional analysis was performed to ascertain the broad-crested trapezoidal weir formulation and to assess the possible dimensionless relationships of overfall characteristics. All factors listed in SECTION II-c, OVERFALL PARAMETERS, are included in

the analysis. From the detailed dimensional analysis, which is discussed in APPENDIX A1, the resultant function for a trapezoidal weir is:

$$Q/g^{1/2} H^{5/2} = f\left(\frac{u}{eg^{1/2} H^{3/2}}, \frac{H}{P}, \frac{H}{L}, \frac{H}{b}, Z, Z_A \right)$$

rearranging:

$$Q = f\left(\frac{u}{eg^{1/2} H^{3/2}}, \frac{H}{P}, \frac{H}{L}, \frac{H}{b}, Z, Z_A \right) g^{1/2} H^{5/2}$$

or: $Q = CH^{5/2}$ .....(II-6)

which has the same structure as the basic formula for a triangular weir.

So mathematical formulations of broad-crested trapezoidal weirs are possible and good dimensionless relationships are obtainable. Thus, weir studies can usefully simulate overfall sections and the ensuing results can be plotted in a dimensionless form to enable synthetic rating curve development.

CHAPTER III

EXPERIMENTAL STUDIES

A. Weir Studies

(a) Weir design

Since the weir studies were introduced to gather data from various combinations of overfall parameters, and not model one particular prototype overfall, geometrical similarity was the prime concern. Thus the bottom width and the side slopes at the overfall section, the height of the overfall crest above the upstream channel bed, the length of the crest in the direction of flow and the adverse approach slope were the

PHOTOGRAPH III-1 Typical Test Weir

major design parameters. The only controls on the weir design were

(1) the available space in the flume

(2) that the operating conditions never resulted in H/L values exceeding 0.333 which ensured that the weir remained in the broad-crested region.

All weir edges were rounded on the upstream face to prevent separation from occuring on the crest. A complete record of weirs tested is listed in APPENDIX A2. A typical weir tested is shown in PHOTOGRAPH III-1.

(b) Testing apparatus

All weir tests were conducted in a 2.5' x 3' x 46' flume. The discharge was controlled by recirculating water through a centrifugal pump and sump system. Water surface profiles were measured by means of a point gauge located on a four-wheel carriage which moved the length of the flume on pre-levelled rails. Actual discharge values were calculated by timing the volume changes in a holding tank located at the flume outlet.

(c) Testing procedure

For each particular channel geometry analyzed, various upstream heads, H, were established and the corresponding discharges were measured. Since velocities at the point where H was measured were negligible, the height of the upstream water surface above the weir crest was used as H. Several water surface profiles were measured under a variety of heads. A complete range of submergence conditions were also studied for selected

discharge values. These procedures were followed for all three adverse approach slopes studies, namely 10:1, 5:1, and 0:1 (90° edge), before a new channel geometry was formed.

(d) Limitations of weir studies

Due to the limited width of the flume, only two side slope values, Z could be tested, namely 1:1 and 3:1. However, this was not deemed a problem since, as the side slopes flatten, the trapezoidal shape of the overfall section approaches the conditions for a regular broad-crested weir, for which relations are known. Therefore, both the extreme values of the side slope factor are accounted for and extrapolation for other intermediate side slopes can be obtained if necessary.

B. Burntwood River Model Study

(a) Introduction

As previously mentioned, a comparison of the rating curve technique developed from weir studies to an actual field overfall would greatly aid in ascertaining the reliability of the synthetic rating curve method. Consequently, a section of the Burntwood River was chosen to be modelled. The actual river reach selected lies downstream of Manasan Falls and upstream of Apassigamassi Lake in the immediate vicinity of Thompson, Manitoba. More specifically, the model extends around the northern edge of Thompson, from the water supply pumphouse on the west side, to just downstream of the Government Air Services base in the northeast. A reasonable amount of hydrometric and survey data was available for both the Thompson over-

fall and the modelled reach, so field conditions in terms of stage-discharge relations can be well simulated. Location plans and site plans for the modelled reach are found in FIGURES B1-1 and B1-2 respectively, of APPENDIX B1.

(b) Model scales

(i) Basic principles

In order for complete similitude, a model and its prototype are required to be geometrically, kinematically and dynamically similar.

Geometric similarity exists if the ratios of all linear dimensions are equal. It is independent of motion of any kind and involves only similarity of form.

Kinematic similarity concerns motion. If ratios of components of velocity at all similar points in geometrically similar systems are equal, the status of motion is kinematically similar.

Dynamic similarity requires that the ratios of forces in geometrically and kinematically similar systems must be the same.

(ii) Model Design

The factors which influenced the choice of model scales were:

(1) similitude laws

(2) available space

(3) available discharge

(4) type of problem (influences vertical distortion)

On consideration of these factors a rigid bed model was chosen with distorted scales of horizontal 1:320 and vertical 1:60. The detailed scaling analysis is discussed in APPENDIX B2.

(iii) Layout of the model

The layout of the Burntwood River Model is shown in APPENDIX B3. Known channel cross-sections in the modelled reach are also shown in APPENDIX B3 and listed as FIGURES B3-1, 2, 3 and 4.

(c) Operation and instumentation

The discharge in the model is controlled by recirculating through a pump and sump system. The actual discharge is controlled by a valve leading into a six-foot weir box with a rated V-notched sharp-crested weir as an outlet. Depths are controlled by means of a downstream flap gate. Actual depths are measured by a series of point gauges which are situated at all known cross-sections.

Flow patterns are measured by dye releases, or float observations. Velocities are measured by observing floats in the area under consideration.

In a given test, the model is operated for sufficient time to allow water levels to stabilize.

(d) Introductory testing

The testing and adjusting of the channel profile and the calibration of the measuring gauges is discussed in detail in APPENDIX B4.

Minor errors in the channel profile were encountered which

caused small errors in the discharge values. For example, for an expected prototype discharge of 30,000 cfs the actual modelled prototype discharge would be 30 cfs higher. Since this amounts to only 0.1% error which is indistinguishable in the model, no further corrections were deemed necessary.

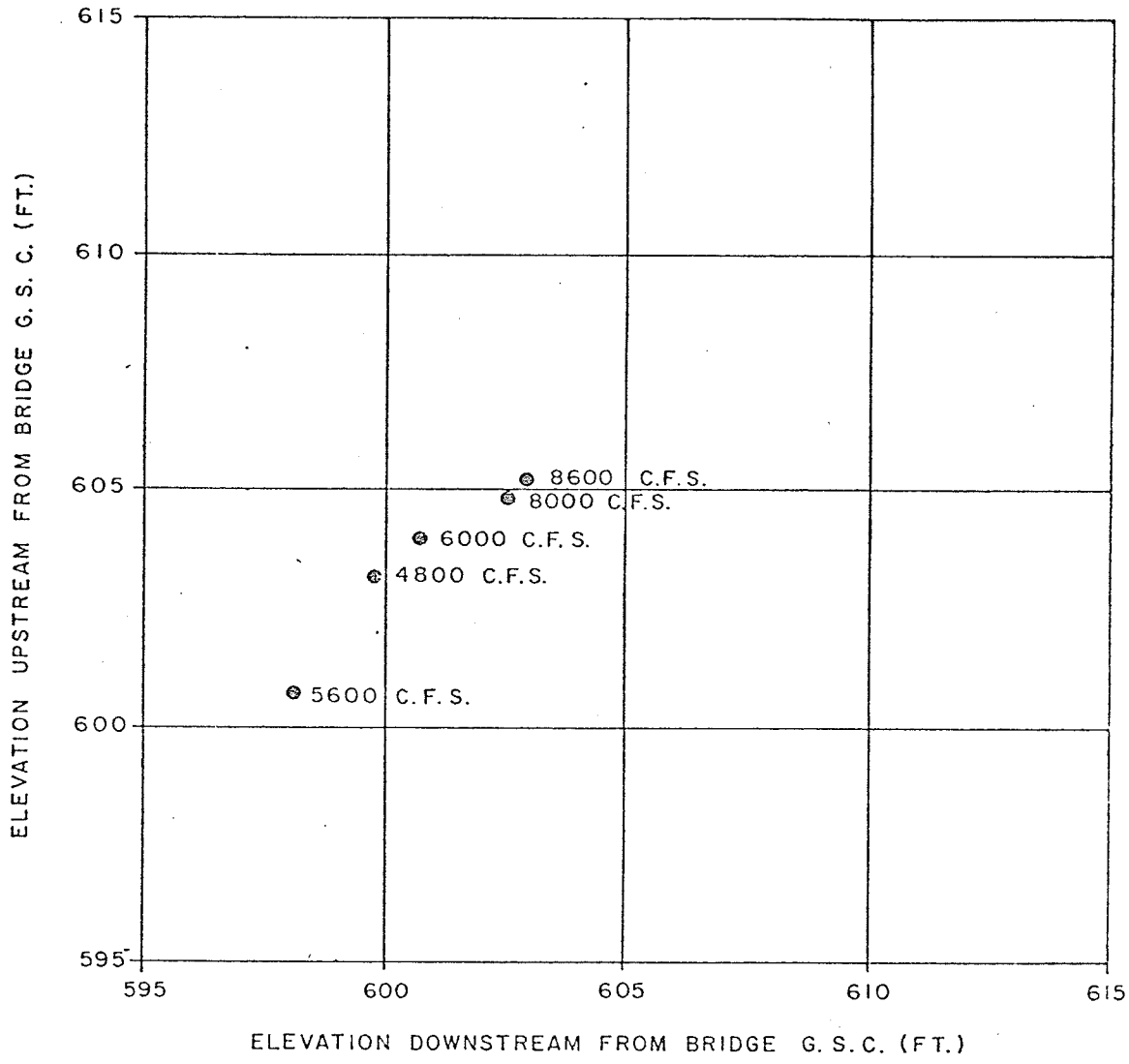

FIGURE III-1 Stage Relation at Thompson Bridge

(e) Testing in known flow range

To further establish the model's relationship to the prototype, tests were conducted with discharges in the known range of stage-discharge conditions. In these tests a rather liberal assumption was made, in that a 2.5 foot difference in stage upstream and downstream of the Thompson Overfall applied throughout the known flow range. FIGURE III-1 shows a relation for stages upstream and downstream of the overfall as presented by Galay and Baracos (1973). This plot indicates that this condition may be correct. In any case, it did establish a basis for further testing.

(f) Testing in extrapolated high flow region

The initial tests to extend flows above the known range followed the extrapolation of the Thompson Overfall rating curve, as shown by Galay and Baracos (1973) in FIGURE III-2. The assumption of the 2.5 foot stage difference at the overfall was again incorporated in the testing. The procedure followed was to assume an upstream stage for a given discharge from the proposed rating curve. The downstream water surface elevation in the model was set from the 2.5 foot observed difference in water levels at the overfall. Once steady state conditions were attained, measurements of the water surface profile were taken. From this, the observed stage at cross-section 5 could be compared to the proposed extrapolation.

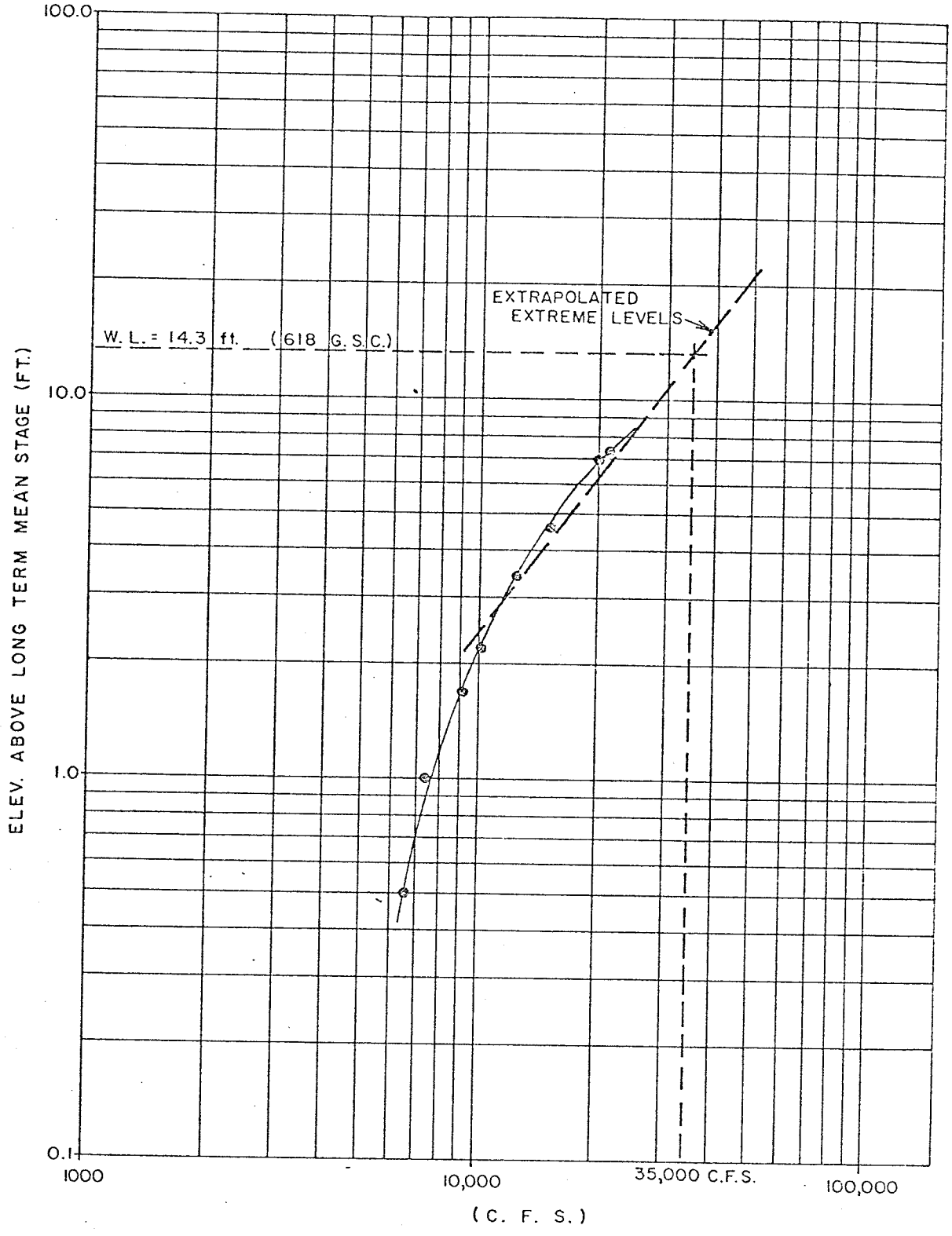

LONG TERM MEAN FLOW = 5800 C. F. S.
LONG TERM MEAN STAGE = 603.7 FT. (G.S.C.)

FIGURE III-2 Rating Curve of Thompson Overfall

(g) Testing with varying downstream water levels

If the Thompson Overfall acts in a manner similar to that of a weir, the stage-discharge relationships upstream of the overfall could be dependent on the depth of water below the overfall. To analyze this possibility, a variety of downstream levels above and below the 2.5 foot drop were studied for each of the following prototype discharges: 5800, 8400, 30,000 and 35,000 cfs.

(h) Testing incorporating 5th Rapids rating curve

The problem apparant at this point was to establish the correct surface water elevations at cross-section 1 for a variety of discharges. Two approaches were studied:

(i) derived backwater elevations from Manitoba Hydro

From a backwater analysis, Manitoba Hydro has derived natural open water elevations for a variety of cross-sections downstream of the Thompson Overfall. These were used to establish the water level conditions at cross-section 1. The detailed calculations for this analysis are presented in APPENDIX B5.

(ii) synthetic rating curve at 5th Rapids

Using the technique for synthetic rating curve development which is presented in CHAPTER V, a rating curve for 5th Rapids was constructed. Using Manitoba Hydro backwater relations, the water level conditions at cross-section 1 were established. The detailed analysis, including the calculation of the 5th Rapids rating curve is listed in

APPENDIX B5.

The procedure used in testing was to establish a discharge in the model and to set the surface-water elevation at cross-section 1 to the corresponding calculated value. Once steady-state conditions prevailed, the water surface elevations at the various cross-sections were measured.

(i) Velocity patterns and parameters

Studies of velocity patterns and parameters were conducted in the reach of the model downstream of the Thompson Bridge. Two discharge conditions, namely 5000 cfs and 35,000 cfs, were analyzed using the synthetic 5th Rapids rating curve as a criterion for establishing water elevations at cross-section 1.

CHAPTER IV

TEST RESULTS

A. Weir Studies

Tabulated data and calculations for all weirs tested are listed in TABLE C1-1 of APPENDIX C1.

(a) Adverse approach slope

From tests conducted on four weirs it was determined that adverse approach slopes have no effect on the head-discharge relationship. The only noticeable change was in the water level conditions upstream of the weir. It was observed that as the adverse approach slope became progressively flatter, the position of the level water surface upstream of the weir migrated upstream. Selected water surface profiles shown the effect of adverse approach slopes on upstream surface levels are shown in FIGURE IV-1. Head-discharge plots, involving the three approach slopes tested are shown in FIGURE IV-2.

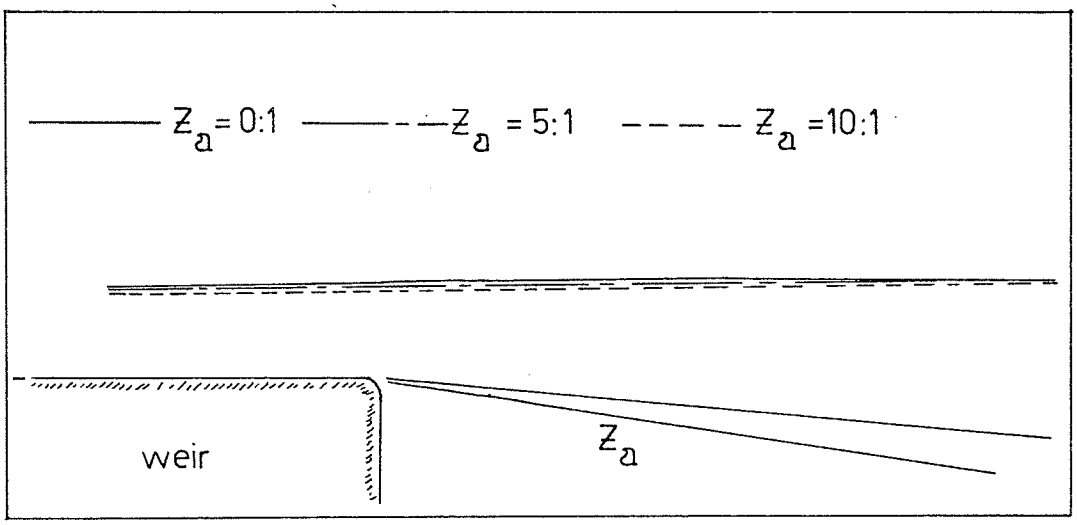

FIGURE IV-1 Effects of Adverse Approach Slope on Surface Water Level

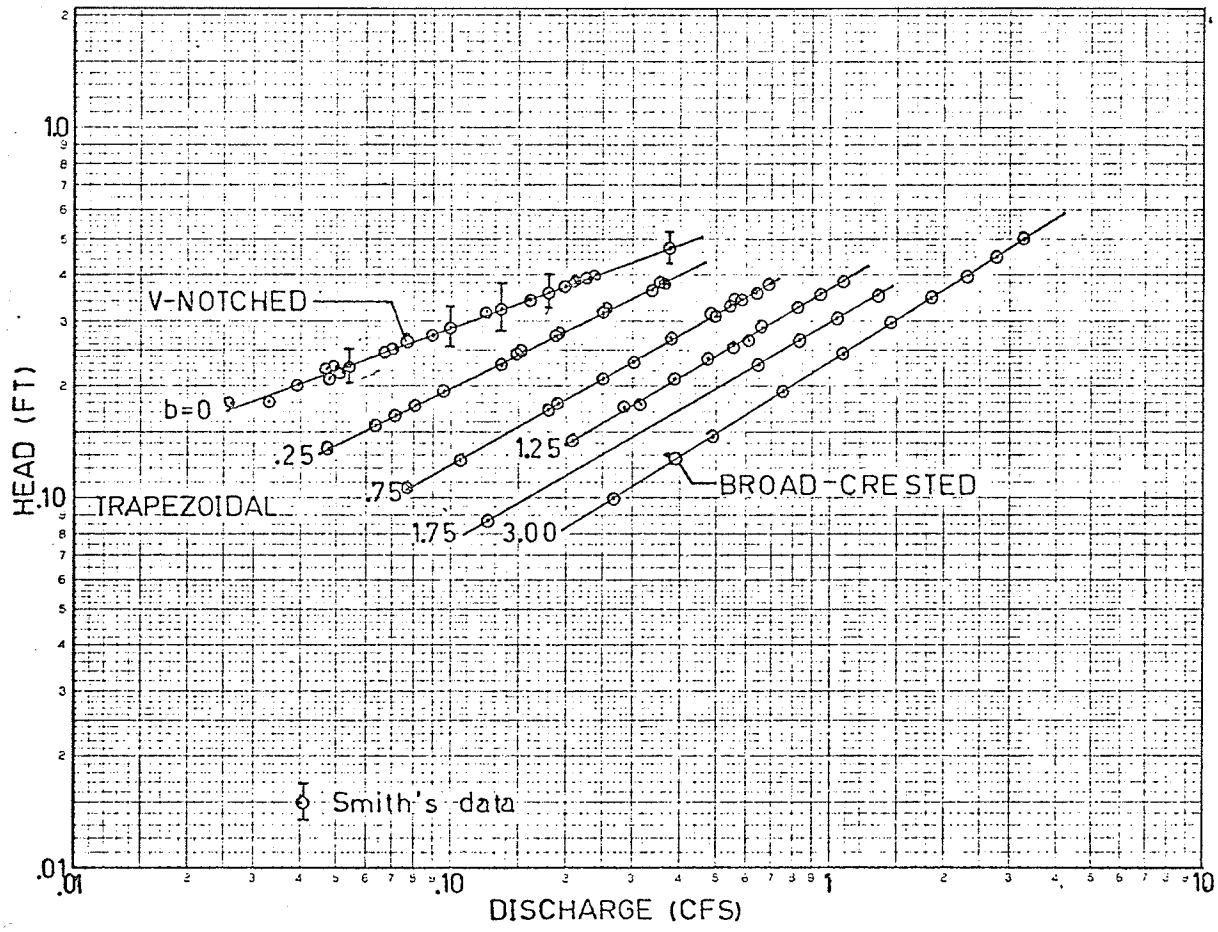

FIGURE IV-2 Head-discharge Relations

(b) Head discharge relations

Typical head-discharge relationships are shown in FIGURE IV-2. From this diagram, it appears that the channel side-slope and the bottom width are the dominant factors. The V-notched broad-crested relation and the standard broad-crested relation form the outer boundaries; all trapezoidal broad-crested relations lie between these two plots with their positioning dependant upon the magnitude of the bottom width. The complete set of head-discharge relations are found in APPENDIX C2, FIGURES C2-1 and C2-2.

(c) Submergence relations

The test results show that for H/L < 0.333, free flow conditions are maintained for $h_s/H < 0.80$. For submergence values in excess of 0.80, stage-discharge relations are altered. Examples of this are shown in FIGURE IV-3.

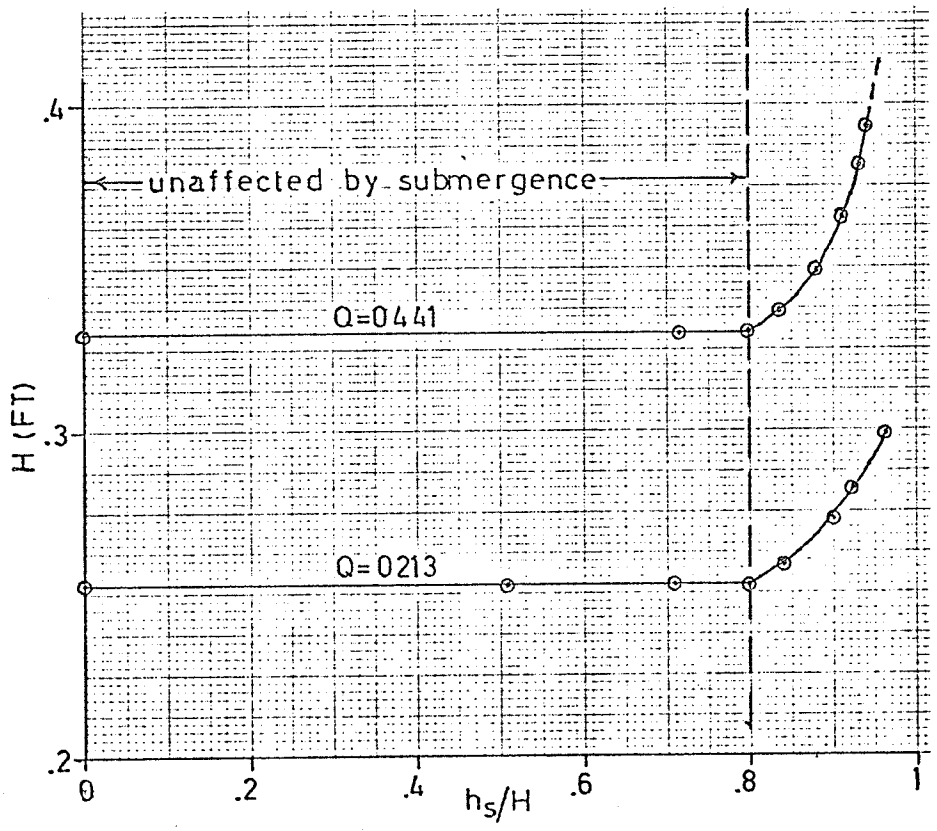

FIGURE IV-3 Effects of Submergence on Head

From the plots of FIGURE IV-3, stage-discharge values were calculated for submergence ratios of 0.80, 0.85, 0.90, and 0.95. The resulting relations are shown plotted in FIGURE IV-4.

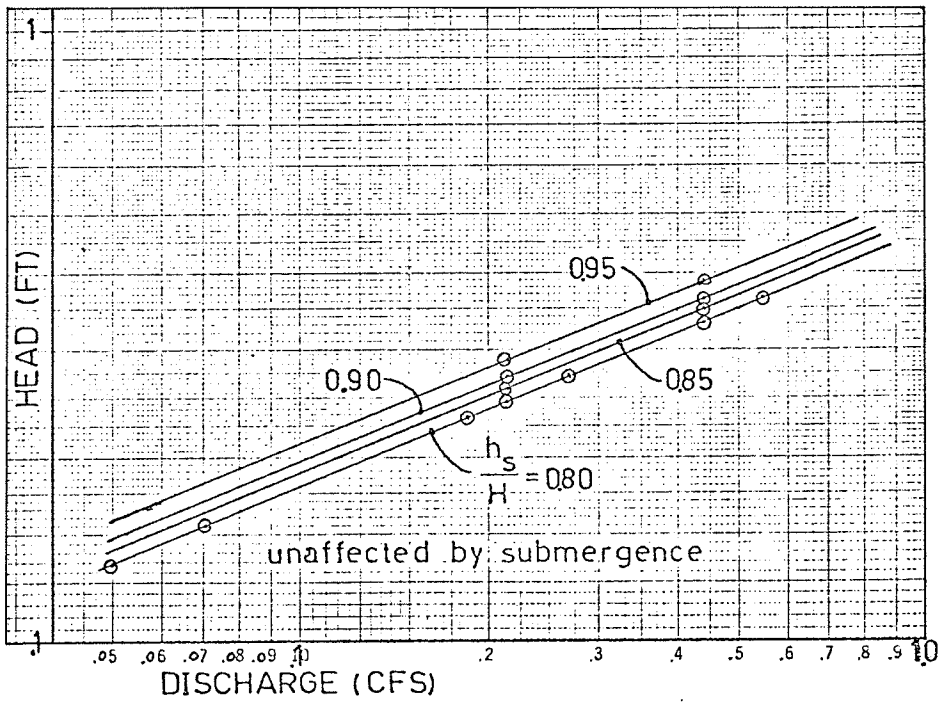

FIGURE IV-4 Head-discharge Relations Involving Submergence

A complete listing of submergence relations are shown in APPENDIX C3, FIGURES C3-1, -2, -3, and -4.

(d) Dimensionless relations

Since the head-discharge plots indicated a major dependancy on the side-slope and the bottom width factors, a dimensionless relation was constructed for:

$$H/b \text{ and } Q/g^{1/2} H^{5/2}$$

for various values of Z. The resulting plot is shown in FIGURE IV-5. This relation distinctively shows the dependence of the side slope factor. However, since data was not obtainable for side slopes greater than 3:1 the plot is limited in its use.

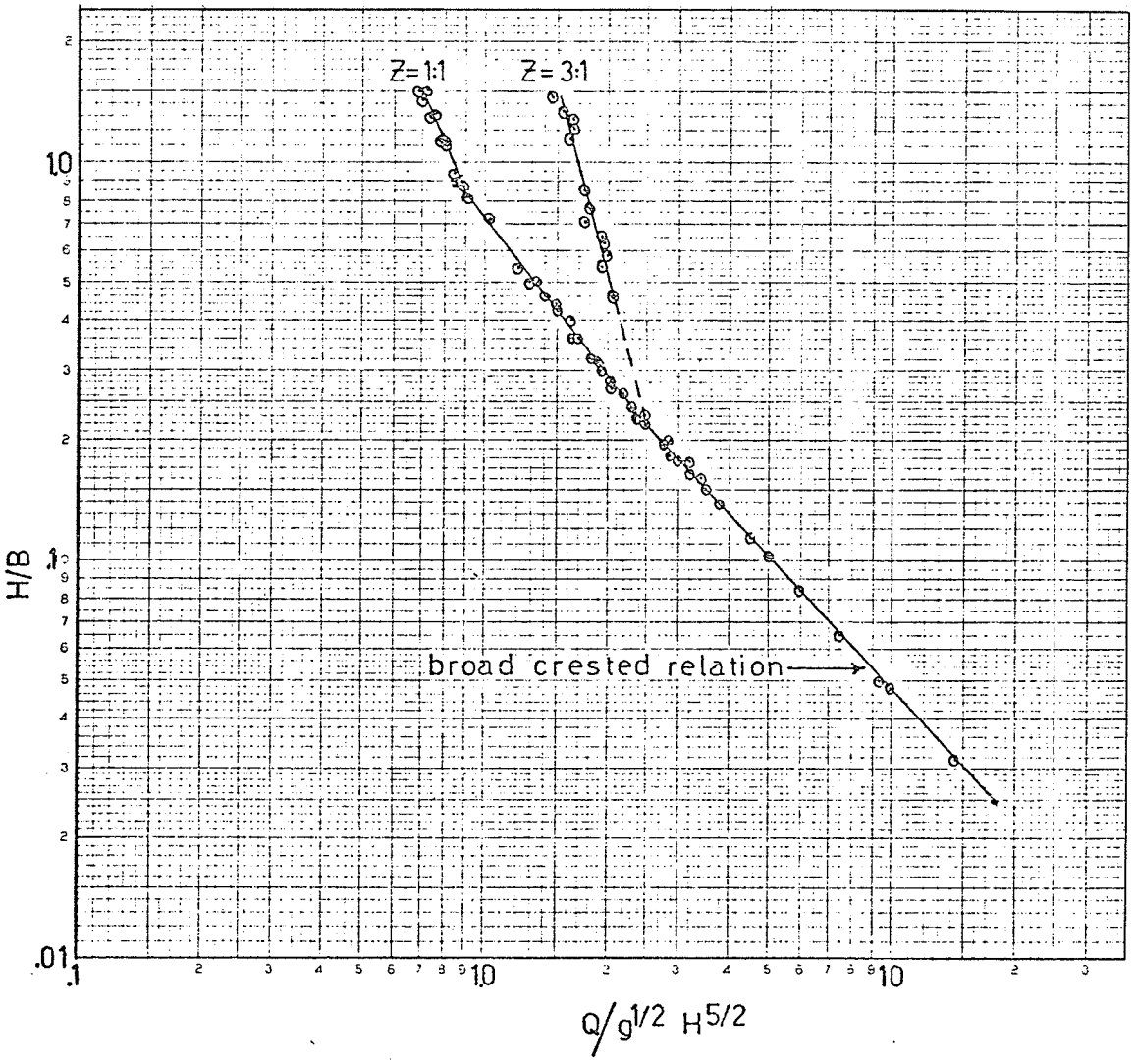

FIGURE IV-5 Dimensionless Relation for Side Slopes and Bottom Widths

To overcome this lack of data the side slope and the bottom width were combined to form the average width, $b_{ave.}$. The average width is defined as:

$$b_{ave.} = \frac{HZ*_L}{2} + b + \frac{HZ*_R}{2} \qquad \text{..... (IV-1)}$$

where: $Z*$ is the horizontal component of the side slope resulting

when the vertical component is equal to 1.0, and subscripts L and R refer to the left and right side of the channel when viewed in a downstream direction.

For cases where both the left and right side slopes are equal EQUATION (IV-1) simplifies to:

$$b_{ave} = b + H\bar{Z}^* \qquad .....(IV\text{-}2)$$

Using the average width relation, a dimensionless plot was constructed for H/b_{ave} and $Q/g^{1/2} H^{5/2}$ for various $\bar{Z}$. The resulting plot is shown in FIGURE IV-6. Incorporating the side slope into the ordinate has resulted in a single plot for trapezoidal conditions. The relation must hold for values of $\bar{Z}$ flatter than 3:1 since the standard broad-crested values also plot on the same relation.

One problem that does arise from the relation shown in FIGURE IV-6 is that the V-notched broad-crested values plot on horizontal lines. For a particular $\bar{Z}$: $H/b_{ave} = H/b + H\bar{Z}^* = H/H\bar{Z}^* = 1/\bar{Z}^*$ = a constant. Thus, knowing just the H/b_{ave} value would not be sufficient to calculate the discharge for V-notched broad-crested weirs, since any abscissa value can be chosen for the relation.

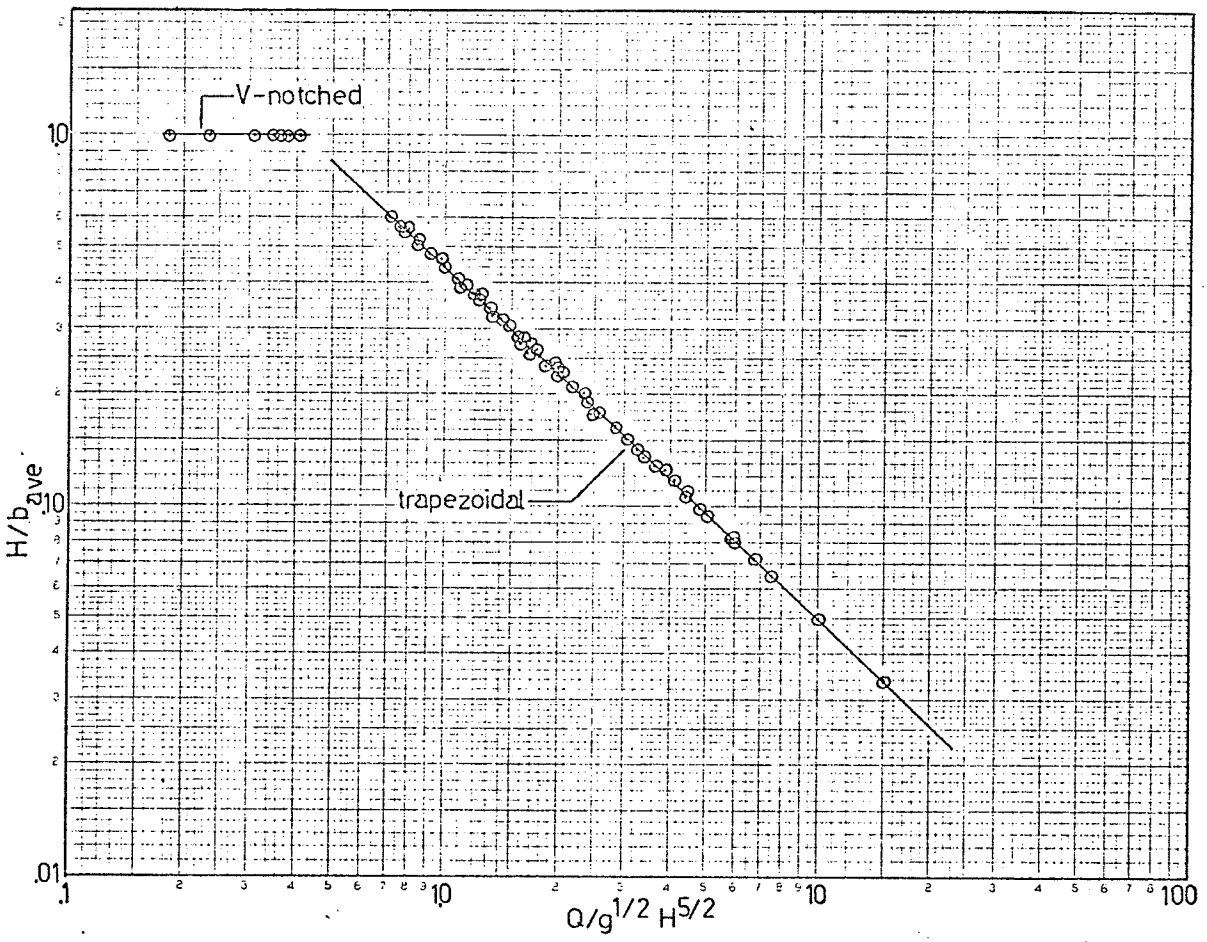

FIGURE IV-6 Dimensionless Relation for b_{ave}

B. Burntwood River Model Studies

(a) Tests in known flow range

The stage-discharge relations of the river model at cross-section 5, when converted to prototype values, was plotted against the known stage-discharge curve from Water Survey of Canada's stage-discharge table. The resulting plot is shown in FIGURE D2-1 of

APPENDIX D2. Note that since FIGURE D2-1 is a logarithmic plot, a small deviation from the known curve represents a much larger error for high flows (say 15,000 cfs.) than does the same deviation for low flows (say 7,000 cfs.). The maximum deviation from the curve is 0.5 ft. at Qp = 13,600 cfs.; the next largest is 0.4 ft. at Qp = 10,000 cfs., while the remainder of the plots show a close agreement with the known curve. The data and calculations of these tests are listed in TABLE D1-1 of APPENDIX D1.

(b) Tests in extrapolated high flow region

The complete results of all extrapolated high flow tests conducted are listed in TABLE D1-1 of APPENDIX D1. Plots of the stage-discharge relations are shown in FIGURE D3-1 of APPENDIX D3. Surface profiles of these tests are shown in FIGURE D3-2 of APPENDIX D3. The results show that there is a close agreement between the model results and the straight line approximation as shown in FIGURE III-2.

(c) Tests with varying downstream water level

The complete results of the tests with varying downstream water levels are listed in TABLE D1-1 of APPENDIX D1. For any of the constant discharges shown, the effect of varying downstream water levels on the surface profile can be seen in the range of upstream levels. Examples of surface profile variations for varying downstream water levels are shown in FIGURE IV-7.

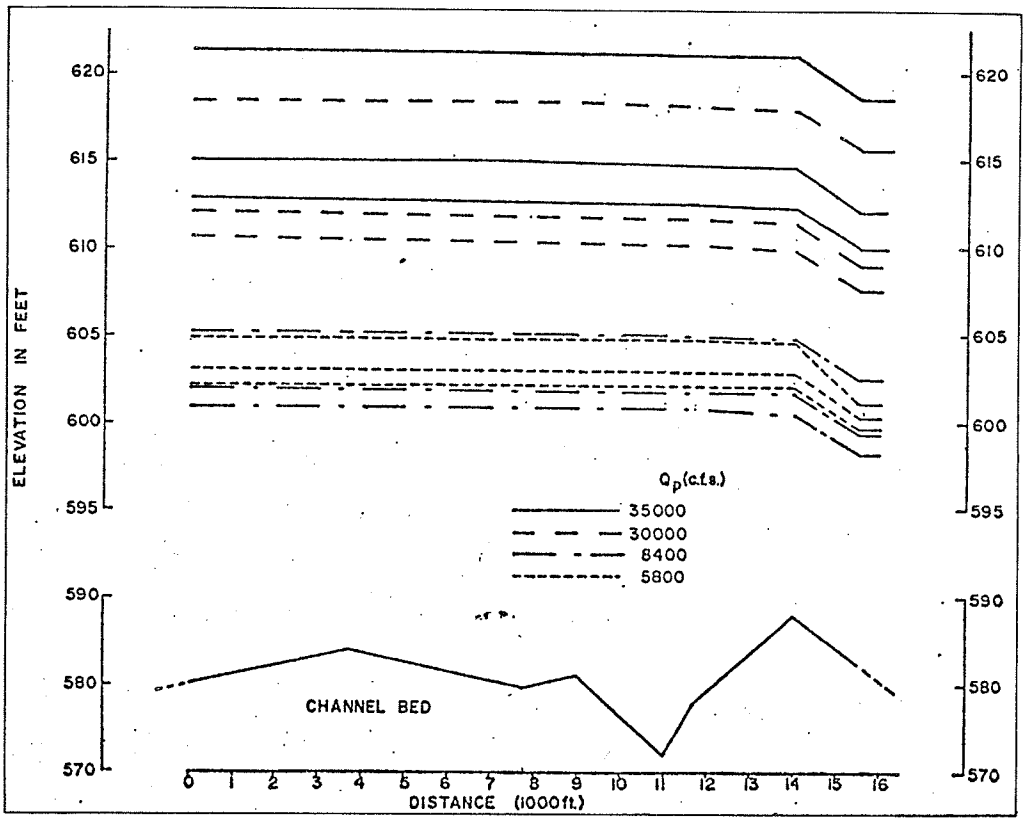

FIGURE IV-7 Effects of Varying Downstream Water Levels

(d) Tests incorporating 5th Rapids rating curve

The complete results of tests incorporating a 5th Rapids rating curve to establish surface water elevations at cross-section 1 are shown in TABLE D1-2 of APPENDIX D. The subsequent rating curves for the Thompson Overfall, one using Manitoba Hydro derived backwater elevations and the other synthetic rating curve approach, are shown in FIGURE IV-8. Note that the derived backwater curve closely follows the proposed extrapolation whereas the synthetic backwater curve tends to follow the curvature of the known flow curve.

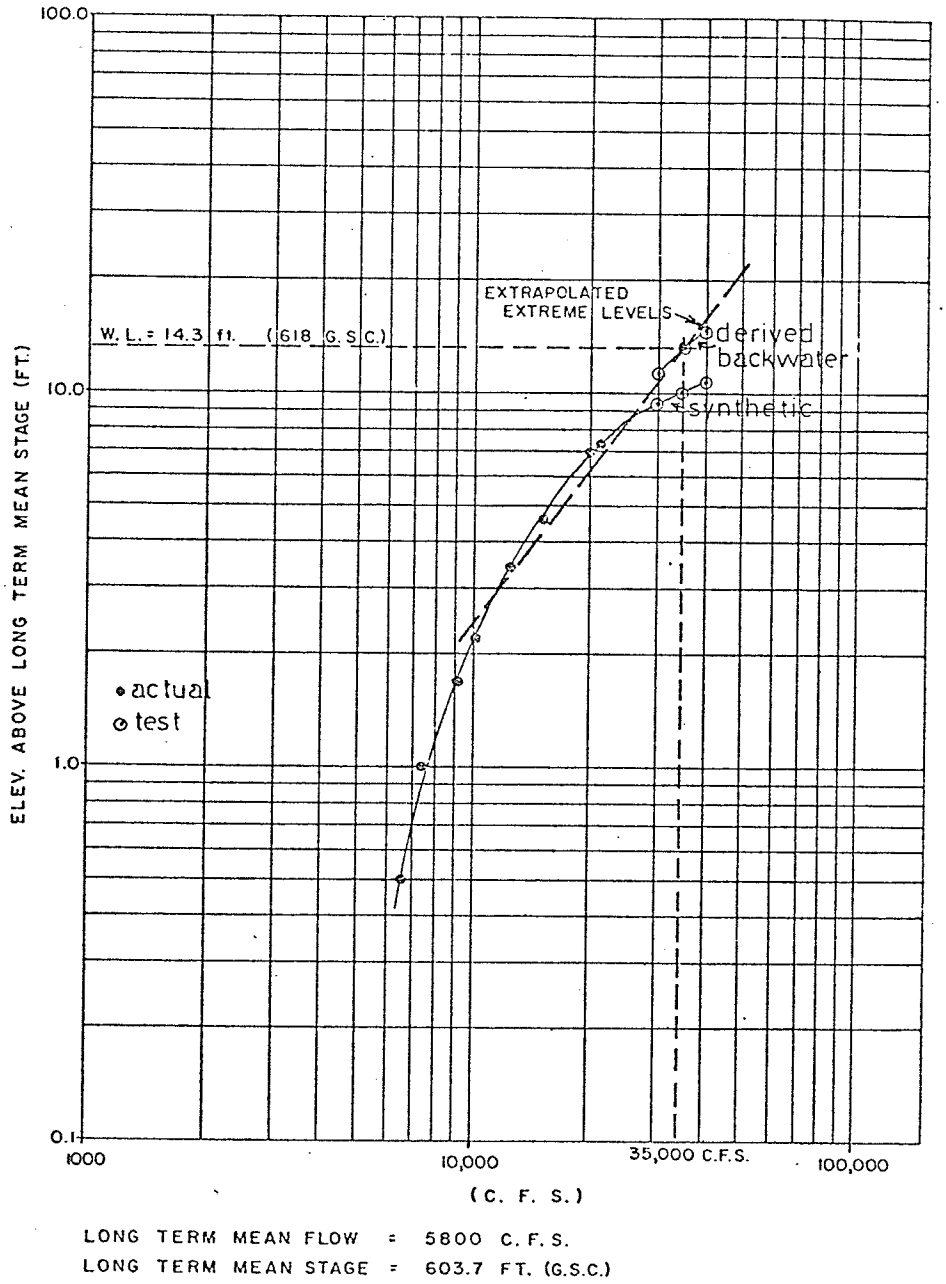

FIGURE IV-8 Developed Rating Curves

(e) Velocity tests

The calculated values for the surface velocity parameters studied are listed in TABLE D7-1 of APPENDIX D7. Flow patterns in the reach for discharges of 5000 cfs and 35,000 cfs are illustrated on FIGURES D7-1 and D7-2 respectively; of APPENDIX D7.

CHAPTER V

DISCUSSION

A. Weir Studies

(a) Comparison of test results

(i) head-discharge relations

The head-discharge relations for trapezoidal weirs form straight-line relations on log-log plots. The channel geometry, namely the side-slope and the bottom width of the section, dictate the positioning of the relation. All trapezoidal weir plots lie between the relations for the V-notched and the broad-crested weirs, and act as an intermediate transition zone between the two.

The necessity of determining the channel geometry is clearly established in the head-discharge relations. Applying standard broad-crested weir theory to a trapezoidal section could result in the actual heads being much larger than the predicted. From FIGURES C2-1 and C2-2 of APPENDIX C2 it appears that as the discharge increases, the V-notched and trapezoidal relations approach the plotted broad-crested relation. Note that this broad-crested relation is for $b = 3.00$ ft.; other values of b would result in a different positioning of the broad-crested relation. Since the width of the test flume was 3 feet, this broad-crested relation is the limiting plot for any trapezoidal section that could be tested.

(ii) submergence relations

All submergence tests showed that for trapezoidal sections with $H/L \leq 0.333$, free flow conditions are maintained for $h_s/H < 0.80$. This has a close agreement with a triangular section, which has a critical depth of 80 percent of the upstream head. Actually, depending on the magnitude of the bottom width, trapezoidal weirs should be affected by submergence values less than 80 percent and ranging downward to 66 percent for a rectangular section. However, due to the small bottom width values tested in the weir studies plus the fact that simultaneous readings of both the H and h_s values to determine the critical condition were impossible, the 80 percent submergence factor was chosen to be representative.

Plots of head-discharge relations for various submergence levels are shown in APPENDIX C3. They show the basic trend that submergence has on stage-discharge relations, in that, to pass the same discharge in a submerged state, an increase in the free flow head must occur.

(iii) dimensionless plots

As previously mentioned in SECTION V-a(i), all trapezoidal relations on a head-discharge plot tend toward the broad-crested for increasing discharge values. It would therefore appear that for flows in the order of several thousand cfs., a broad-crested

analysis would suffice. However this is not so. In a dimensionless form, the weir channels studied are distinctly separated in terms of their channel side-slopes and bottom widths as shown in FIGURE IV-5. The dishcarge relation only approaches the broad-crested when the bottom width b becomes large enough to make the H/b value very small.

Basically the dimensionless plot of FIGURE IV-5 relates channel geometry, H/b, to a discharge constant, $Q/g^{1/2} H^{5/2}$. To further understand the relationship, compare the following two trapezoidal overfalls. Assume that overfall 1 has a channel bottom width of 100 feet and an upstream head of 30 feet, and that overfall 2 has a channel bottom width of 1 foot and a head of 0.3 feet. Both channel sections have 1:1 side-slopes and no significant submergence affects either overfall.

Both these overfall channel sections are geometrically similar, with H/b = 0.30. They also have the same discharge constant, $Q/g^{1/2} H^{5/2} = 1.45$. The difference in the discharge values between the two overfalls comes from substituting the corresponding head into the discharge constant relation and solving for the flow. Thus the discharge at overfall 1 is 40,500 cfs. as compared to 0.405 cfs. at overfall 2.

Since FIGURE IV-5 is dependent on side-slope, the parameter b_{ave} was incorporated to combine the side-slope and the bottom width. Thus the dimensionless relation for trapezoidal channels was reduced

to a single plot of

$$H/b_{ave} \text{ and } Q/g^{1/2} H^{5/2}$$

which applies for all side-slope values, as shown in FIGURE IV-6. The use of geometrical similarity is applied in this relation in the same manner as was discussed for FIGURE IV-5.

In terms of dimensionless relations similar to FIGURE IV-6, which include submergence factors, several parameters were analyzed. These included such dimensionless terms as H/b, H/b_{ave} and H/L. In all cases studied, no dimensionless relations were obtainable for submergence factors. The dimensionless plot of

$$H/b_{ave} \text{ and } Q/g^{1/2} H^{5/2}$$

shown in FIGURE V-1, illustrates the difficulty encountered. The plots show no correlation between various submergence levels and appear to be more dependant of specific channel geometries and discharge conditions.

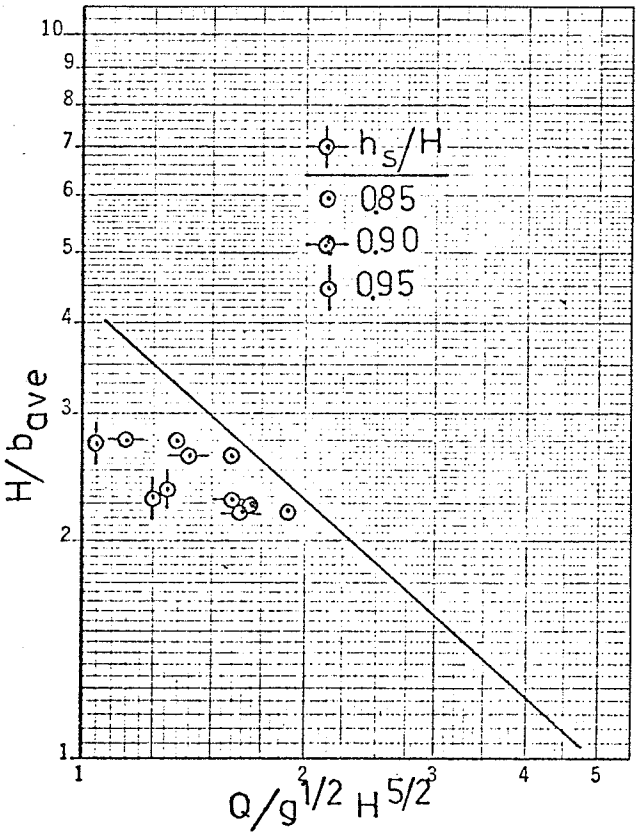

FIGURE V-1 Effects of Submergence on Dimensionless Plots

(b) Comparison of weir data with existing theories

The data obtained from the weir studies compares favourably with previous studies conducted by C.D. Smith. In terms of head-discharge relations for 90° V-notched broad-crested weirs, FIGURE C2-1 of APPENDIX C2 shows that the data collected from this weir agrees

perfectly with Smith's relation.

As previously mentioned, Smith speculated that the weir coefficient, C, for any angle, ϕ, would be the value of the coefficient given in FIGURE II-5d multiplied by tan ($\phi/2$). Calculations using this procedure were conducted utilizing weir data obtained from 143.2° V-notched (3:1 side-sloped) broad-crested weir. The resulting discharges were lower than actual discharges by as much as 10 percent. These errors could possibly be caused by neglecting the velocity heads in the calculation of H, however these values were so small that it seems unlikely. TABLE V-1 shows the results of these calculations.

TABLE V-1 Verification of Smith's Theory
(For ϕ = 143.2°)

Test	C(90°)	C(143.2°)*	$Q_{ca/c}$	Q_{act}	%error**
1	2.13	6.29	0.044	0.049	10.2
2	2.153	6.459	0.065	0.072	10.75
3	2.205	6.615	0.171	0.183	7.02
4	2.23	6.69	0.542	0.550	1.41
5	2.225	6.675	0.380	0.393	3.42
6	2.22	6.66	0.260	0.280	7.69

* C(143.2°) = C(90°) x tan (143.2/2)

** % error = $(Q_{act} - Q_{ca/c})$ (100) / Qca/c

(c) Synthetic rating curve technique

Using the dimensionless plot of FIGURE V-1 which involves

H/b_{ave} and $Q/g^{1/2}\ H5/2$

a synthetic rating curve technique for overfalls in bedrock rivers was developed. The only data necessary is a cross-section at the overfall and some idea as to the possible degree of submergence. As previously mentioned, dimensionless relations involving submergence factors was unobtainable, thereby limiting this synthetic rating curve technique to only free flow conditions. The detailed design procedure is outlined in APPENDIX E1.

To further establish the validity of this technique, overfalls with existing rating curves were analyzed using the developed synthetic rating curve technique. Obtaining overfall data complete with rating curve was difficult therefore few sections were analyzed. For results and discussion of these tests, see APPENDIX E2.

B. Burntwood River Model

(a) Known low flow analysis

From the close agreement between the model tests and the known rating curve, it can be concluded that the constructed and adjusted model represents the field situation. The minor errors in the channel profile remained insignificant in terms of rating curve development as was previously discussed in APPENDIX B4. The assumption that a 2.5 foot difference in the stage upstream and downstream of the Thompson Overfall was correct and applied throughout the known flow range.

Since the model conformed to the known rating curve without utilizing any artificial roughening, it is likely the model will perform similarly in the extrapolated high-flow region. Water levels in this region should also be as accurate as in the low flow case since the same degree of accuracy, namely 5 foot (prototype) contours, was used throughout the entire model construction.

(b) Extrapolated high-flow analysis

The points on FIGURE D3-1 of APPENDIX D3 show that there is a close agreement between the model results and the straight line approximation, utilizing the 2.5 foot difference in upstream and downstream heads at the overfall. The problem still remaining is whether or not this 2.5 foot difference applies in the extrapolated high-flow region. Different submergence conditions might be encountered which would alter the stage-discharge pattern that applies in the known low-flow range.

(c) Varying downstream water levels

Comparing the water surface profiles for constant flows shown in FIGURE D4-1 of APPENDIX D4, the stage upstream of the Thompson Overfall is very much dependant on the downstream water level condition. This indicates that not only does the 2.5 foot water level difference affect the upstream stage, but that the whole realm of downstream water levels plays an integral part in the rating curve.

The range of downstream water levels tested in the model is probably much higher than what may actually occur in the field. In fact, the downstream water level may rise only a few feet compared to the 12 to 15 foot rise expected upstream of the Overfall.

An interesting point to note is that the difference in elevation between the upstream and downstream water levels varied from 2.66 feet to 3.02 feet for the tests conducted at discharges above the known flow range. This may or may not be representative of field conditions. The control of the water level difference would be based on the downstream water level and the influence of the overfall. At high discharges it would appear that open channel flow conditions would prevail over the overfall control.

(d) Rating curves for Thompson Overfall

The rating curves for the Thompson Overfall, one from Manitoba Hydro's derived backwater elevations and the other a synthetic rating curve developed from an analysis of 5th Rapids, are shown in FIGURE D6-1 of APPENDIX D6.

The derived backwater curve basically agrees with the proposed extrapolated extreme level curve. This should be expected since calculations of downstream water levels were based on the proposed extrapolated stage-discharge relation. In other words, the calculations and tests performed complete a full circle with the final results equal to the initial assumptions. Yet this does not allow the downstream

water elevations to be calculated independant of the Thompson rating curve. Since the tests incorporating various downstream water level conditions showed the great dependency of the upstream stage on the downstream water levels, this rating is questionable.

The proposed synthetic rating curve of the Thompson Overfall was established from model tests where the downstream water elevation was calculated utilizing a synthetic rating curve at 5th Rapids. These downstream water level calculations were totally independent of any Thompson rating curve. Consequently, the author feels that this rating curve better simulates the actual rating curve for the Thompson Overfall.

Note that for both rating curves, flow was assumed steady and design rather than operating conditions were analyzed.

(e) Inundation of low lying areas and facilities

In terms of elevation, the estimated maximum water elevation for 35,000 cfs. will be 613.8 (GSC), just upstream from the Thompson Bridge. This level will be affected by the backwater of the proposed First Rapids Dam, although increases in the upstream stage should not be more than approximately 1 foot.

With the expected increased water levels, the following low lying areas or facilities will be affected:

(1) Raised water levels will necessitate modifications of the

Thompson Waterworks Pumphouse.

(2) A portion of the Government Air Services base will be inundated.

(3) The elevation of the top of the Thompson Bridge piers is well above anticipated high water levels.

(4) Increased levels will submerge the discharge end of the sewer outfall.

(f) Velocity considerations and bank erosion

The velocity patterns shown in APPENDIX D7 closely represent the actual flow conditions. Velocity parameters, however, are only estimates and should only be used in comparing zones of relative slow and fast flowing water. The velocity parameters listed in TABLE D7-1 of APPENDIX D7 were derived utilizing the synthetic rating curve.

Following are the findings of the velocity tests. Note that since surface velocities could only be estimated, the discussions are of a qualitative form.

(1) One area of the right bank downstream of the Thompson Bridge currently shows erosion and some incipent instability of recent fill. Under proposed 35,000 cfs. conditions, approximately 4,000 feet in length of this bank would require protective measures. PHOTOGRAPHS D7-1, -2, -3 and -4 show the flow pattern around this bank.

(2) In the area of the Government Air Services facilities, surface velocities are slow and should not pose problems. In the main channel, however, increased velocities may cause some operating difficulty.

(3) Lowering downstream water levels, for example, by blasting at 5th Rapids, would greatly increase the velocity parameters and erosion capabilities downstream of the Thompson Bridge.

(4) Raising downstream water levels would result in somewhat lower velocities in the area downstream of the Thompson Bridge.

CHAPTER VI

CONCLUSIONS

(a) Summary

The weir analysis performed verified Smith's studies on V-notched broad-crested weirs. Dimensionless plots involving trapezoidal weirs were also developed and incorporated into a synthetic rating curve technique for overfalls in bedrock rivers. This technique holds only for free flow conditions; dimensionless submergence relations for various overfall sections were unobtainable.

Stage-discharge relations for the modelled reach of the Burntwood River were analyzed and found to be lower than previously predicted. The effects of the higher water elevations were discussed and velocity patterns and parameters downstream of the Thompson Bridge were established for 35,000 cfs. Possible difficulties in terms of increased velocities and bank erosion were also mentioned.

(b) Conclusions

A synthetic approach to rating curve development of trapezoidal overfalls in bedrock rivers utilizing dimensionless plots is possible for free flow conditions. A cross-section of the overfall and the degree of anticipated submergence is the only necessary

data. Rating curves for V-notched overfalls can be estimated by assuming small values for the bottom width.

(c) Recommendations

(1) The developed synthetic rating curve technique should be applied to more overfalls where stage-discharge relations are known in order to further test its validity in the field.

(2) Further trapezoidal weir studies should be undertaken to ascertain the possibilities of obtaining dimensionless relations involving effective submergence conditions. These relations could then be incorporated into the developed synthetic rating curve technique.

LIST OF REFERENCES

Baracos, A. and Galay, V.J., 1973 - "Effects of Increased Flow in the Burntwood River Near Thompson, Manitoba", Water Resources Branch, Department of Mines, Resources and Environmental Management, Province of Manitoba

Bauer, S.W. and Graf, W.H., 1971 - "Free Overfall as Flow Measuring Device", A.S.C.E. Proc., Irrigation and Drainage Division

Fonstad, G.D. and Gibson, D.G., 1974 - "Hydraulics of an Overfall on the Burntwood River", Department of Civil Engineering, University of Manitoba

Pilgram, D.H., et al, 1966 - "Hydraulic Model Rating of Gauging Stations on Small Catchments", Journal of the Institution of Engineers, Australia

Rao, S.S. and Shukla, M.K., 1971 - "Characteristics of Flow over Weirs of Finite Crest Width", A.S.C.E. Proc., Hydraulic Division

Smith, C.D., 1956 - "Open Channel Water Measurement with the Broad-Crested Weir", P.F.R.A. Design Bulletin No. 7

Smith, C.D., 1969 - "Triangular Broad-Crested Weir", A.S.C.E. Proc., Irrigation and Drainage Division

Underwood McLellan and Assoc. Ltd., 1973 - "Sediment Transport Investigations for Rat-Burntwood Mitigation Study, Winnipeg

Wilson, E.H., 1972 - "Broad-Crested Weirs and the Equation of Gradually Varied Flow", Water Power

APPENDIX A

WEIR STUDIES

A1. Dimensional Analysis of Trapezoidal Weir

The science of dimensional analysis is based on the concept that all the quantities to be added must be of the same dimension or combination of dimensions.

There are generally four applications of dimensional analysis:

(1) to reduce the number of variables in an experimental program

(2) to convert from one set of unit to another set

(3) to enable scientists and engineers to efficiently plan their model testing programs

(4) to check equations

Fundamental variables are variables which will influence the test and can be changed without altering the other variables. Everything that one may measure after setting the fundamental variables can be termed controlled variables, and is completely determined by the fundamental variables.

From an examination of the various dimensions one finds that there are only three fundamental dimensions: feet, seconds, pounds and these are simplified to: L, T, F - (length, time, force).

The number of variables to consider can be reduced through the application of the Buckingham Pi Theorum which states: "If any equation is dimensionally homogeneous, it can be reduced to a relationship among a complete set of dimensionless products." In other words, if there are a large number, n, of fundamental and controlled

variables having k fundamental dimensions (usually k=3), then the result would be n-k dimensionless groups which are usually called Pi (or π) terms.

In the case of the trapezoidal broad-crested weir, the variables are grouped as:

$$f\ (Q,\ e,\ \mu,\ P,\ H,\ b,\ Z,\ g,\ L,\ Z_A)$$

Therefore: n = 10

and as previously established k = 3.

Thus the variables should be able to grouped into n-k=10-3=7 π-terms.

There are several basic steps involved in obtaining these 7 π-terms. These steps are:

(1) Select k repeating variables, in this case 3 out of 10, making sure that all the fundamental dimensions are included in the chosen quantities. It is usually better to choose these repeating variables from the fundamental variables.

In this case, e, g, and H are chosen as repeating variables.

(2) Take these three variables and assign unknown exponents or powers to them, and, to obtain the first π-term combine these with another variable having an exponent = 1:

$$\pi_1 = e^a \times g^b \times H^c \times \mu^1$$

(3) By using dimensional analysis, solve for the unknown exponents - insert the fundamental dimensions into the above arrangement:

$$F^{\circ}L^{\circ}T^{\circ} = \left(\frac{FT^2}{L^4}\right)^{a} \times \left(\frac{L}{T^2}\right)^{b} \times L^{c} \times \left(\frac{FT}{L^2}\right)^{1}$$

Equating exponents of F, L, and T obtains:

F: $0 = a + 1 \qquad a = -1$

L: $0 = -4a + b + c - 2$

T: $0 = 2a - 2b + 1 \qquad b = -1/2$

and substituting into the L arrangement

$0 = 4 + 1/2 + c - 2 \qquad c = -3/2$

$$\pi_1 = e^{-1}\, g^{-1/2}\, H^{-3/2}\, \mu$$

or $$\pi_1 = \frac{\mu}{e\, g^{1/2}\, H^{5/2}}$$

The same steps are followed to obtain dimensionless π-terms which includes the other variables. Therefore:

$\pi_2 = H/P$

$\pi_3 = H/L$

$\pi_4 = H/b$

$\pi_5 = \not{Z}$

$\pi_6 = \not{Z}_A$

$\pi_7 = Q/g^{1/2}\, H^{5/2}$

$$Q/g^{1/2}\, H^{5/2} = f(\mu/eg^{1/2}\, H^{3/2},\ H/P,\ H/L,\ H/b,\ \not{Z},\ \not{Z}_A)$$

$$Q = f(\mu/eg^{1/2}\, H^{5/2},\ H/P,\ H/L,\ H/b,\ \not{Z},\ \not{Z}_A \quad g^{1/2}\, H^{5/2})$$

or: $Q = CH^{5/2}$

This is similar to the basic formula for a triangular weir.

A2. Weir types tested

Listed in TABLE A2-1 are the various weir combinations tested.

TABLE A2-1 Weir Combinations Tested

Weir No.	b(ft.)	$\not{z}$	$\not{z}_A$	Weir type
1 #	0.000	1:1	0:1	V-notched
2	0.000	1:1	5:1	"
3	0.000	1:1	10:1	"
4	0.250	1:1	0:1	trapezoidal
5	0.250	1:1	5:1	"
6	0.250	1:1	10:1	"
7	0.750	1:1	0:1	"
8	0.750	1:1	5:1	"
9	0.750	1:1	10:1	"
10	1.250	1:1	0:1	"
11	1.250	1:1	5:1	"
12	1.250	1:1	10:1	"
13	1.750	1:1	0:1	"
14 *	0.000	3:1	0:1	V-notched
15 *	0.167	3:1	0:1	trapezoidal
16 *	0.333	3:1	0:1	"
17 #	3.000	1:0	0:1	broad-crested

All weirs were designed with

P = 0.50 feet and L = 2.00 feet

\# Submergence values available from C.D. Smith
* Submergence tests conducted

APPENDIX B

BURNTWOOD RIVER MODEL

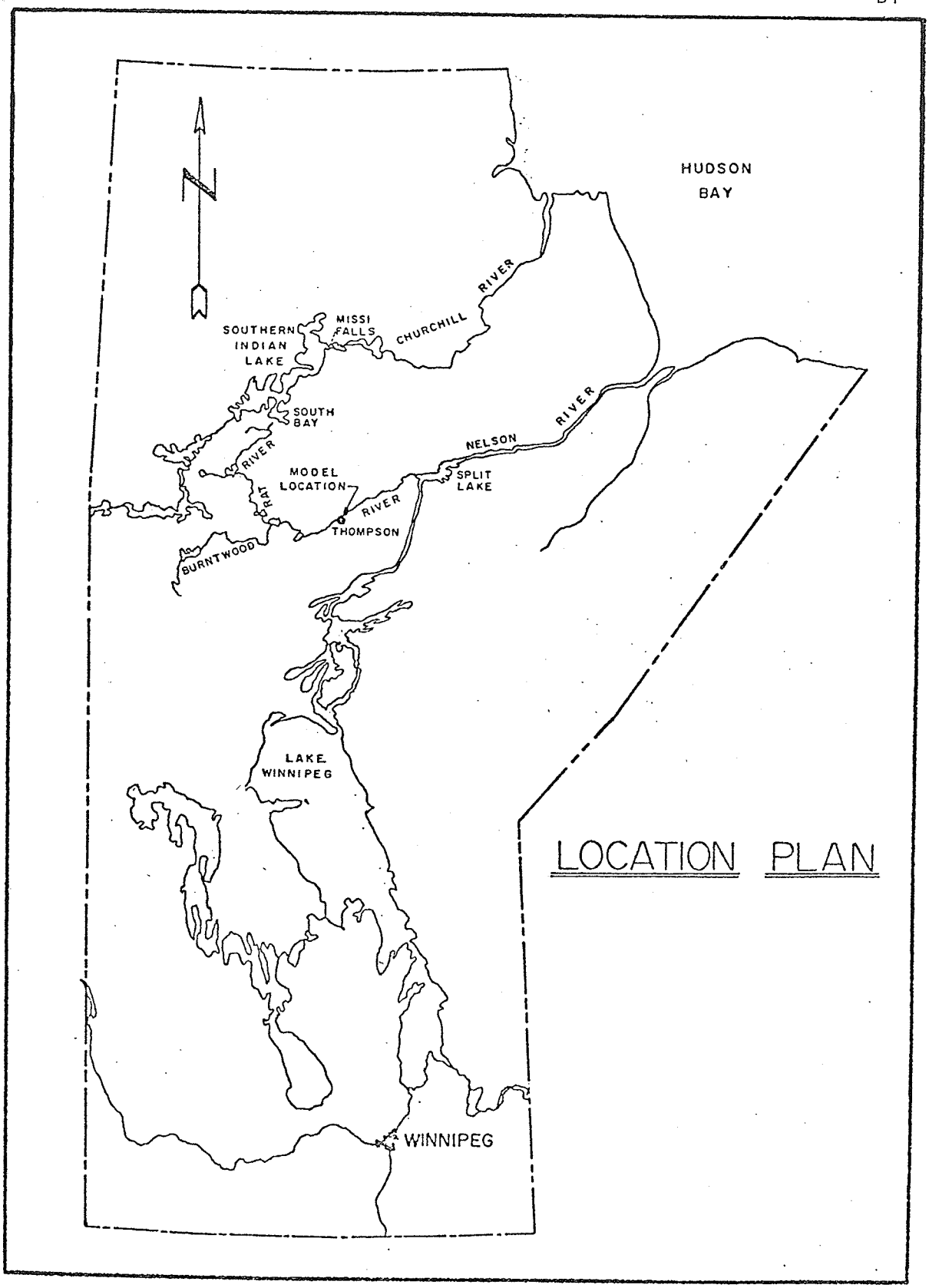
HUDSON
BAY
SOUTHERN
INDIAN
LAKE
MISSI
FALLS
CHURCHILL
RIVER
SOUTH
BAY
RIVER
NELSON
RIVER
MODEL
LOCATION
SPLIT
LAKE
RAT
RIVER
THOMPSON
BURNTWOOD
LAKE
WINNIPEG
WINNIPEG
LOCATION PLAN

FIGURE B1-1

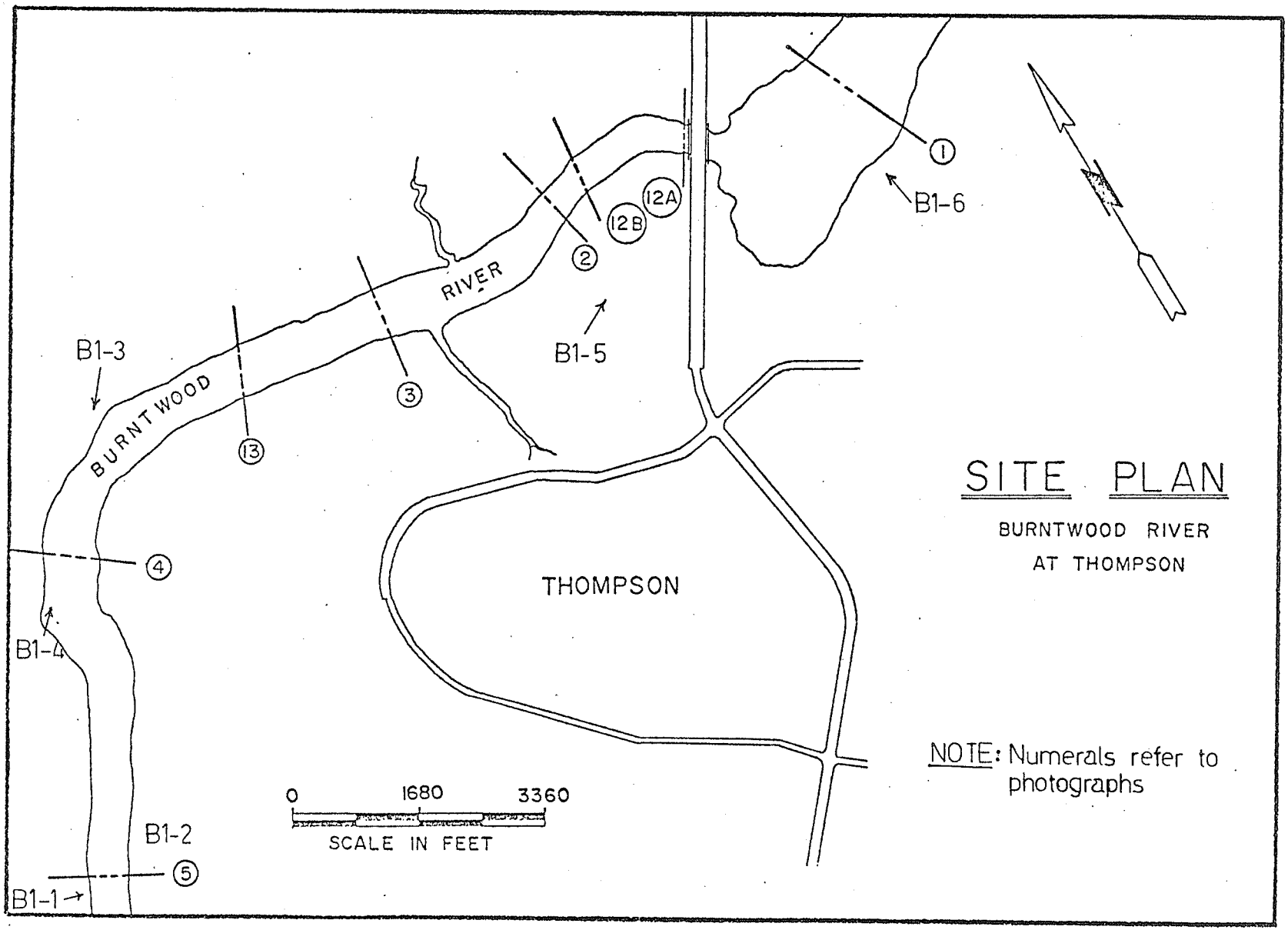
SITE PLAN
BURNTWOOD RIVER
AT THOMPSON
NOTE: Numerals refer to photographs
THOMPSON
RIVER
BURNTWOOD
B1-1
B1-2
B1-3
B1-4
B1-5
B1-6
1
2
3
4
5
12A
12B
13
0
1680
3360
SCALE IN FEET

FIGURE B1-2

PHOTOGRAPH B1-1 Thompson Waterworks Pumphouse

PHOTOGRAPH B1-2 Burntwood River Near Pumphouse

PHOTOGRAPH B1-3 Burntwood River Upstream of Cross-Section 4

PHOTOGRAPH B1-4 Cross-Section 4 Located at Promontory in Lower Center of Photograph

PHOTOGRAPH B1-5 Reach Near Thompson Bridge

PHOTOGRAPH B1-6 Government Air Services Base

B2. Model Design

(i) proposed scaling

In the initial analysis for scaling the Burntwood River model, the following controls were established:

(1) maximum model discharge, $Q_m(max)$ = 5 cfs.

(2) maximum prototype discharge, $Q_p(max)$ = 35,000 cfs.

The proposed scales are:

horizontal 1:320

vertical 1:60

Scale ratios based on Fronde Relationship are:

length ratio $\frac{X_p}{X_m} = X_r$

height ratio $\frac{Y_p}{Y_m} = Y_r$

undistorted model $X_r = Y_r$

distorted model $X_r \neq Y_r$

ratio	undistorted	distorted	model scales
horizontal	X_r	X_r	1:320
vertical	Y_r	Y_r	1:60
area	Y_r^2	X_rY_r	1:19,200
velocity	$Y_r^{1/2}$	$Y_r^{1/2}$	1:7.74
discharge	$X_r^{5/2}$	$X_rY_r^{3/2}$	1:148,722

(ii) verification of proposed scales

FIGURE B1-1 shows cross-section 3 of the model with:

channel bed = 581.0 ft (G.S.C.)

stage = 605.1 ft. (G.S.C.)

area of flow = 7187 ft.^{2} (by planimeter)

$\simeq$ 7190 ft.^{2}

discharge = 8400 cfs.

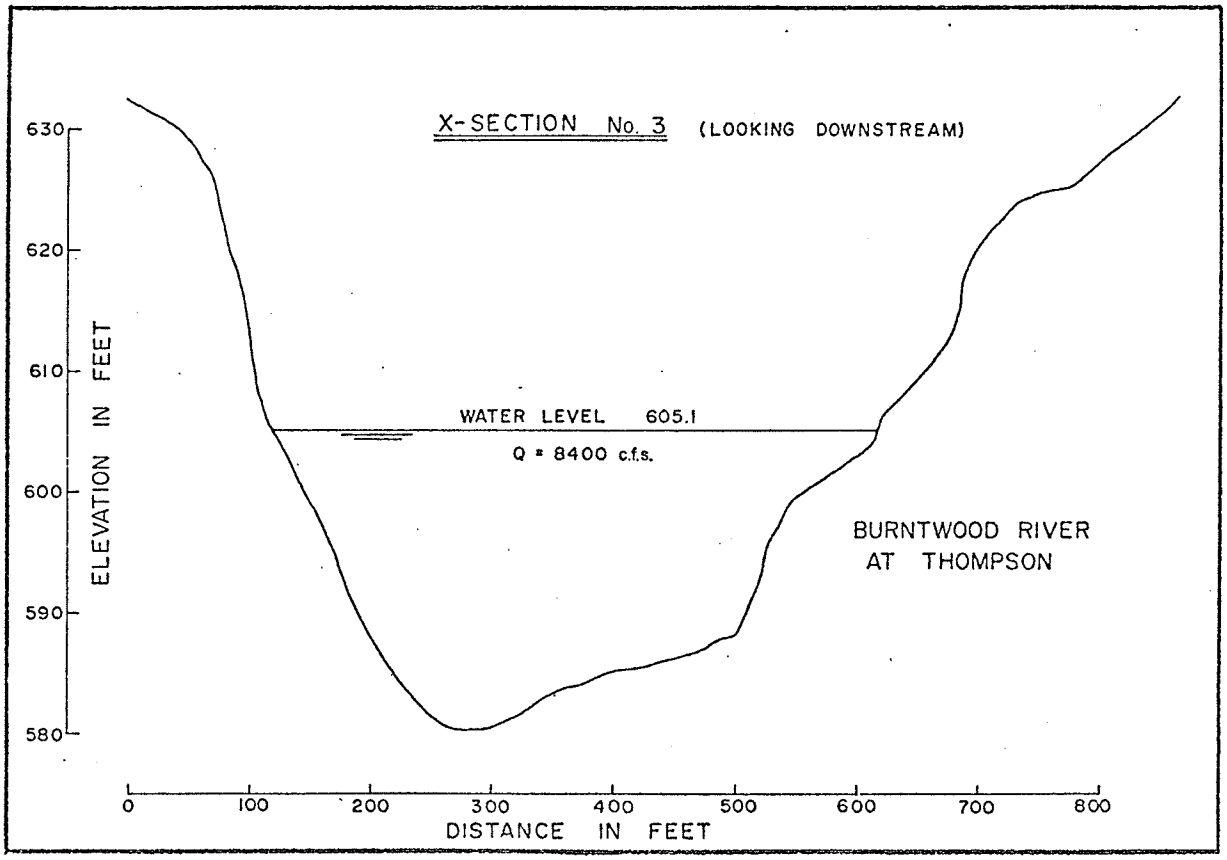

FIGURE B1-1 Cross-Section 3

At 8400 cfs., the depth of flow Y_p = 24.1 ft.. This results in a model depth of Y_m = 0.402 ft. = 4.83 inches. This depth is easily measurable in the model so no problems should occur when studying low discharge values.

In terms of velocities

$$V_p = Q_p/A_p = \frac{8400 \text{ ft}^3/\text{sec}}{7190 \text{ ft}^2} = 1.168 \text{ ft/sec}$$

Now for an assumed water temperature of 50°F, the Reynolds Number for the prototype is:

$$\mathbb{R}e_p = \frac{4VpYp}{\nu} = \frac{4 \times 1.168 \times 24.1}{1.41 \times 10\text{-}5} \quad \frac{ft/sec \times ft}{ft^2/sec}$$

$$\mathbb{R}e_p = 7.98 \times 10^6$$

and for the model

$$\mathbb{R}e_m = \frac{4VmYm}{\nu} = \frac{4 \times V_p/V_r \times Y_p/Y_r}{\nu}$$

$$\mathbb{R}e_m = \frac{4 \times (1.168/7.746) \times (24.11/60)}{1.41 \times 10\text{-}5}$$

$$\mathbb{R}e_m = 1.718 \times 10^4$$

$\mathbb{R}e_m$ is greater than 4000, as required to be in the rough turbulent region of flow, which agrees with the prototype conditions.

Due to the size of the model and the low velocities encountered in the model, roughness has not been considered. If during testing it appears to be a factor, artifical roughening techniques will be employed.

The degree of distortion is not critical for a model in which stage-discharge relationships are studied. However, further studies involving velocities were later included. Distortion in this case should not exceed a factor of 6 and preferably be less than 5. The model scales result in a distortion factor of 5.3 thereby allowing velocity patterns to be studied and estimates of actual surface velocities to be made.

From the above analysis and discussion, it appears that the chosen scales of 1:320 horizontal and 1:60 vertical are suitable for the considerations of the study.

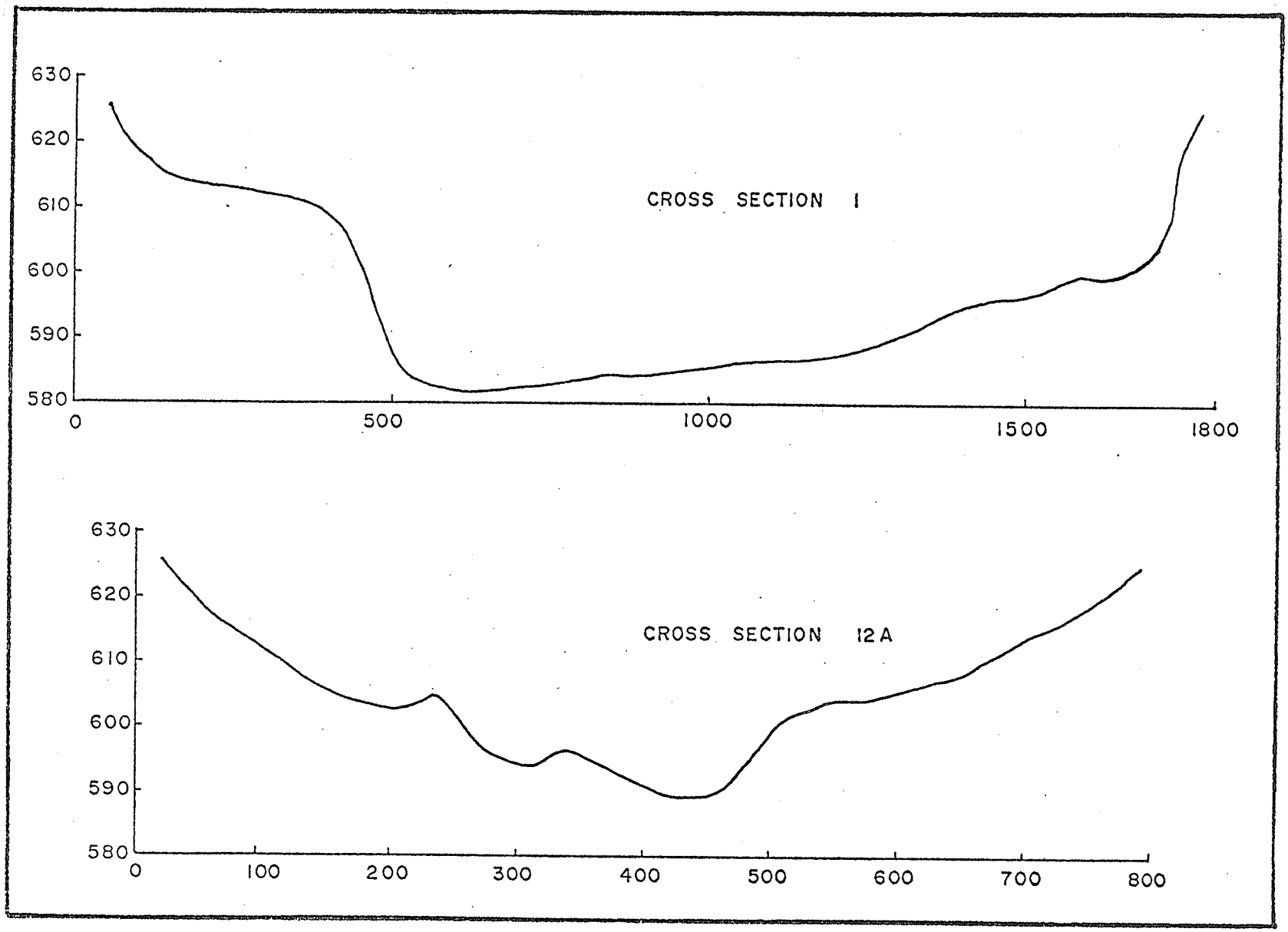

FIGURE B3-1 MODEL CROSS-SECTIONS

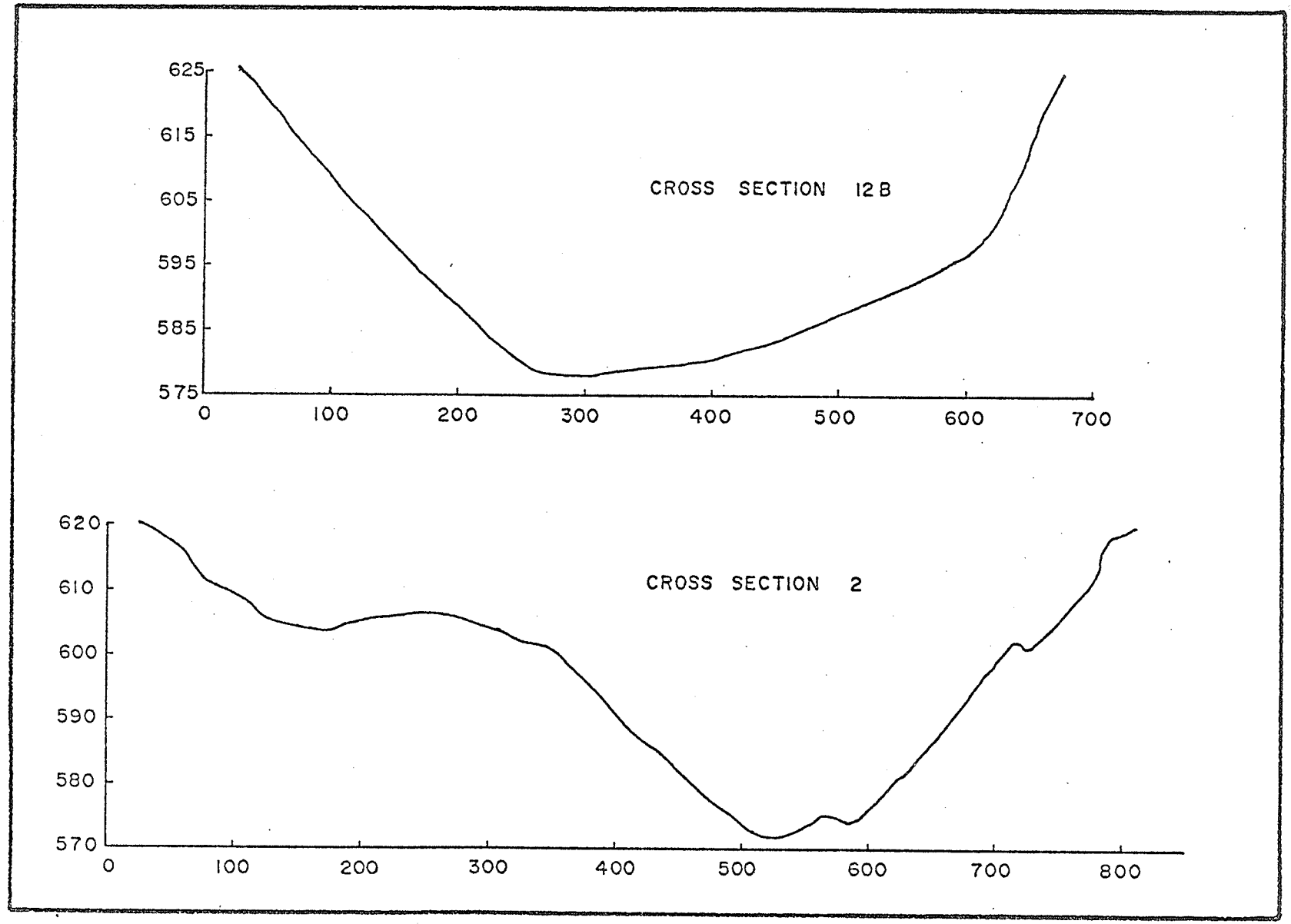

FIGURE B3-2 MODEL CROSS-SECTIONS

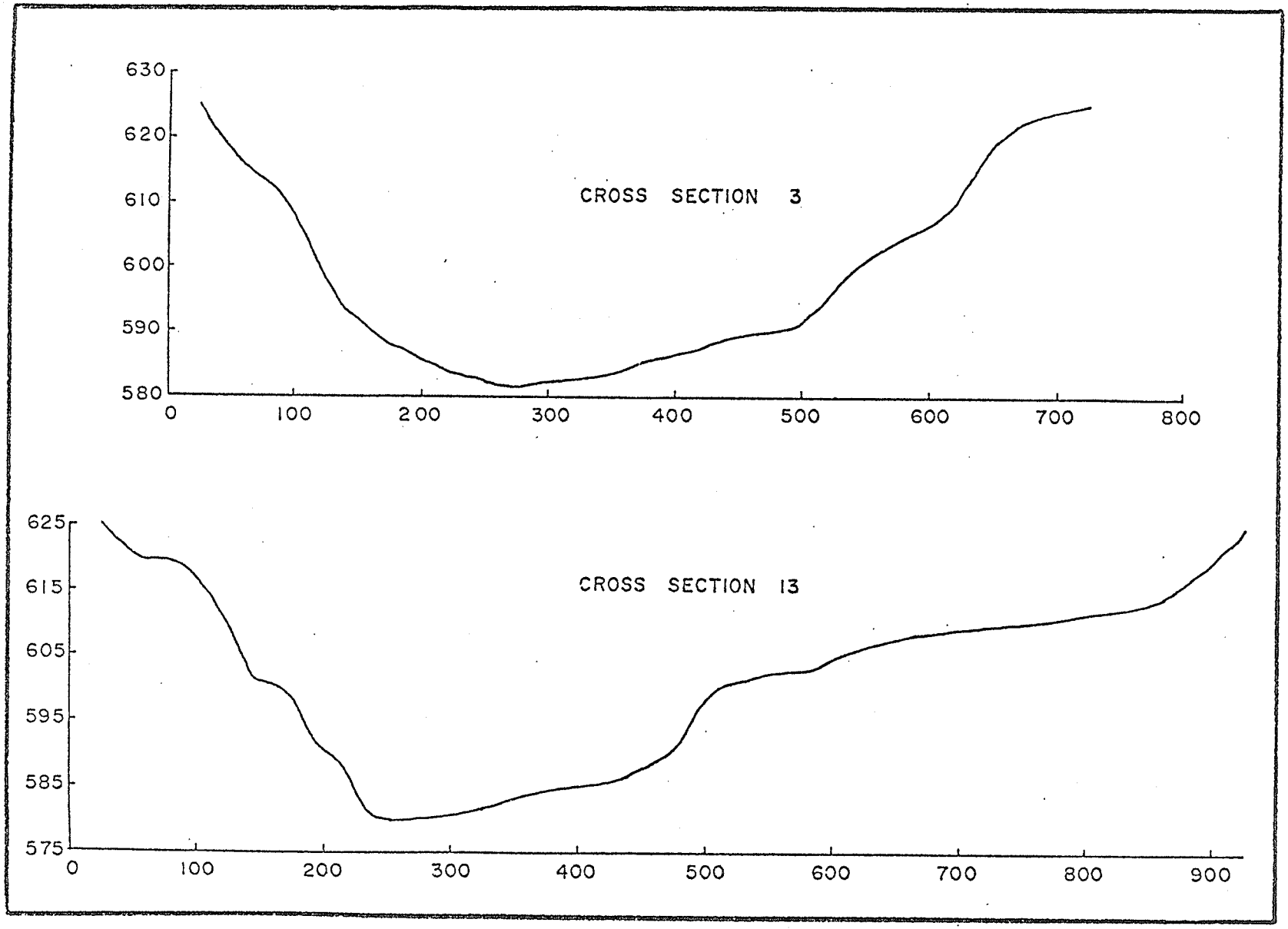

FIGURE B3-3 MODEL CROSS-SECTIONS

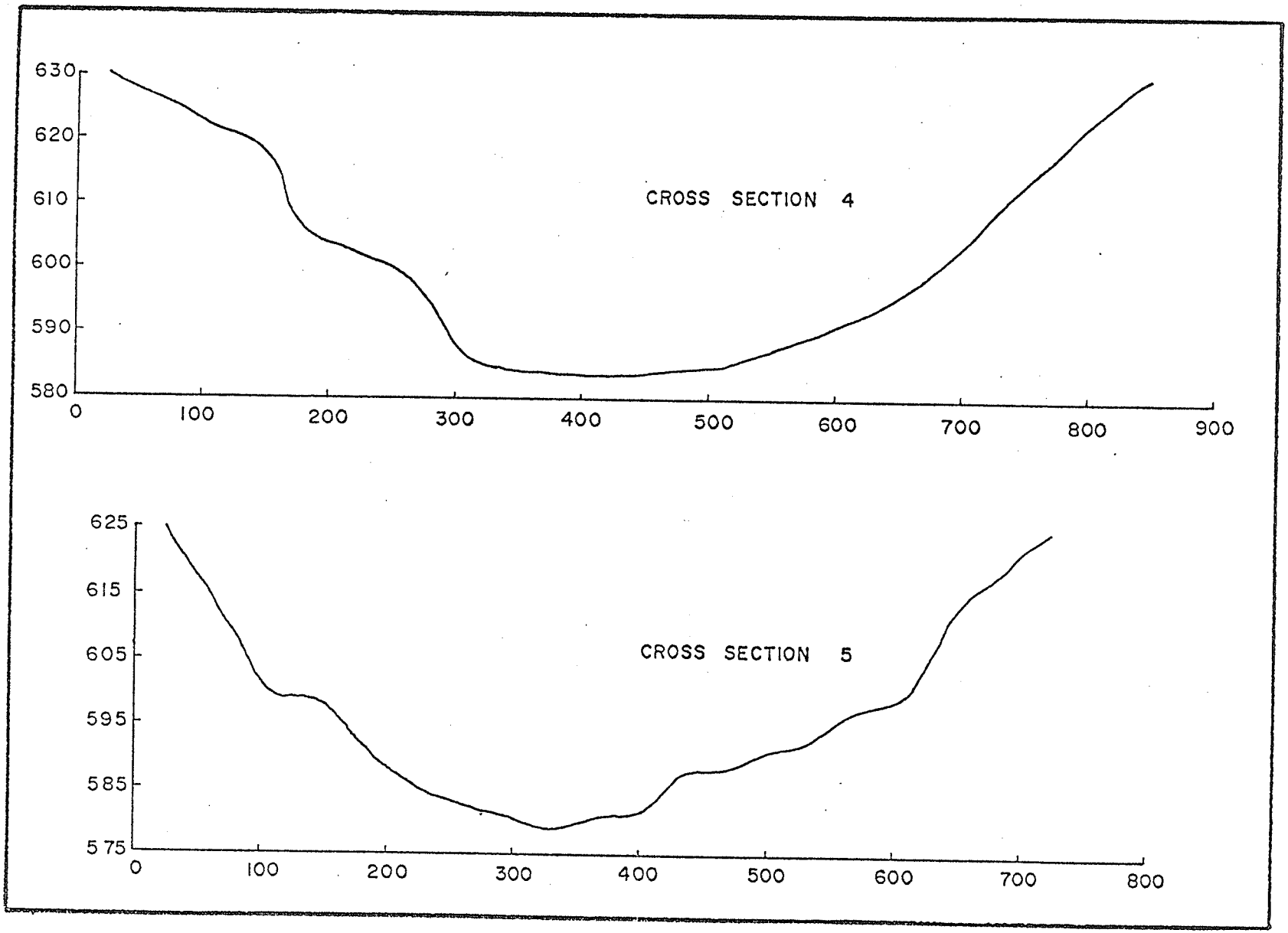

FIGURE B3-4 MODEL CROSS-SECTIONS

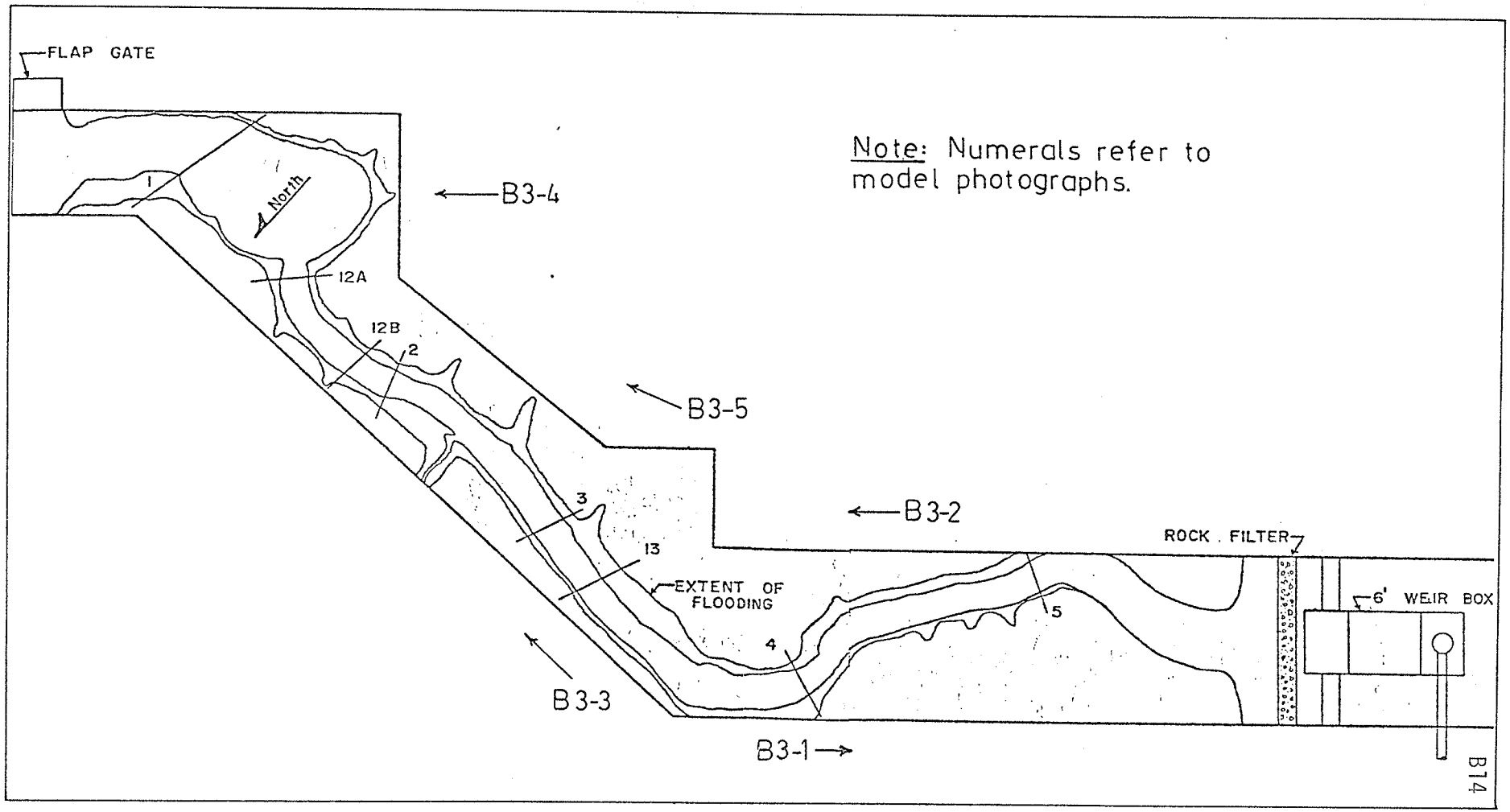

FIGURE B3-5 MODEL LAYOUT

PHOTOGRAPH B3-1 Burntwood River Model Cross-Section 4 and Upstream

PHOTOGRAPH B3-2 Burntwood River Model Cross-Section 4 as in Photograph B1-4

PHOTOGRAPH B3-3 Burntwood River Model
Upstream of Bridge

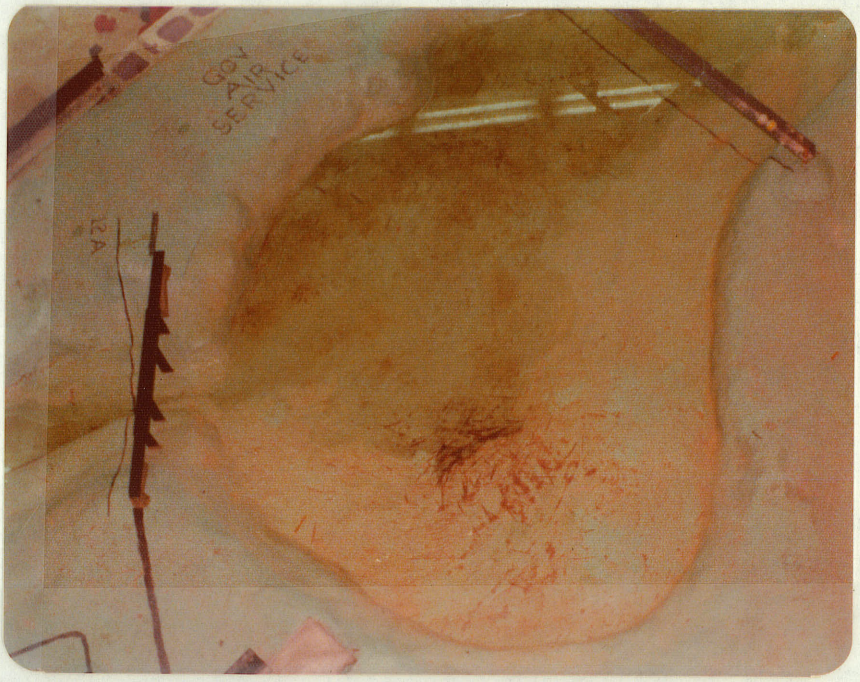

PHOTOGRAPH B3-4 Burntwood River Model
Downstream of Bridge

PHOTOGRAPH B3-5 Burntwood River Model
Reach Near Bridge

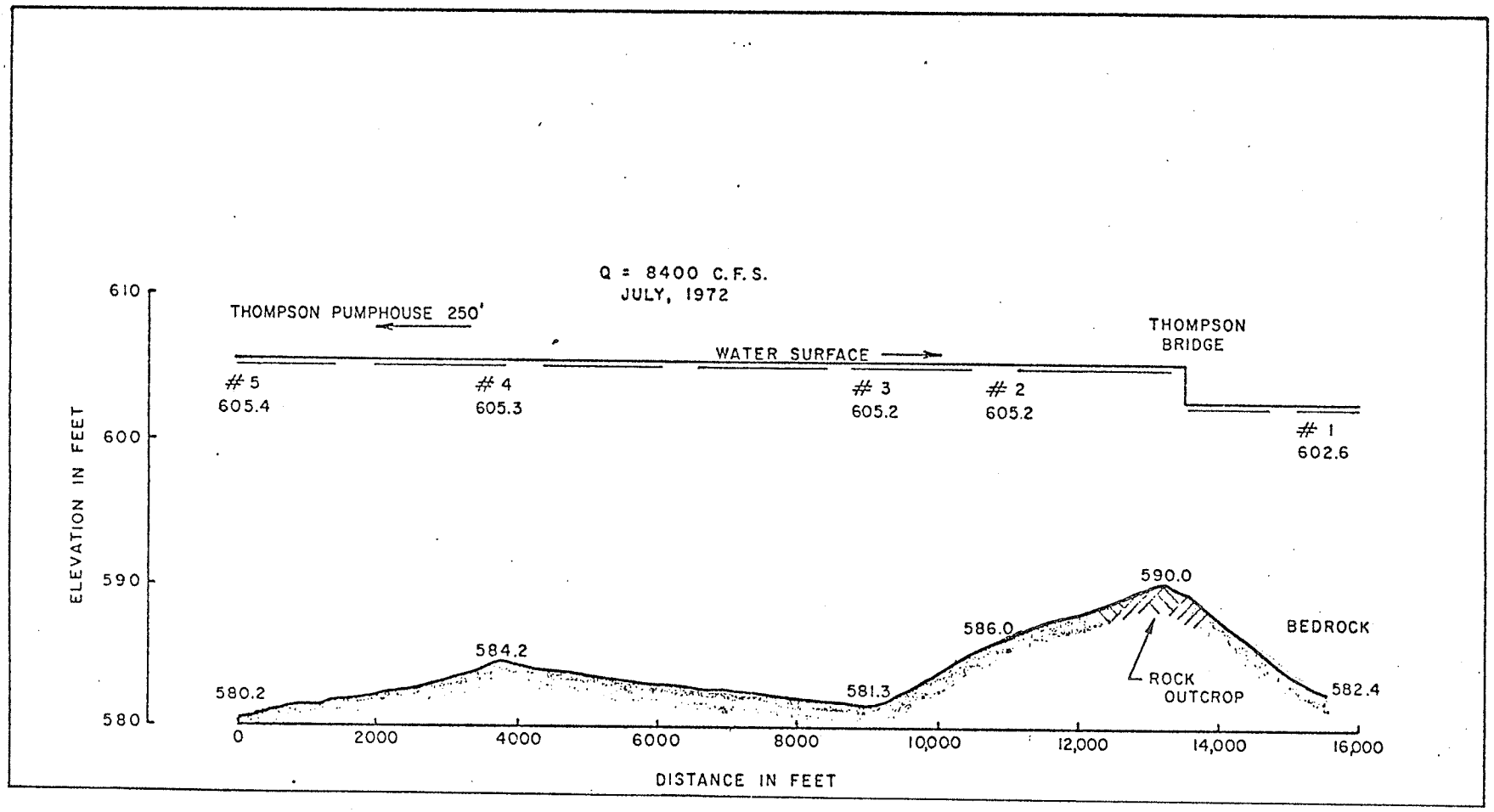

FIGURE B3-6 SAMPLE WATER SURFACE PROFILE

Leaf blank to correct numbering

B4. Introductory Testing

(a) checking and adjusting channel profile

Once construction of the model was completed, a level survey of the constructed channel profile was undertaken. The results of this survey showed that the profile was constructed with an average error of 1.64 feet (prototype scale) lower than the actual, with cross-section 5 being an exception at 6.05 feet low.

The error in cross-section 5 was corrected by reshaping the section.

In order to compensate for the average profile error of 1.64 feet, a level-water, zero-flow test was conducted. Using the invert of cross-section 12A (as constructed) as a datum, point gauge readings to the still water surface and the channel bed were taken at all cross-sections upstream of 12A. The bed elevations of these cross-sections could then be calculated based on the level water surface elevation. The constructed and the actual profiles are found in FIGURE B4-1. It can be seen that the constructed channel was still lower than the actual.

To compensate for the remaining error, water surface calculations were based on the correct channel elevations. However this necessitated ignoring the flow between the prototype channel elevation and the constructed channel elevation. For the invert case, this would amount to a flow equal to that through a depth of

0.035 feet extending over no more than 0.20 feet of width. This small amount of flow, approximately 30 cfs., could be omitted without introducing significant errors.

To allow for this change, the point gauge readings to channel bed were adjusted, based on the difference in elevation of the constucted model and the actual. The calculations for this adjustment procedure are listed in TABLE B4-1.

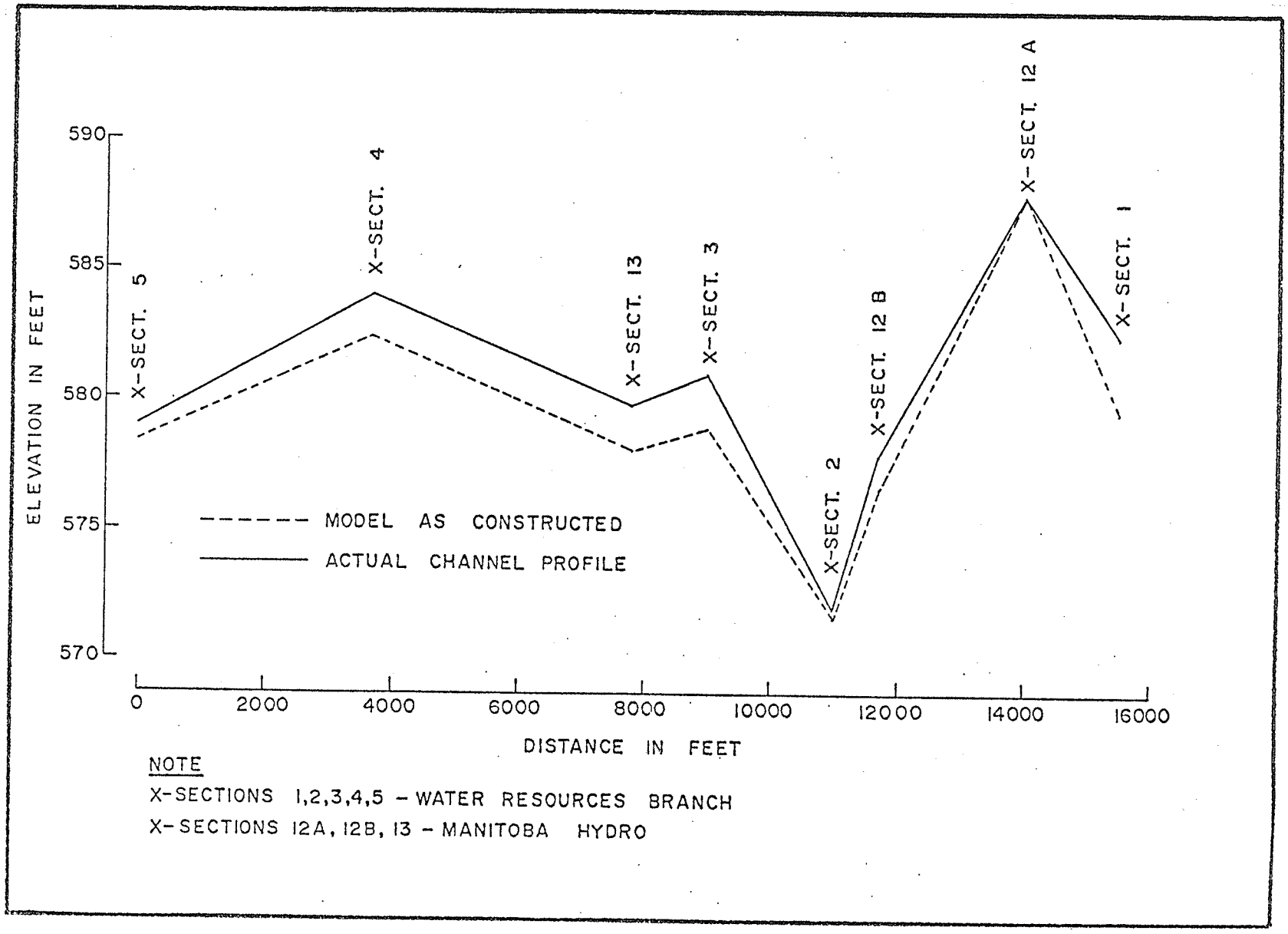

FIGURE B4-1 MODEL PROFILES

TABLE B4-1 Channel Bed Adjustment Calculations

Sta.	Prototype Channel Elevation	Gauge Water Level	Gauge Bed Level	ΔEl_m	ΔEl_p	Bed Elevation	$Diff_p$	$Diff_m$	Adjusted Gauge Reading Bed Level
	(ft.)	(ft.)	(ft.)	(ft.)	(ft.)	(ft.)	(ft.)	(ft.)	(ft.)
1	582.40		.239			576.90	5.5	.091	.330
12A	587.90	.568	.568	0	0	587.90	0	0	.568
12B	577.90	.565	.377	.188	11.28	576.62	1.28	.021	.398
2	572.00	.568	.297	.271	16.26	571.64	0.36	.006	.303
3	581.00	.567	.417	.150	9.00	578.90	2.10	.035	.452
13	579.80	.198	.033	.165	9.90	578.00	1.80	.030	.063
4	584.00	.562	.469	.093	5.58	582.32	1.68	.028	.497
5	579.00	.624	.465	.158	9.54	578.36	0.64	.011	.476

B5. Calculated Stage-Discharge Conditions for Cross-Section 1

(a) derived backwater calculations from Manitoba Hydro

The derived backwater elevations for natural water conditions for cross-sections 5B and 6, presented by Manitoba Hydro, are listed in TABLE B5-1.

TABLE B5-1 Natural Open Water Elevations

Cross-Section 5B		Cross-Section 6	
Q(cfs)	Elevation(GSC)	Q(cfs)	Elevation(GSC)
5,000	594.80	5,000	598.37
10,000	597.48	10,000	602.06
20,000	602.11	20,000	606.78
30,000	605.12	30,000	609.96
34,000	606.20	34,000	611.04
40,000	607.00	40,000	612.88
50,000	609.63	50,000	614.95

The stage-discharge relation used at cross-section 1 was derived as shown in TABLE B5-2.

TABLE B5-2 Stage-Discharge Relations at Cross-Section 1

(Manitoba Hydro)

Q(cfs)	Elev. X-Sect. 6	+ Incremental Rise	= Elev. X-Sect. 1 (GSC)
5,000	598.37	4.00	602.37
10,000	602.06	*3.80	605.86
20,000	606.78	*3.70	610.48
30,000	609.96	*3.60	613.56
34,000	611.04	3.50	614.54
40,000	612.88	*3.50	616.38

*interpolated values

(b) Synthetic rating curve at 5th Rapids

The procedure followed in deriving the 5th Rapids rating curve is discussed in detail in APPENDIX E.

Cross-section 5B, shown in FIGURE B5-1, was chosen as the study section. The section has a bottom width of 35 ft. with side-slopes of 7:1 and 5:1. The trapezoidal cross-section chosen to represent this section is:

bottom width b = 35ft.

average side-slope, Z = 6:1

For a comparison of b_{ave} values for the actual channel and the theoretical 6:1 sided channel:

for H = 20ft.

actual: $$b_{ave} = \frac{Z*_L H}{2} + b + \frac{Z*_R H}{2}$$

$$b_{ave} = \frac{5(20)}{2} + 35 + \frac{7(20)}{2} = 155 \text{feet}$$

theoretical: $b_{ave} = Z_* H + b$

$$b_{ave} = 6(20) + 35 = 155 \text{feet}$$

Values are equal therefore the average side-slope factor does not affect results.

TABLE B5-3 lists the calculations for the 5th Rapids rating curve. The synthetic 5th Rapids rating curve at cross-section 5B and Manitoba Hydro's derived backwater elevations for the same section are shown in FIGURE B5-2.

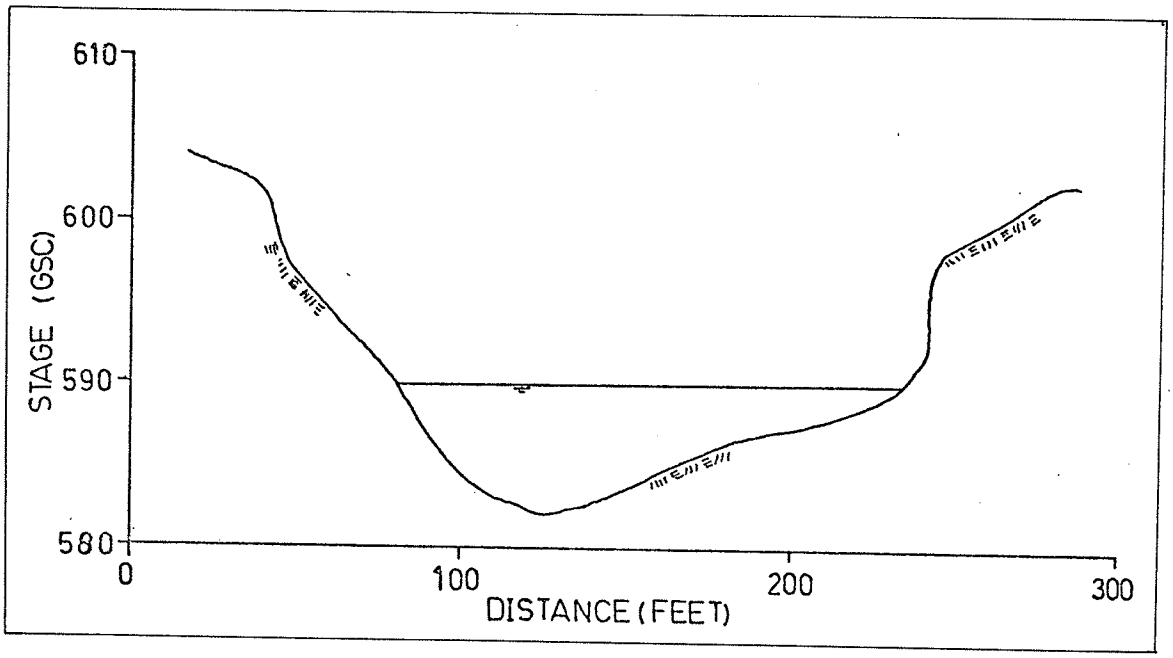

FIGURE B5-1 Cross-Section 5B

TABLE B5-3 5th Rapids Rating Curve

H (ft)	b_{ave} (ft)	H/b_{ave}	$Q/g^{1/2} H^{5/2}$	Stage (GSC)	Q (cfs)
0	-	-	-	583.5	0.0
5.0	65.0	0.076	6.40	587.0	2,030.2
7.5	80.0	0.094	5.15	589.5	4,501.8
10.0	95.0	0.106	4.70	592.0	8,433.8
12.5	110.0	0.114	4.20	594.5	13,165.9
15.0	125.0	0.120	3.90	597.0	19,285.0
17.5	140.0	0.125	3.70	599.5	26,898.3
20.0	155.0	0.129	3.60	602.0	36,543.1

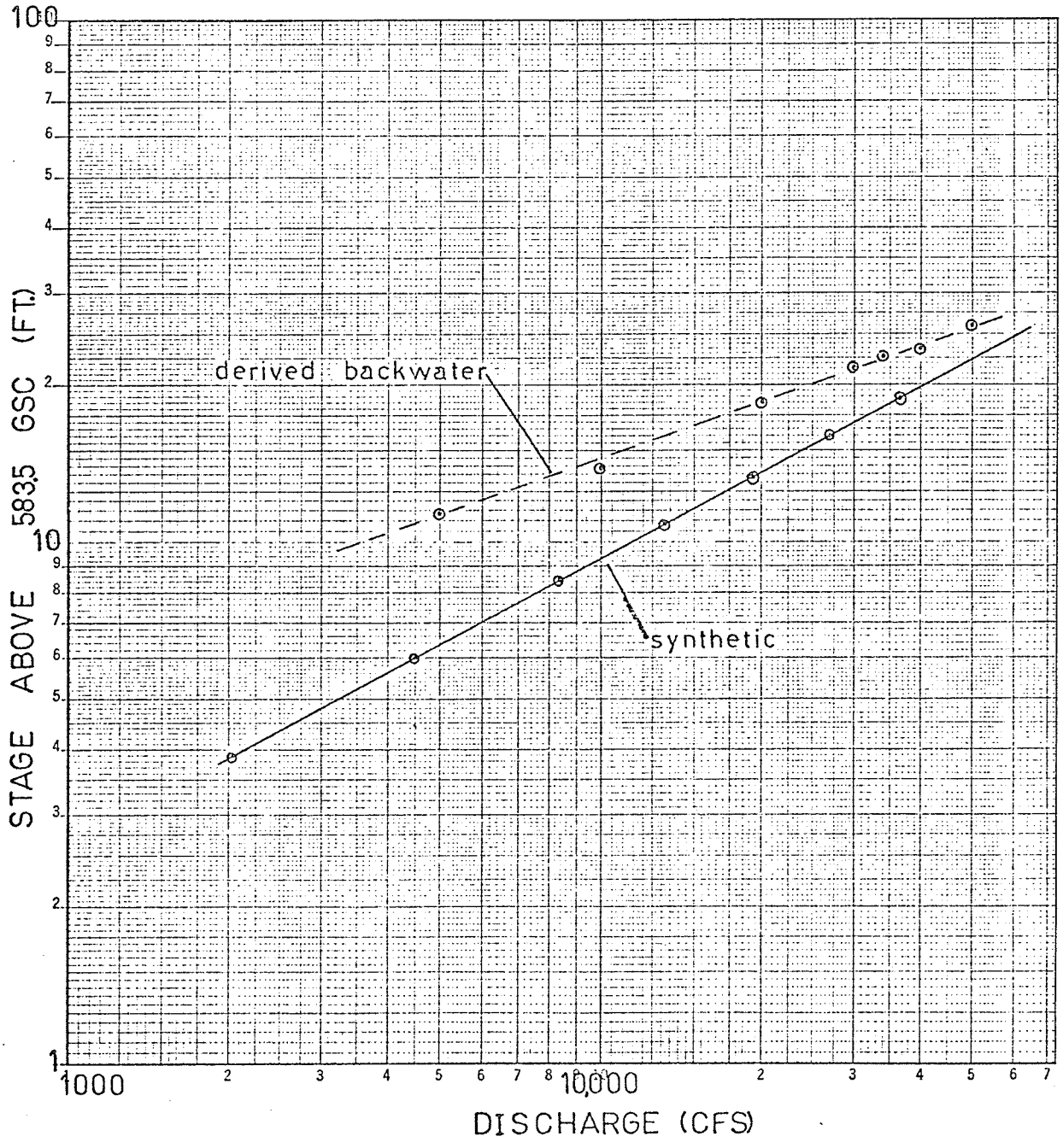

FIGURE B5-2 Rating Curves for 5th Rapids

The stage-discharge relations between cross-section 5B and 6 was calculated using Manitoba Hydro's backwater relation between the two sections. Calculations for the stage-discharge relations at cross-section 1 are listed in TABLE B5-4.

TABLE B5-4 Stage-Discharge Relations at Cross-Section 1
(synthetic)

Q (cfs)	Elevation X-Sect. 5B	+	Increment to 6	+	Increment to 1	=	Elevation X-Sect. 1 (GSC)
5,000	591.30		3.57		4.00		598.87
10,000	594.30		4.58		*3.80		602.68
20,000	598.60		4.67		*3.70		606.97
30,000	601.80		4.84		*3.60		610.24
34,000	602.90		4.84		3.50		611.24
40,000	604.40		4.89		*3.50		612.79

*interpolated values

APPENDIX C

WEIR TEST RESULTS

TABLE C1-1 Weir Data and Calculations

V-notched weir 1-1 sides b = 0.000 ft.

Test	H	Q	b_{ave}	H/b_{ave}	$Q/g^{1/2}H^{5/2}$	h_s	h_s/H	H/L	H/b	C
1	0.186	0.035	0.186	1.000	0.413	0.000	0.000	0.093	****	2.346
2	0.217	0.047	0.217	1.000	0.378	0.000	0.000	0.109	****	2.143
3	0.297	0.100	0.297	1.000	0.367	0.000	0.000	0.148	****	2.080
4	0.337	0.135	0.337	1.000	0.361	0.000	0.000	0.169	****	2.048
5	0.377	0.179	0.377	1.000	0.361	0.000	0.000	0.188	****	2.051
6	0.418	0.232	0.418	1.000	0.362	0.000	0.000	0.209	****	2.054
7	0.385	0.189	0.385	1.000	0.362	0.000	0.000	0.192	****	2.055
8	0.191	0.028	0.191	1.000	0.309	0.000	0.000	0.095	****	1.756
9	0.231	0.050	0.231	1.000	0.344	0.000	0.000	0.115	****	1.950
10	0.275	0.085	0.275	1.000	0.378	0.000	0.000	0.137	****	2.143
11	0.326	0.124	0.326	1.000	0.360	0.000	0.000	0.163	****	2.044
12	0.368	0.175	0.368	1.000	0.375	0.000	0.000	0.184	****	2.130
13	0.394	0.207	0.394	1.000	0.374	0.000	0.000	0.197	****	2.124
14	0.231	0.052	0.231	1.000	0.357	0.000	0.000	0.115	****	2.028
15	0.275	0.086	0.275	1.000	0.382	0.000	0.000	0.137	****	2.169
16	0.325	0.121	0.325	1.000	0.354	0.000	0.000	0.162	****	2.009
17	0.380	0.183	0.380	1.000	0.362	0.000	0.000	0.190	****	2.056
V-notched Broad-Crested weir 3-1 sides										
1	0.139	0.049	0.417	0.333	1.199	*****	*****	0.069	****	6.802
2	0.159	0.072	0.477	0.333	1.259	*****	*****	0.080	****	7.142
3	0.233	0.183	0.699	0.333	1.231	*****	*****	0.116	****	6.983
4	0.366	0.550	1.098	0.333	1.196	*****	*****	0.183	****	6.787
5	0.319	0.393	0.957	0.333	1.205	*****	*****	0.160	****	6.838
6	0.272	0.280	0.816	0.333	1.279	*****	*****	0.136	****	7.257

Test	H	Q	b_{ave}	H/b_{ave}	$Q/g^{1/2}H^{5/2}$	h_s	h_s/H	H/L	H/b	C
V-notched Broad-Crested weir 3-1 sides										
1	0.253	0.213	0.759	0.333	1.167	*****	*****	0.127	****	6.624
2	0.253	0.213	0.759	0.333	1.167	0.130	0.514	0.127	****	6.624
3	0.253	0.213	0.759	0.333	1.167	0.180	0.711	0.127	****	6.624
4	0.269	0.213	0.807	0.333	1.001	0.241	0.896	0.135	****	5.683
5	0.295	0.214	0.885	0.333	0.799	0.283	0.959	0.148	****	4.534
6	0.280	0.214	0.840	0.333	0.908	0.259	0.925	0.140	****	5.153
7	0.258	0.213	0.774	0.333	1.112	0.217	0.841	0.129	****	6.308
8	0.331	0.450	0.993	0.333	1.258	*****	*****	0.166	****	7.139
9	0.330	0.441	0.990	0.333	1.243	0.252	0.764	0.165	****	7.052
10	0.337	0.441	1.011	0.333	1.179	0.282	0.837	0.168	****	6.692
11	0.360	0.439	1.080	0.333	0.995	0.328	0.911	0.180	****	5.646
12	0.375	0.411	1.125	0.333	0.841	0.350	0.933	0.188	****	4.772
13	0.387	0.435	1.161	0.333	0.822	0.364	0.941	0.194	****	4.667
14	0.347	0.435	1.041	0.333	1.080	0.307	0.885	0.174	****	6.130
Submergence tests V-notched weir 3-1 sides										
1	0.253	0.213	0.759	0.333	1.166	0.202	0.800	0.127	****	6.616
2	0.260	o.213	0.780	0.333	1.089	0.221	0.850	0.130	****	6.179
3	0.270	0.213	0.810	0.333	0.991	0.243	0.900	0.135	****	5.623
4	0.290	0.213	0.870	0.333	0.829	0.276	0.950	0.145	****	4.703
5	0.331	0.441	0.993	0.333	1.233	0.265	0.800	0.165	****	6.996
6	0.339	0.441	1.017	0.333	1.161	0.288	0.850	0.169	****	6.591
7	0.356	0.441	1.068	0.333	1.028	0.320	0.900	0.178	****	5.832
8	0.395	0.441	1.185	0.333	0.793	0.375	0.950	0.197	****	4.497

Test	H	Q	b_{ave}	H/b_{ave}	$Q/g^{1/2}H^{5/2}$	h_s	h_s/H	H/L	H/b	C
Trapezoidal weir 1-1 sides b = 0.25 ft.										
1	0.088	0.047	0.338	0.260	3.605	0.000	0.000	0.044	0.352	20.459
2	0.166	0.073	0.416	0.399	1.146	0.000	0.000	0.083	0.664	6.502
3	0.220	0.112	0.470	0.468	0.869	0.000	0.000	0.110	0.880	4.934
4	0.280	0.183	0.530	0.528	0.777	0.000	0.000	0.140	1.120	4.411
5	0.383	0.356	0.633	0.605	0.691	0.000	0.000	0.192	1.532	3.922
6	0.333	0.274	0.583	0.571	0.755	0.000	0.000	0.166	1.332	4.282
7	0.139	0.049	0.389	0.357	1.199	0.000	0.000	0.069	0.556	6.802
8	0.187	0.083	0.437	0.428	0.967	0.000	0.000	0.093	0.748	5.489
9	0.230	0.122	0.480	0.479	0.847	0.000	0.000	0.115	0.920	4.809
10	0.278	0.181	0.528	0.527	0.783	0.000	0.000	0.139	1.112	4.442
11	0.327	0.253	0.577	0.567	0.729	0.000	0.000	0.164	1.308	4.138
12	0.381	0.367	0.631	0.604	0.722	0.000	0.000	0.190	1.524	4.096
13	0.204	0.099	0.454	0.449	0.528	0.000	0.000	0.102	0.816	5.267
14	0.287	0.191	0.537	0.534	0.763	0.000	0.000	0.143	1.148	4.328
15	0.370	0.336	0.620	0.597	0.711	0.000	0.000	0.185	1.480	4.035
Trapezoidal weir 1-1 sides b = 0.75 ft.										
1	0.166	0.172	0.916	0.181	2.700	0.000	0.000	0.083	0.221	15.320
2	0.213	0.239	0.963	0.221	2.012	0.000	0.000	0.106	0.284	11.414
3	0.272	0.378	1.022	0.266	1.726	0.000	0.000	0.136	0.363	9.796
4	0.303	0.486	1.053	0.288	1.695	0.000	0.000	0.151	0.404	9.617
5	0.350	0.584	1.100	0.318	1.420	0.000	0.000	0.175	0.467	8.058
6	0.376	0.682	1.126	0.334	1.386	0.000	0.000	0.188	0.501	7.867

Test	H	Q	b_{ave}	H/b_{ave}	$Q/g^{1/2}H^{5/2}$	h_s	h_s/H	H/L	H/b	C
7	0.129	0.107	0.879	0.147	3.155	0.000	0.000	0.064	0.172	17.902
8	0.178	0.192	0.928	0.192	2.531	0.000	0.000	0.089	0.237	14.363
9	0.242	0.303	0.992	0.244	1.853	0.000	0.000	0.121	0.323	10.517
10	0.276	0.377	1.026	0.269	1.660	0.000	0.000	0.138	0.368	9.420
11	0.308	0.497	1.058	0.291	1.664	0.000	0.000	0.154	0.411	9.440
12	0.326	0.542	1.076	0.303	1.574	0.000	0.000	0.163	0.435	8.932
13	0.377	0.643	1.127	0.335	1.298	0.000	0.000	0.188	0.503	7.368
14	0.107	0.078	0.857	0.125	3.670	0.000	0.000	0.053	0.143	20.827
15	0.213	0.247	0.963	0.221	2.079	0.000	0.000	0.106	0.284	11.796
16	0.308	0.481	1.058	0.291	1.610	0.000	0.000	0.154	0.411	9.136
17	0.345	0.566	1.095	0.315	1.427	0.000	0.000	0.173	0.460	8.096
Trapezoidal weir 1-1 sides b = 1.25 ft.										
1	0.149	0.211	1.399	0.107	4.339	0.000	0.000	0.074	0.119	24.622
2	0.213	0.411	1.463	0.146	3.459	0.000	0.000	0.106	0.170	19.629
3	0.280	0.596	1.530	0.183	2.532	0.000	0.000	0.140	0.224	14.367
4	0.333	0.804	1.583	0.210	2.214	0.000	0.000	0.166	0.266	12.565
5	0.192	0.317	1.442	0.133	3.458	0.000	0.000	0.096	0.154	19.625
6	0.290	0.667	1.540	0.188	2.595	0.000	0.000	0.145	0.232	14.728
7	0.374	0.947	1.624	0.230	1.951	0.000	0.000	0.187	0.299	11.071
8	0.243	0.484	1.493	0.163	2.930	0.000	0.000	0.121	0.194	16.628
9	0.303	0.759	1.553	0.195	2.647	0.000	0.000	0.151	0.242	15.019
10	0.399	1.093	1.649	0.242	1.915	0.000	0.000	0.199	0.319	10.869
Trapezoidal weir 1-1 sides b = 1.75 ft.										
1	0.091	0.128	1.841	0.049	9.030	0.000	0.000	0.046	0.052	51.240
2	0.240	0.670	1.990	0.121	4.184	0.000	0.000	0.120	0.137	23.744

Test	H	Q	b_{ave}	H/b_{ave}	$Q/g^{1/2}H^{5/2}$	h_s	h_s/H	H/L	H/b	C
3	0.278	0.857	2.028	0.137	3.706	0.000	0.000	0.139	0.159	21.031
4	0.323	1.023	2.073	0.156	3.040	0.000	0.000	0.161	0.185	17.253
5	0.350	1.274	2.100	0.167	3.098	0.000	0.000	0.175	0.200	17.579
Trapezoidal weir 3-1 sides b = 0.167 ft.										
1	0.145	0.085	0.602	0.241	1.860	*****	*****	0.072	0.868	10.555
2	0.190	0.151	0.737	0.258	1.694	*****	*****	0.095	1.138	9.613
3	0.206	0.197	0.785	0.262	1.798	*****	*****	0.103	1.234	10.203
4	0.226	0.222	0.845	0.267	1.609	*****	*****	0.113	1.353	9.129
5	0.249	0.265	0.914	0.272	1.508	*****	*****	0.124	1.491	8.556
6	0.249	0.265	0.914	0.272	1.508	0.145	0.582	0.124	1.491	8.556
7	0.258	0.265	0.941	0.274	1.380	0.218	0.845	0.129	1.545	7.829
8	0.275	0.265	0.992	0.277	1.176	0.247	0.898	0.137	1.647	6.675
9	0.290	0.265	1.037	0.280	1.030	0.271	0.934	0.145	1.737	5.845
10	0.307	0.265	1.088	0.282	0.893	0.292	0.951	0.154	1.838	5.069
11	0.195	0.168	0.752	0.259	1.759	*****	*****	0.097	1.168	9.981
12	0.195	0.168	0.752	0.259	1.759	0.125	0.641	0.097	1.168	9.981
13	0.203	0.168	0.776	0.262	1.591	0.173	0.852	0.102	1.216	9.027
14	0.213	0.168	0.806	0.264	1.411	0.194	0.911	0.107	1.275	8.004
15	0.225	0.168	0.842	0.267	1.230	0.209	0.929	0.113	1.347	6.979
16	0.241	0.168	0.890	0.271	1.036	0.229	0.950	0.121	1.443	5.878
Submergence tests Trapezoidal weir 3-1 sides b = 0.167 ft.										
1	0.195	0.168	0.752	0.259	1.763	0.156	0.800	0.097	1.168	10.005
2	0.203	0.168	0.776	0.262	1.595	0.173	0.850	0.101	1.216	9.048
3	0.213	0.168	0.806	0.264	1.414	0.192	0.900	0.106	1.275	8.023

Test	H	Q	b_{ave}	H/b_{ave}	$Q/g^{1/2}H^{5/2}$	h_s	h_s/H	H/L	H/b	C
4	0.241	0.160	0.890	0.271	1.038	0.229	0.950	0.120	1.443	5.892
5	0.249	0.265	0.914	0.272	1.509	0.203	0.800	0.124	1.491	8.565
6	0.261	0.265	0.950	0.275	1.342	0.222	0.850	0.130	1.563	7.615
7	0.276	0.265	0.995	0.277	1.167	0.249	0.900	0.138	1.653	6.622
8	0.306	0.265	1.085	0.282	0.902	0.291	0.950	0.153	1.832	5.116
Trapezoidal weir 3-1 sides b = 0.333										
1	0.155	0.122	0.758	0.194	2.278	*****	*****	0.077	0.465	12.928
2	0.188	0.188	0.897	0.210	2.156	*****	*****	0.094	0.565	12.235
3	0.214	0.251	0.975	0.219	2.091	*****	*****	0.107	0.643	11.867
4	0.241	0.288	1.056	0.228	1.783	*****	*****	0.121	0.724	10.117
5	0.257	0.161	1.104	0.233	1.902	*****	*****	0.128	0.772	10.795
6	0.220	0.262	0.993	0.222	2.037	*****	*****	0.110	0.661	11.558
7	0.220	0.262	0.993	0.222	2.037	0.040	0.182	0.110	0.661	11.558
8	0.220	0.262	0.993	0.222	2.037	0.080	0.364	0.110	0.661	11.558
9	0.231	0.262	1.026	0.225	1.803	0.195	0.844	0.115	0.694	10.231
10	0.244	0.262	1.065	0.229	1.572	0.220	0.902	0.122	0.733	8.922
11	0.257	0.262	1.104	0.233	1.381	0.237	0.922	0.128	0.772	7.836
12	0.263	0.262	1.122	0.234	1.304	0.250	0.951	0.131	0.790	7.397
13	0.157	0.214	0.924	0.213	2.192	*****	*****	0.098	0.592	12.440
14	0.197	0.214	0.924	0.213	2.192	0.030	0.152	0.098	0.592	12.440
15	0.197	0.214	0.924	0.213	2.192	0.080	0.406	0.098	0.592	12.440
16	0.197	0.214	0.924	0.213	2.192	0.130	0.660	0.098	0.592	12.440
17	0.209	0.214	0.960	0.218	1.891	0.179	0.856	0.104	0.628	10.731
18	0.229	0.214	1.020	0.225	1.505	0.213	0.930	0.115	0.688	8.539
19	0.240	0.214	1.053	0.228	1.338	0.226	0.942	0.120	0.721	7.594
20	0.253	0.214	1.092	0.232	1.173	0.243	0.960	0.127	0.760	6.656

Test	H	Q	b_{ave}	H/b_{ave}	$Q/g^{1/2}H^{5/2}$	h_s	h_s/H	H/L	H/b	C
Submergence tests		3-1 sides	b = 0.333 ft.							
1	0.220	0.262	0.993	0.222	2.034	0.176	0.800	0.110	0.661	11.541
2	0.232	0.262	1.029	0.225	1.781	0.197	0.850	0.116	0.697	10.106
3	0.244	0.262	1.065	0.229	1.570	0.202	0.900	0.122	0.733	8.909
4	0.262	0.262	1.115	0.234	1.314	0.249	0.950	0.131	0.787	7.457
5	0.197	0.214	0.924	0.213	2.189	0.158	0.600	0.099	0.592	12.424
6	0.208	0.214	0.957	0.217	1.911	0.177	0.850	0.104	0.625	10.846
7	0.220	0.214	0.993	0.222	1.661	0.198	0.900	0.110	0.661	9.427
8	0.246	0.214	1.071	0.230	1.256	0.234	0.950	0.123	0.739	7.130
Broad-Crested weir		b = 3 ft.								
1	0.100	0.262	3.000	0.033	14.601	0.000	0.000	0.050	0.033	82.852
2	0.150	0.490	3.000	0.050	9.909	0.000	0.000	0.075	0.050	56.230
3	0.200	0.763	3.000	0.067	7.517	0.000	0.000	0.100	0.067	42.653
4	0.250	1.076	3.000	0.083	6.068	0.000	0.000	0.125	0.083	34.432
5	0.300	1.425	3.000	0.100	5.094	0.000	0.000	0.150	0.100	28.908
6	0.350	1.868	3.000	0.117	4.542	0.000	0.000	0.175	0.117	25.775
7	0.400	2.224	3.000	0.133	3.873	0.000	0.000	0.200	0.133	21.978
8	0.450	2.664	3.000	0.150	3.456	0.000	0.000	0.225	0.150	19.611
9	0.500	3.145	3.000	0.167	3.135	0.000	0.000	0.250	0.167	17.791

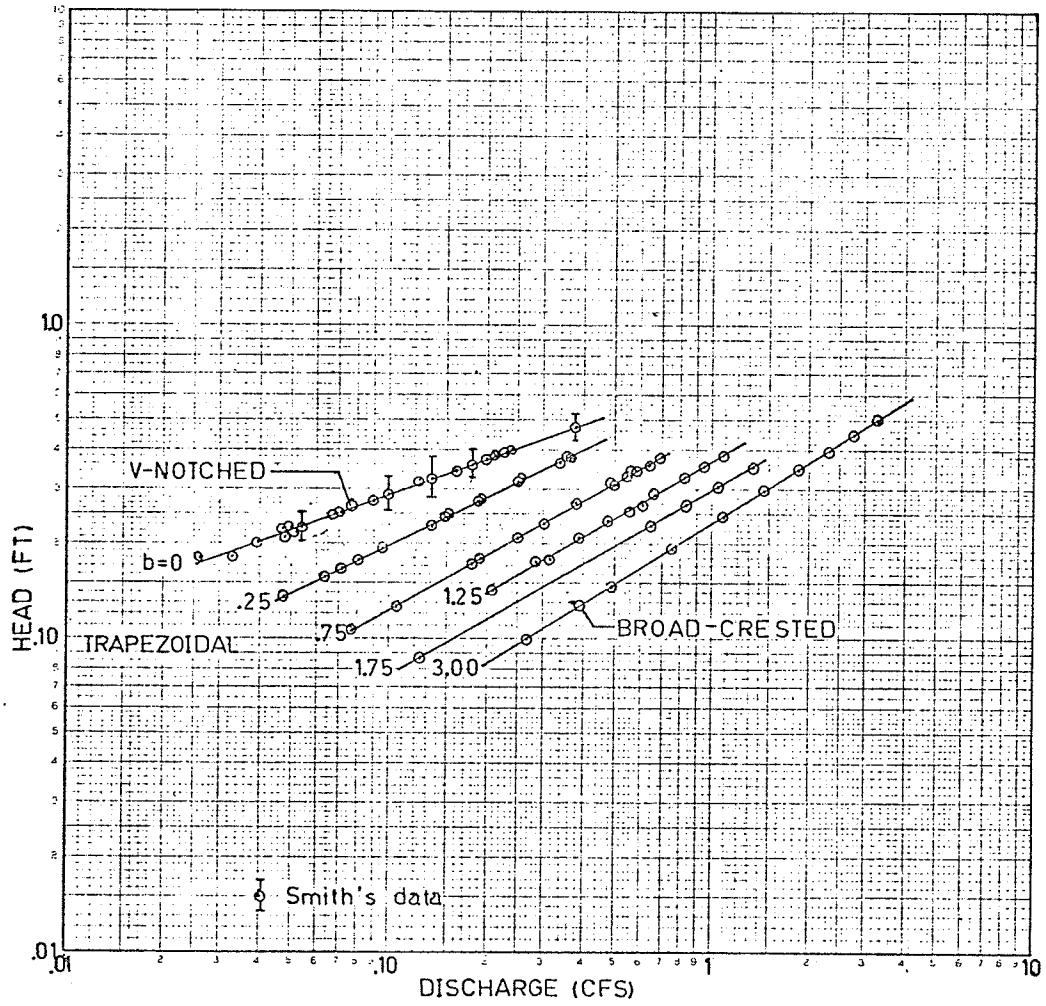

FIGURE C2-1 HEAD-DISCHARGE RELATIONS

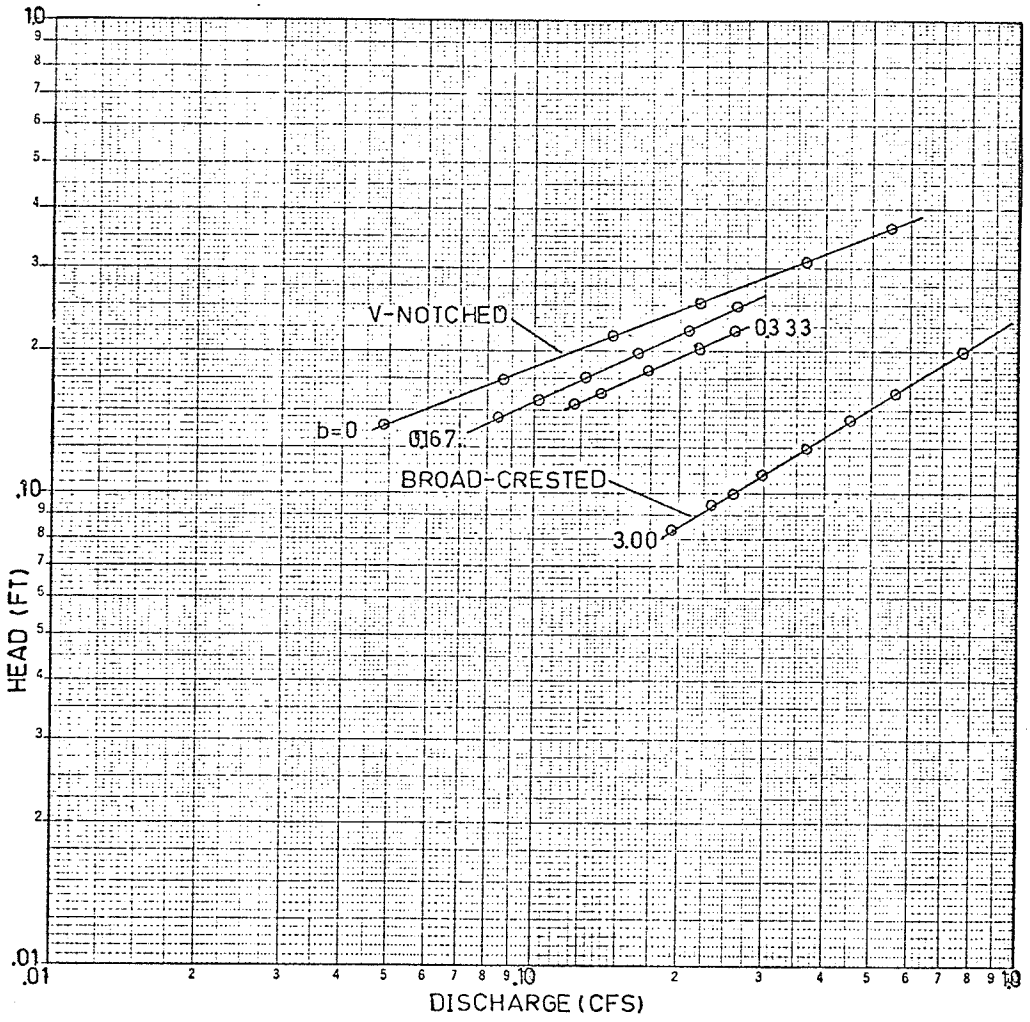

FIGURE C2-2 HEAD-DISCHARGE RELATIONS

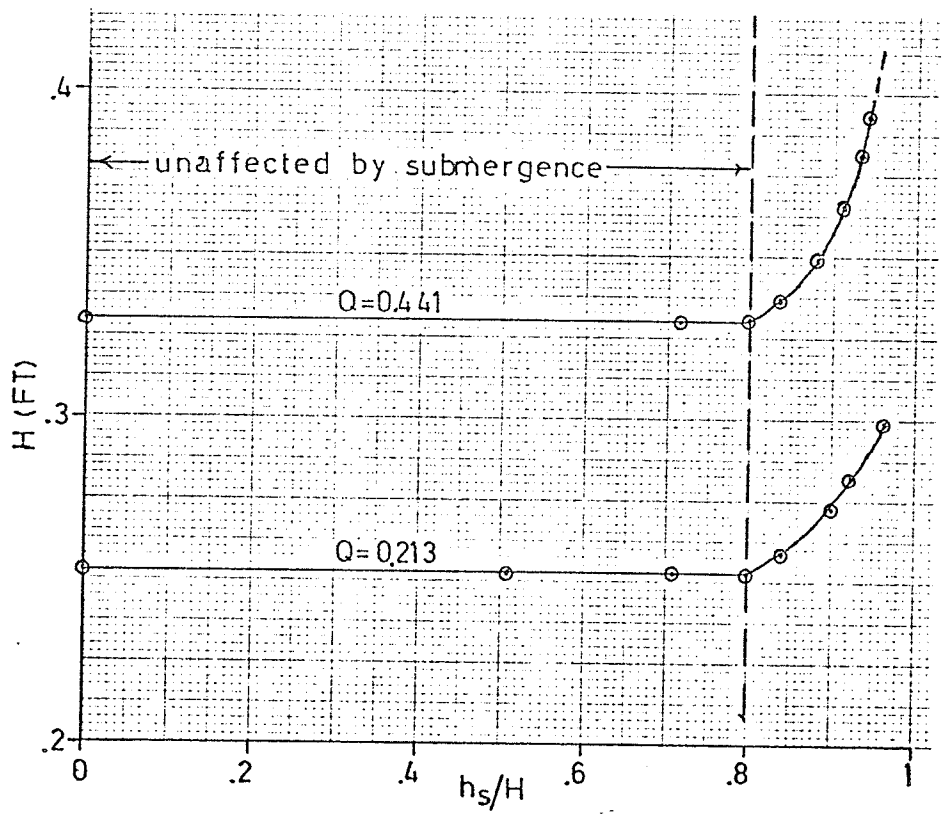

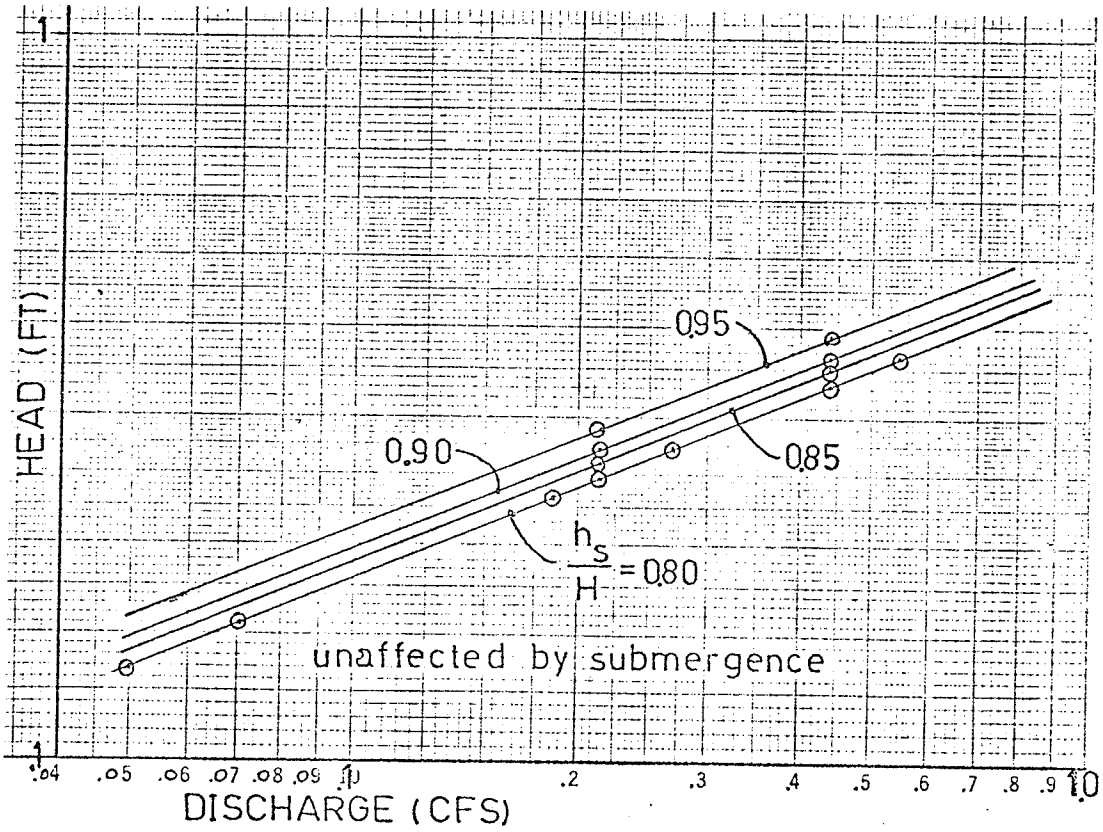

FIGURE C3-1 SUBMERGENCE 3:1 SIDE-SLOPES b=0.000

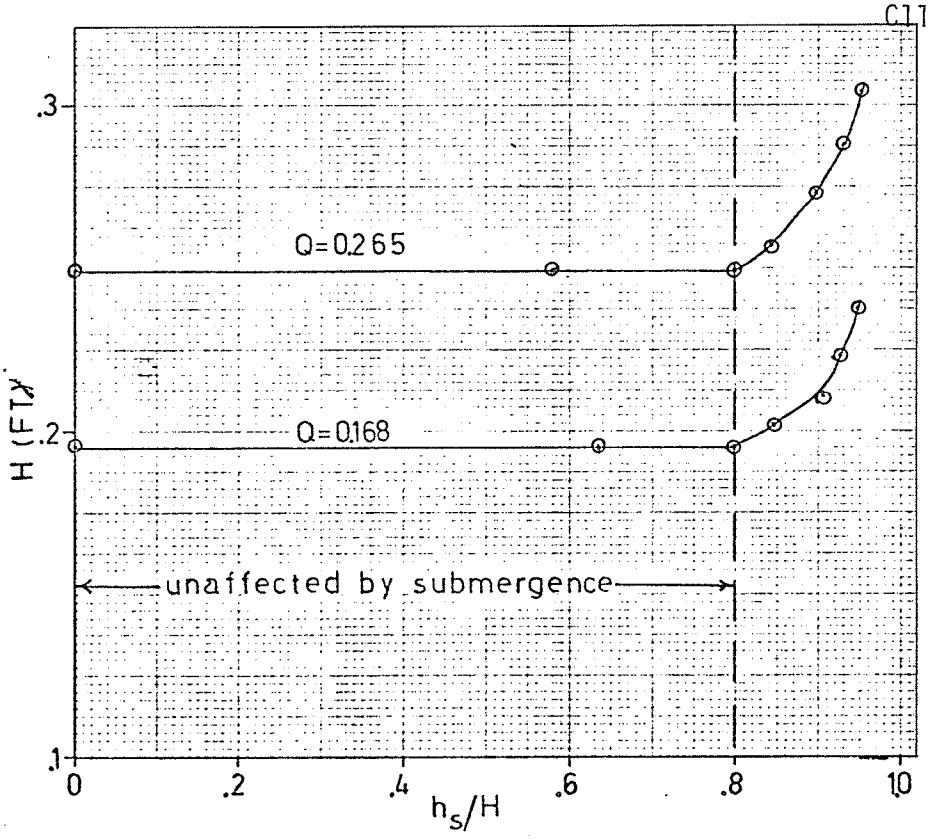

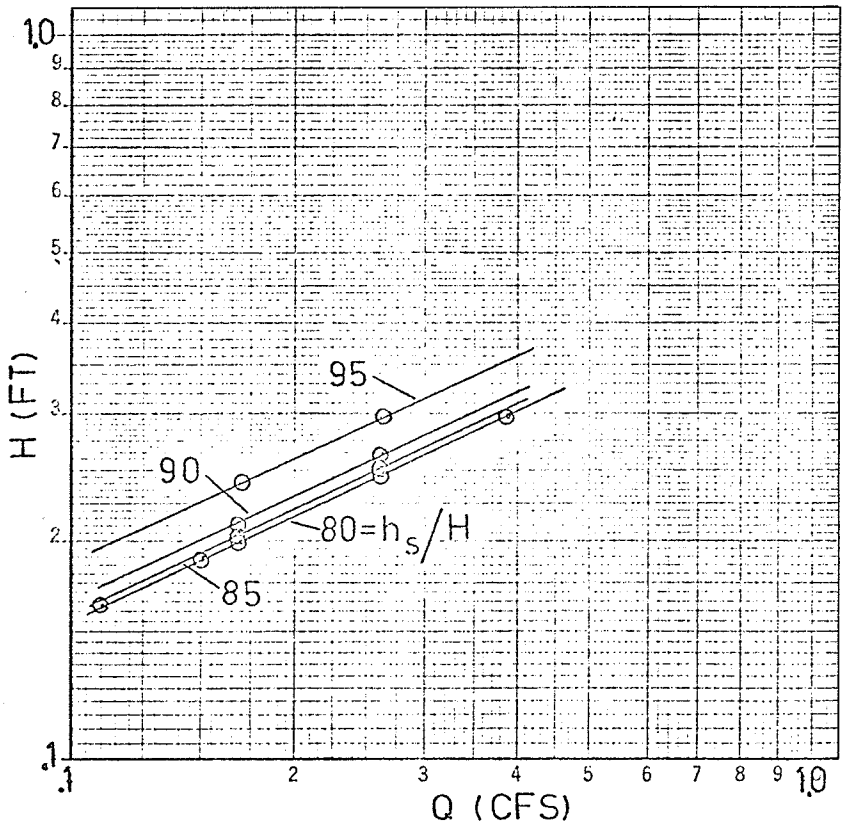

FIGURE C3-2 SUBMERGENCE 3:1 SIDE-SLOPES
b=0.167

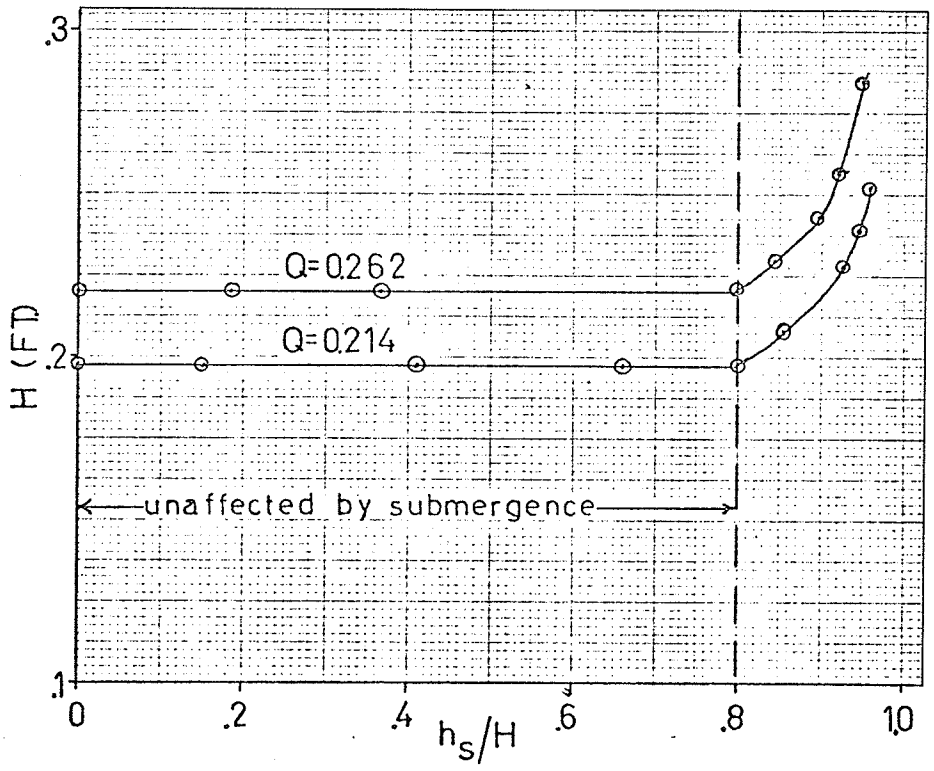

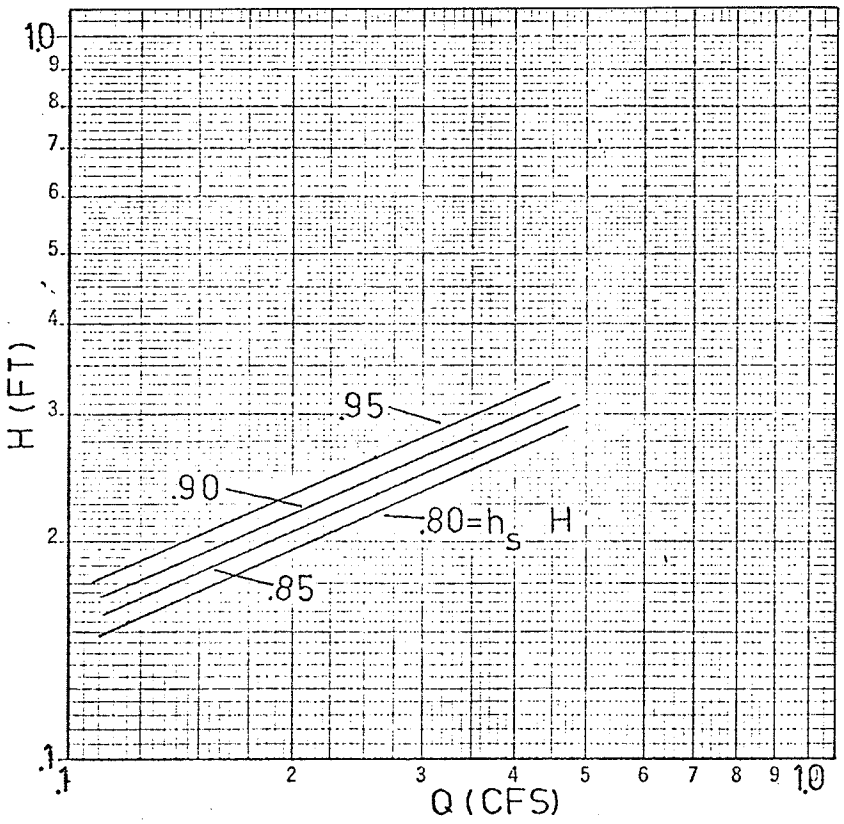

FIGURE C3-3 SUBMERGENCE 3:1 SIDE-SLOPES
b=0.333

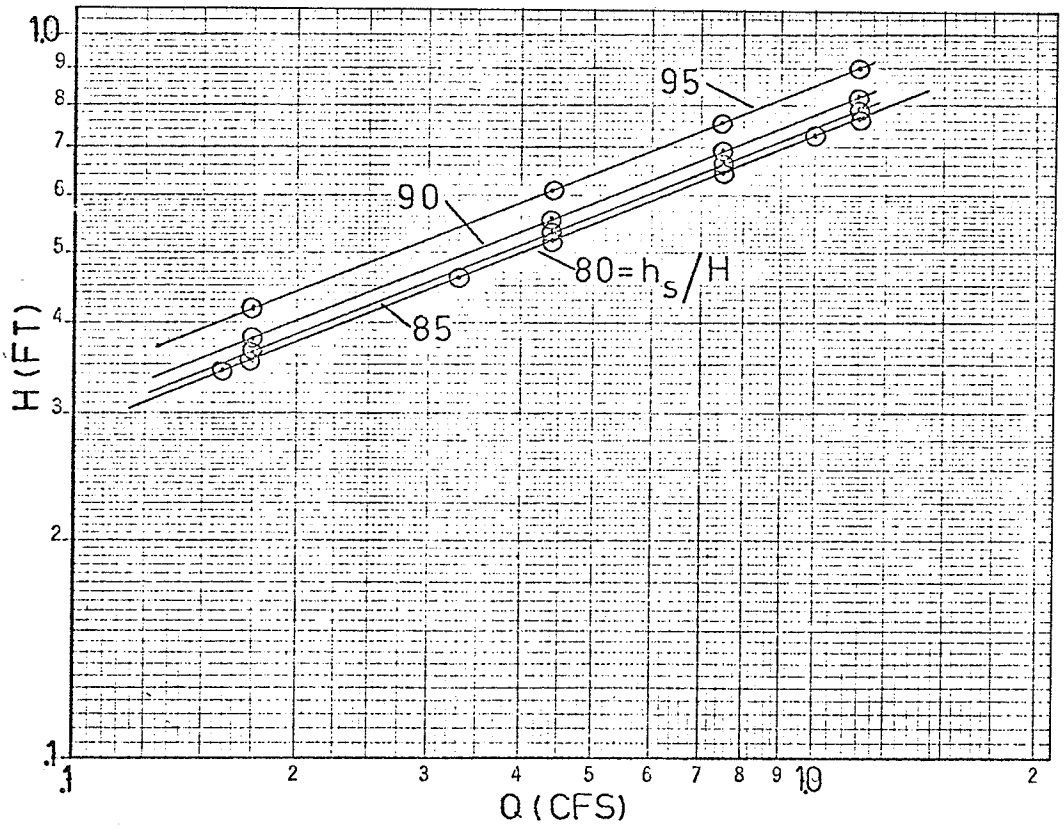

FIGURE C3-4 SUBMERGENCE 1:1 SIDE-SLOPES b= 0.000

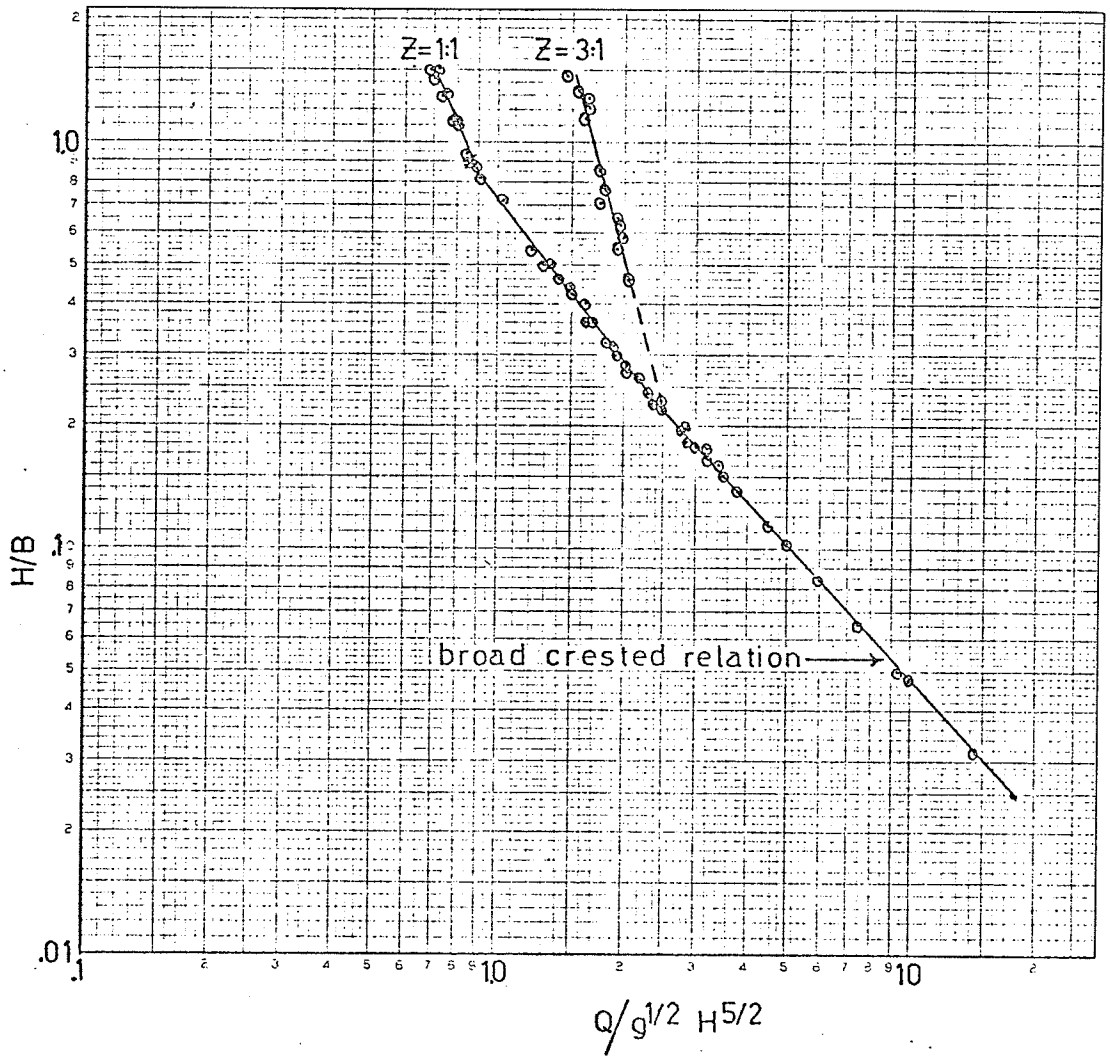

FIGURE C4-1 DIMENSIONLESS RELATIONS

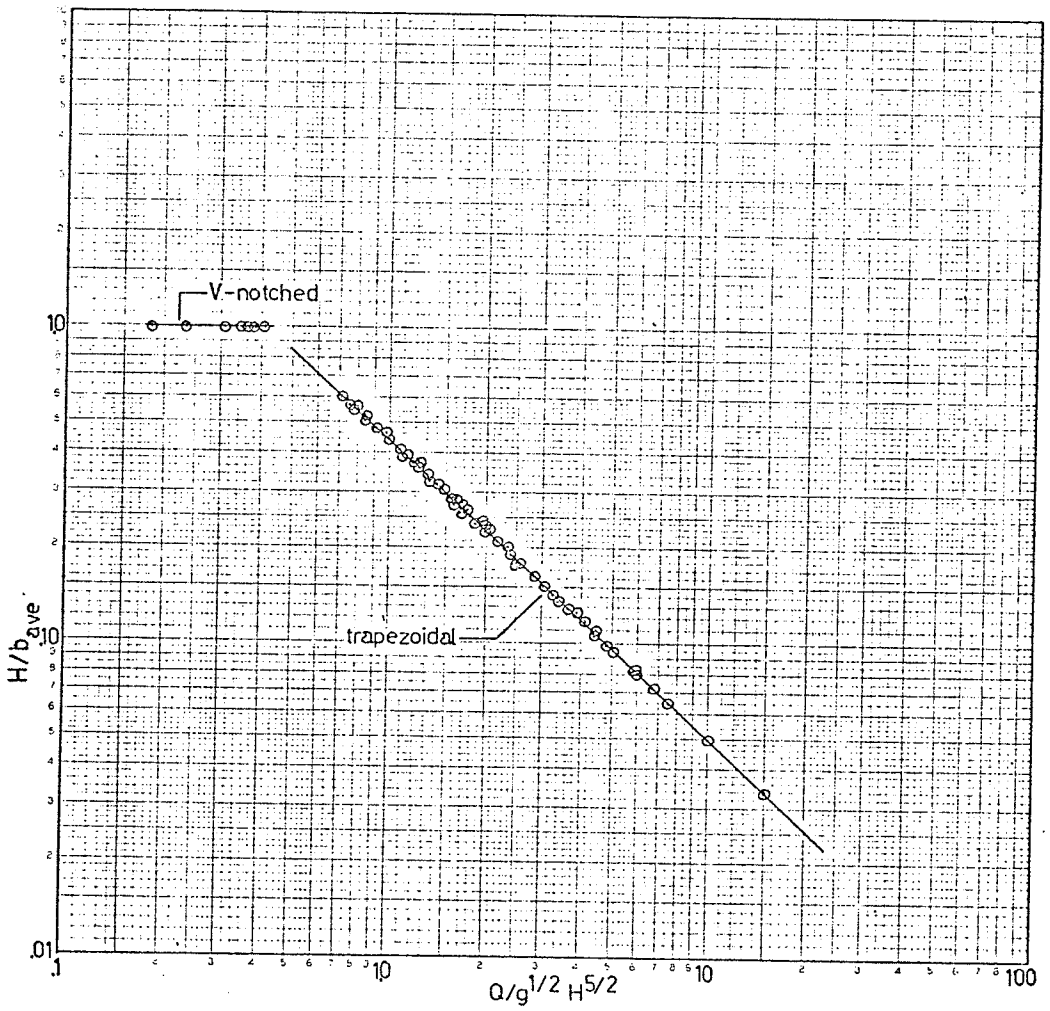

FIGURE C4-2 DIMENSIONLESS RELATIONS

APPENDIX D

BURNTWOOD RIVER MODEL TEST RESULTS

TABLE D1-1 Surface Profile Data from Hydraulic Model Tests

Date	Test No.	2p (cfs)	Water Surface Elevations at X-Secs. (fts.) 1	12-A	12-B	2	3	13	4	5
25/3/74	1*	5800	599.74	602.00	602.08	602.18	602.18	602.18	602.18	602.22
	2*	5800	600.58	602.84	602.92	603.02	602.96	602.96	603.02	603.06
	3*	5800	601.24	604.64	604.78	604.70	604.76	604.82	604.82	604.74
	4*	8400	598.29	600.50	600.82	600.98	600.86	600.98	600.98	600.96
	5*	8400	599.44	601.76	601.84	602.06	602.00	602.06	602.06	602.10
26/3/74	1*	8400	602.59	604.82	604.96	605.00	605.00	605.06	605.12	605.10
	2	10,000	603.82	606.08	606.13	606.20	606.17	606.23	606.26	606.24
27/3/74	1	6600	60.140	604.22	604.24	604.34	604.28	604.34	604.34	604.38
	2	9100	602.80	605.06	605.14	605.24	605.18	605.24	605.30	605.28
	3	13,600	604.48	606.68	606.68	606.82	606.86	606.92	607.10	607.02
	4	17,000	605.80	606.84	608.92	609.02	609.02	609.08	609.14	609.18

* Tests run at a constant discharge and varying downstream water level to test dependence of upstream stage on downstream stage.

TABLE D1-1 (continued)

Date	Test No.	2p (cfs)	Water Surface Elevations at X-Secs. (fts.)							
			1	12-A	12-B	2	3	13	4	5
30/3/74	1	10,000	603.70	606.08	606.76	606.14	606.26	606.26	606.32	606.30
	2	14,600	605.26	607.58	607.78	607.70	607.82	607.88	607.91	607.92
	3	19,900	608.08	610.46	610.57	610.58	610.70	610.76	610.76	610.80
	4	24,500	609.34	611.78	611.92	611.87	612.02	612.08	612.08	612.12
	5	30,000	612.70	615.14	615.22	615.20	615.38	615.38	615.44	615.48
	6	35,800	615.28	617.66	617.68	617.66	617.78	617.90	617.90	617.94
	7	39,400	617.38	619.70	619.84	619.82	619.88	620.00	620.00	620.10
8/4/74	1*	30,000	609.04	611.48	611.68	611.60	611.90	611.84	611.84	612.06
	2*	30,000	615.64	617.90	618.10	617.90	618.26	618.32	618.26	618.30
	3*	30,000	607.60	609.92	610.24	610.10	610.28	610.40	610.46	610.62
	4*	35,000	618.64	621.02	621.04	621.02	621.08	621.20	621.20	621.30
	5*	35,000	612.16	614.60	614.62	614.66	614.84	614.90	614.90	615.00
	6*	35,000	610.00	612.32	612.52	612.50	612.68	612.68	612.74	612.84

* Tests run at a constant discharge and varying downstream water level to test dependence of upstream stage on downstream stage.

PHOTOGRAPH D1-1 Negligible Discharge

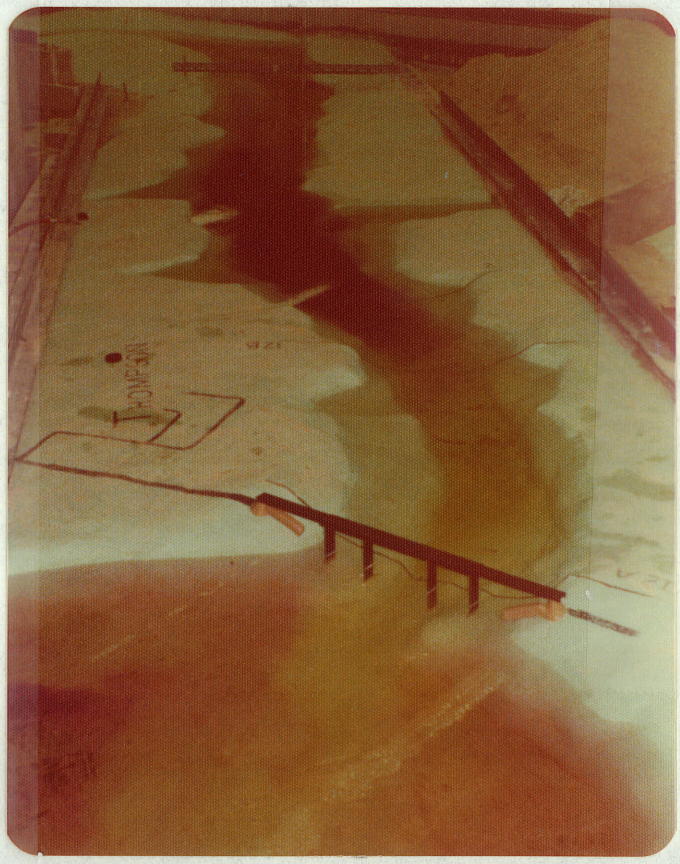

PHOTOGRAPH D1-2 Prototype Discharge = 35,000 cfs.

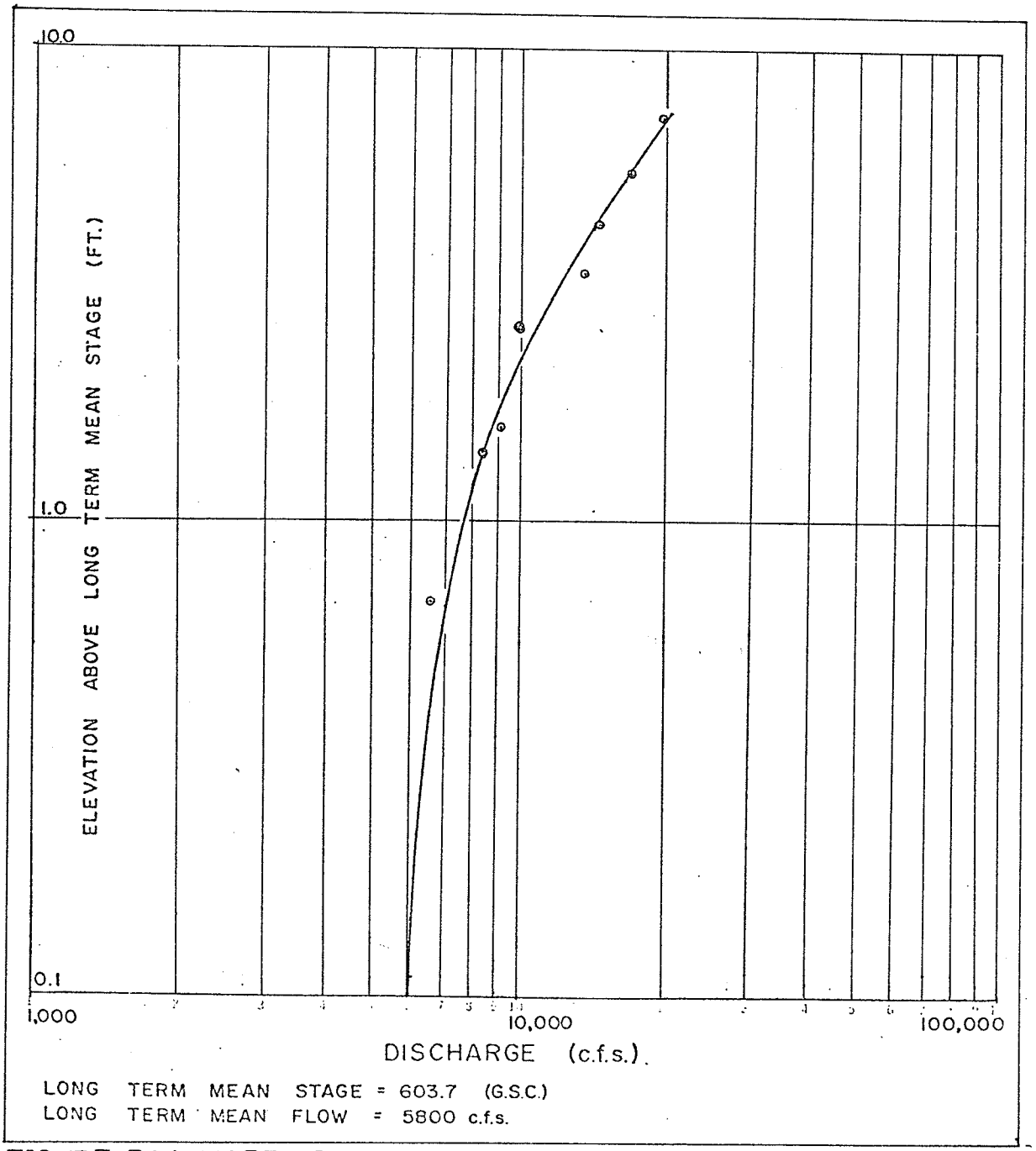

FIGURE D2-1 MODEL COMPARISON TO KNOWN RATING CURVE

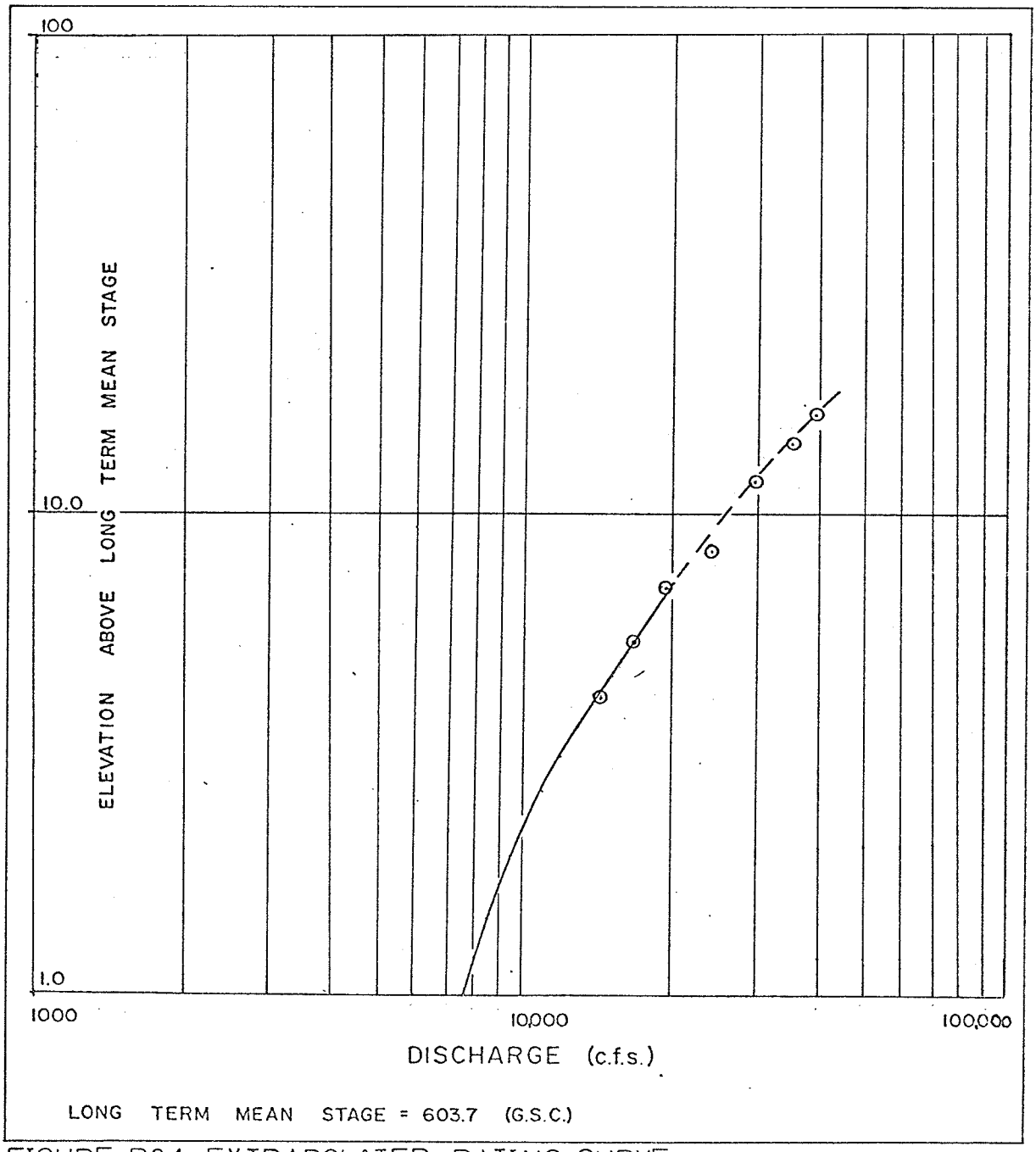

FIGURE D3-1 EXTRAPOLATED RATING CURVE

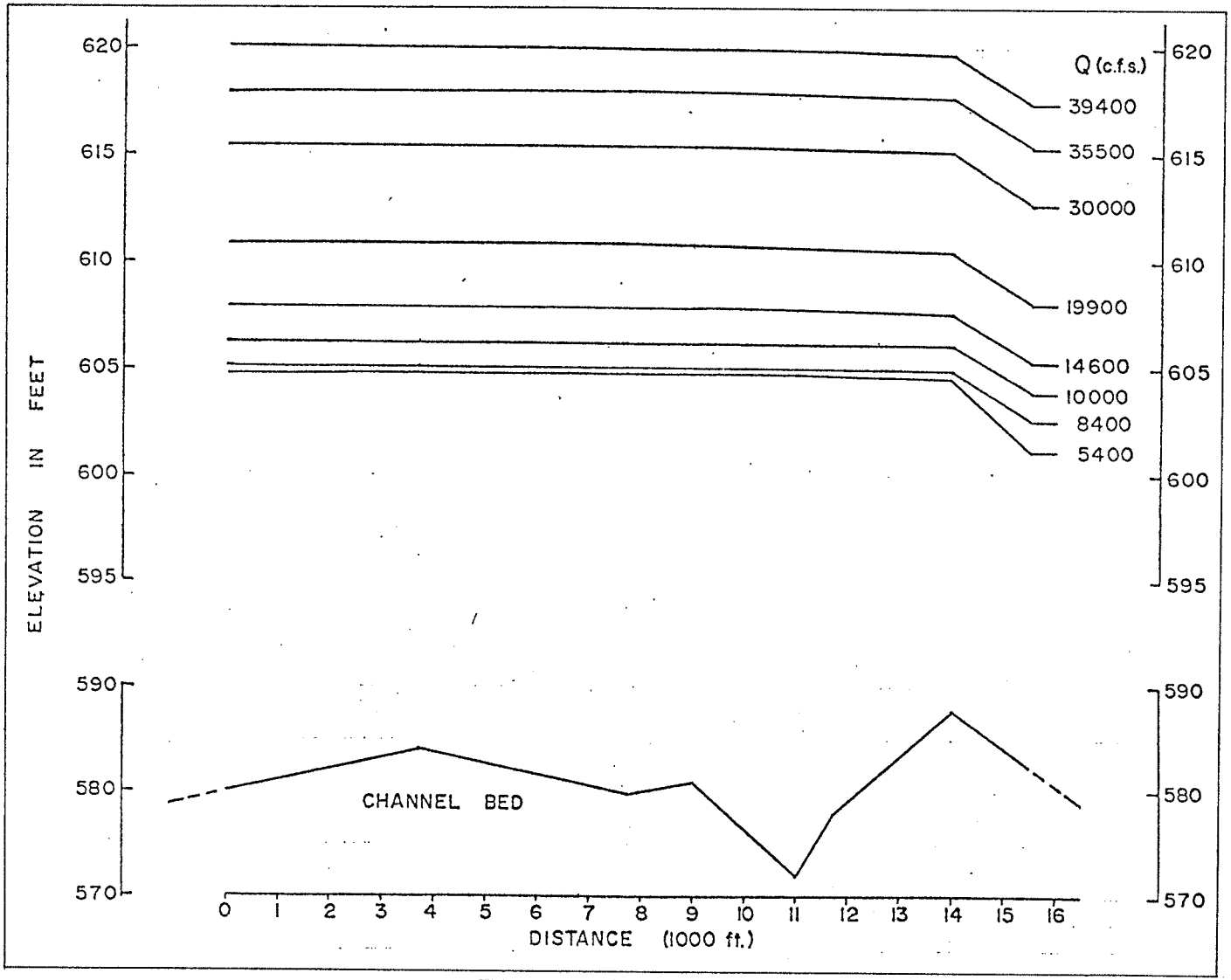

FIGURE D3-2 SURFACE PROFILES

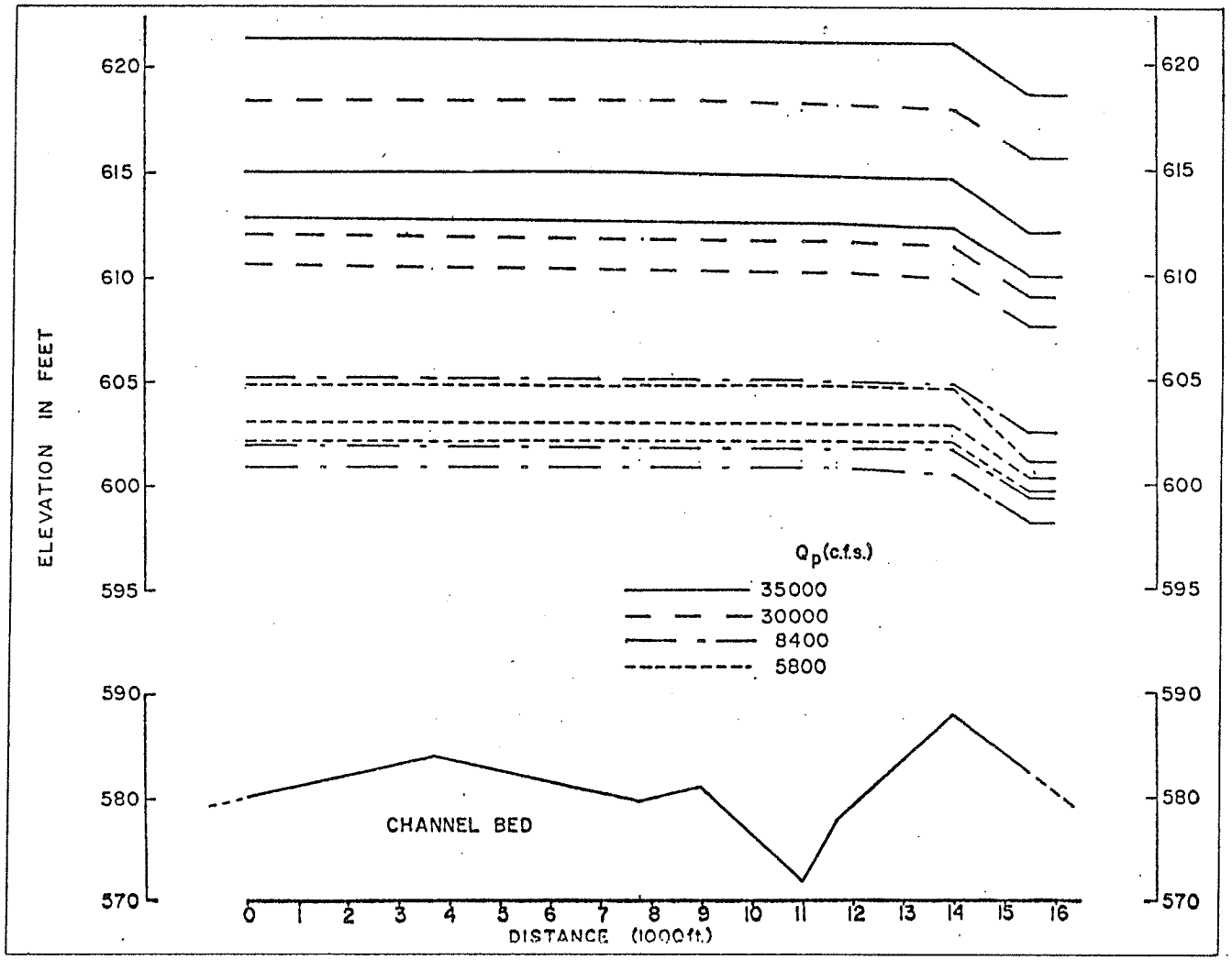

FIGURE D4-1 SURFACE PROFILES (constant Q, varying tailwater)

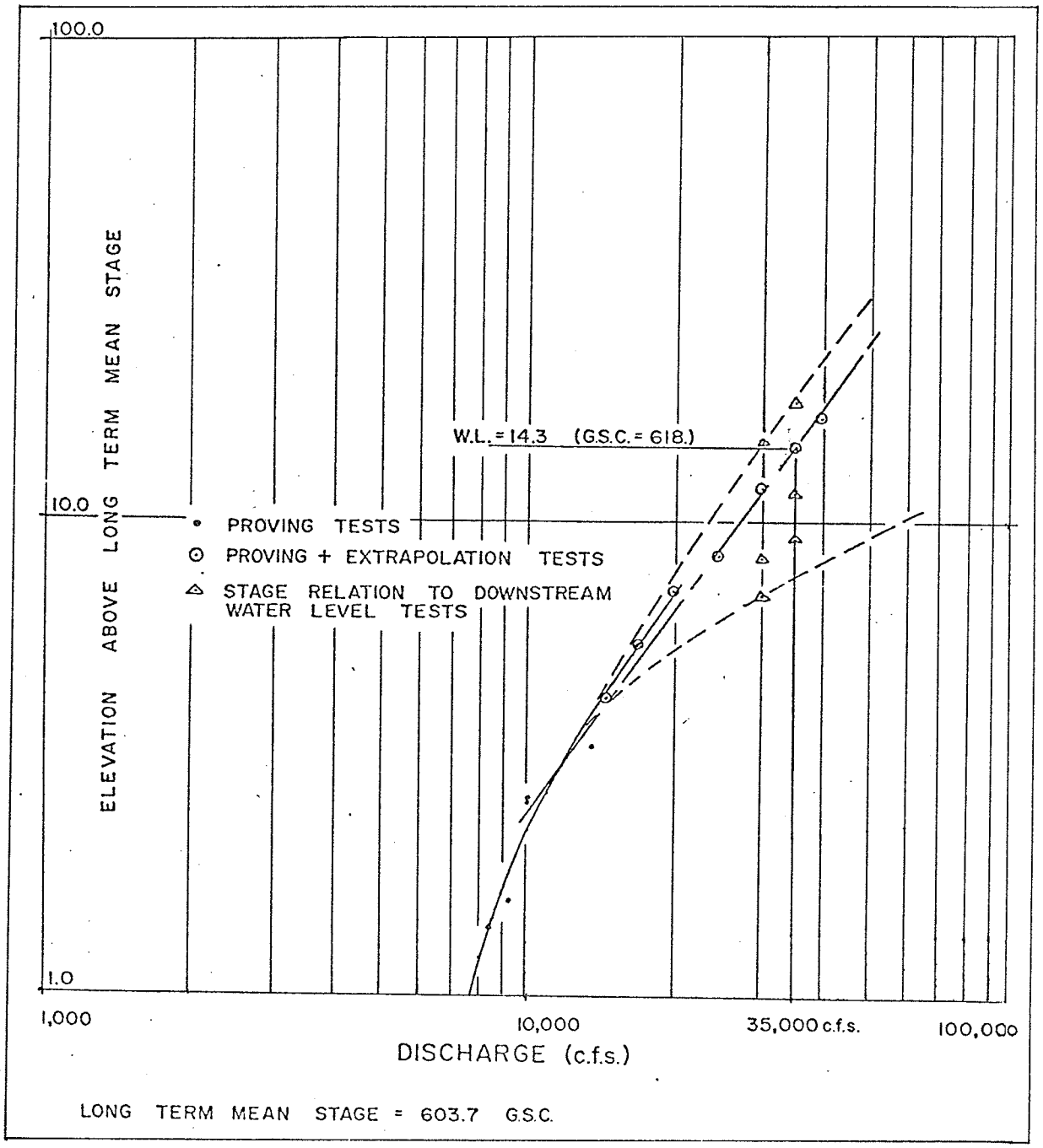

FIGURE D5-1 VARYING WATER-LEVEL TESTS

TABLE D6-1 Surface Profile Data from Hydraulic Model Tests

Date	Test No.	2p (cfs)	Water Surface Elevations at X-Secs. (fts.) 1	12-A	12-B	2	3	13	4	5
20/6/74	*1	5000	598.87	601.37	601.60	601.60	601.60	601.61	601.61	601.61
	*2	10,000	602.68	604.76	604.96	605.23	605.41	605.60	605.70	605.80
	*3	20,000	6.97	609.50	609.70	609.90	610.10	610.20	610.30	610.30
	*4	30,000	610.24	612.56	612.76	612.80	612.89	612.87	612.87	612.87
	*5	34,000	611.26	613.58	613.70	613.78	613.80	613.80	613.80	613.80
	*6	40,000	612.79	614.96	615.16	615.20	615.21	615.21	615.21	615.21
21/6/74	**1	5000	602.37	604.61	604.67	604.68	604.68	604.68	604.68	604.68
	**2	10,000	605.86	607.21	607.27	607.29	607.29	607.29	607.29	607.29
	**3	20,000	610.48	612.79	612.83	612.87	612.87	612.87	612.87	612.87
	**4	30,000	613.56	615.83	615.91	615.97	615.96	615.96	615.96	615.96
	**5	34,000	614.54	616.98	617.01	617.07	617.08	617.10	617.10	617.10
	**6	40,000	616.38	618.77	618.80	613.81	618.83	618.83	618.84	618.84

* Tests utilizing synthetic 5th Rapids rating curve

** Tests utilizing derived backwater calculations

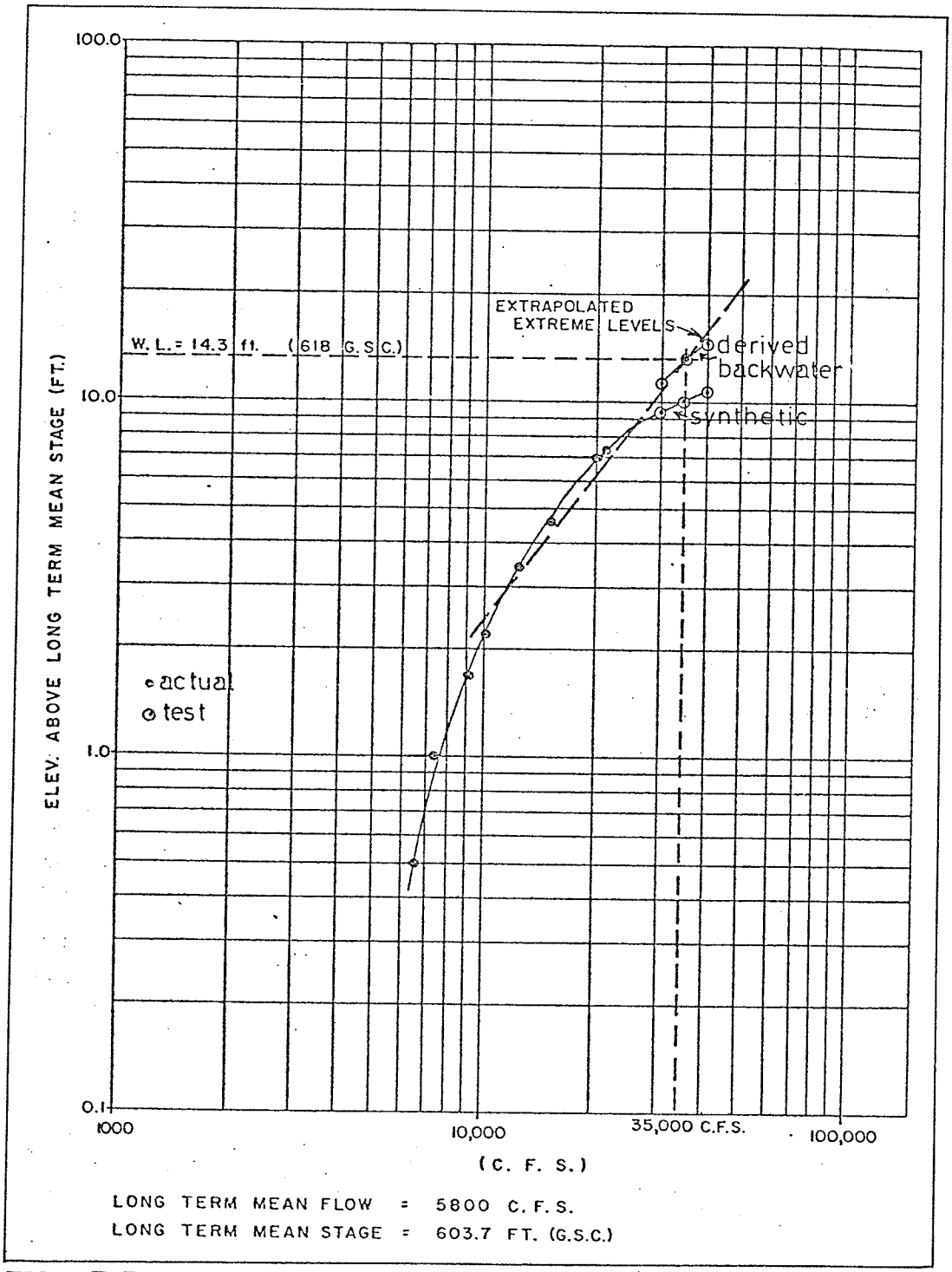

FIGURE D6-1 RATING CURVES

APPENDIX D7

Table D7-1 Surface Velocities

Station No.	Velocity for Q = 5,000 cfs. (ft./sec.)	Velocity for Q = 35,000 cfs. (ft./sec.)
1	-	3.87
2A	2.28	4.30
2B	2.28	4.30
2C	2.28	4.30
3	-	3.52
4	0.15	0.67
5	0.18	negligible
6	1.49	2.76
6A	1.14	3.52
7	0.55	1.76
8	negligible	0.81
9	0.12	0.33
10	0.64	1.46
11	negligible	2.87
12	1.21	2.42
12A	1.11	2.42
13	0.44	1.61
14	0.23	negligible
15	negligible	1.11
16	negligible	0.86
17	-	negligible

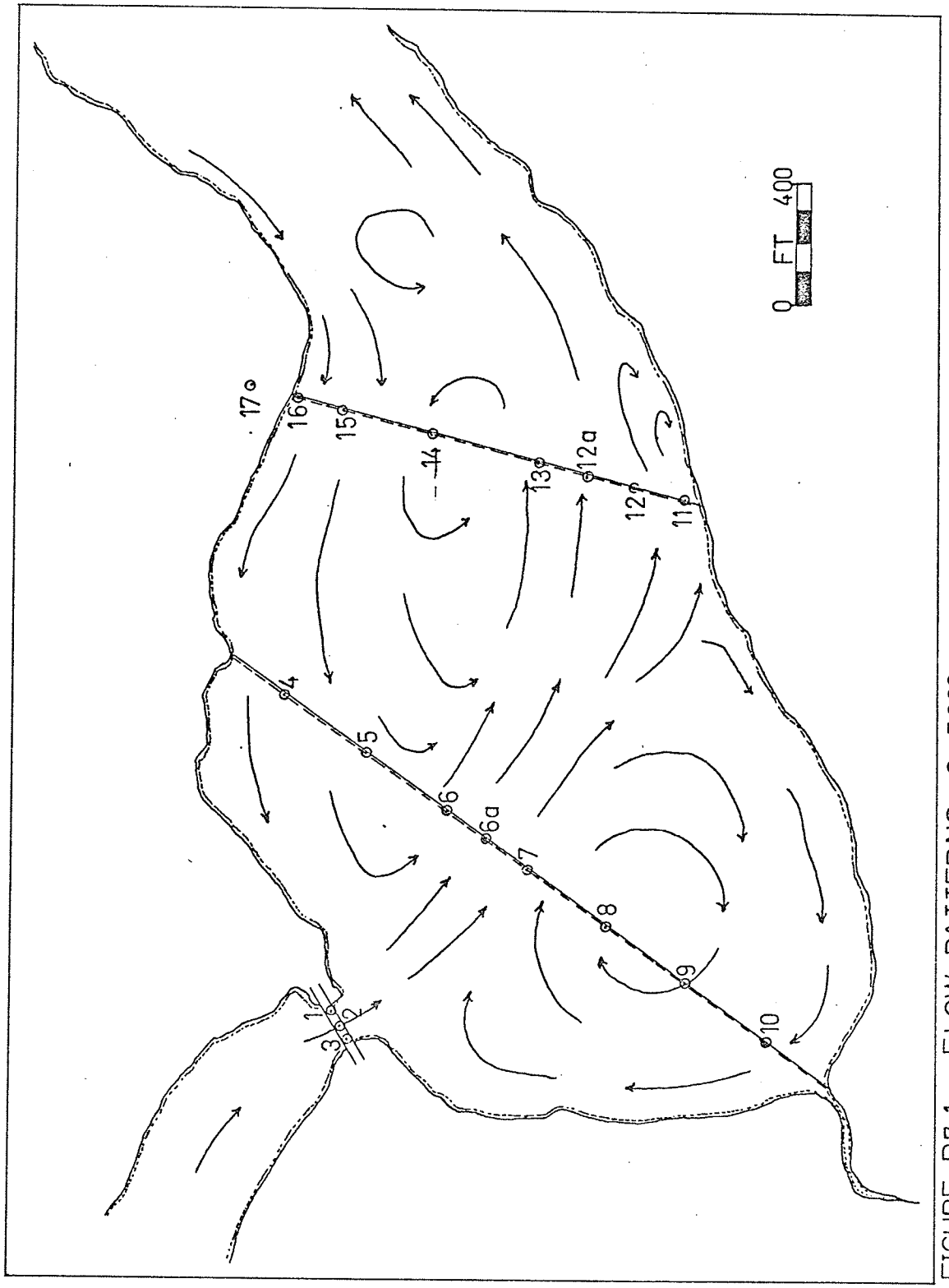

FIGURE D7-1 FLOW PATTERNS Q=5000 cfs

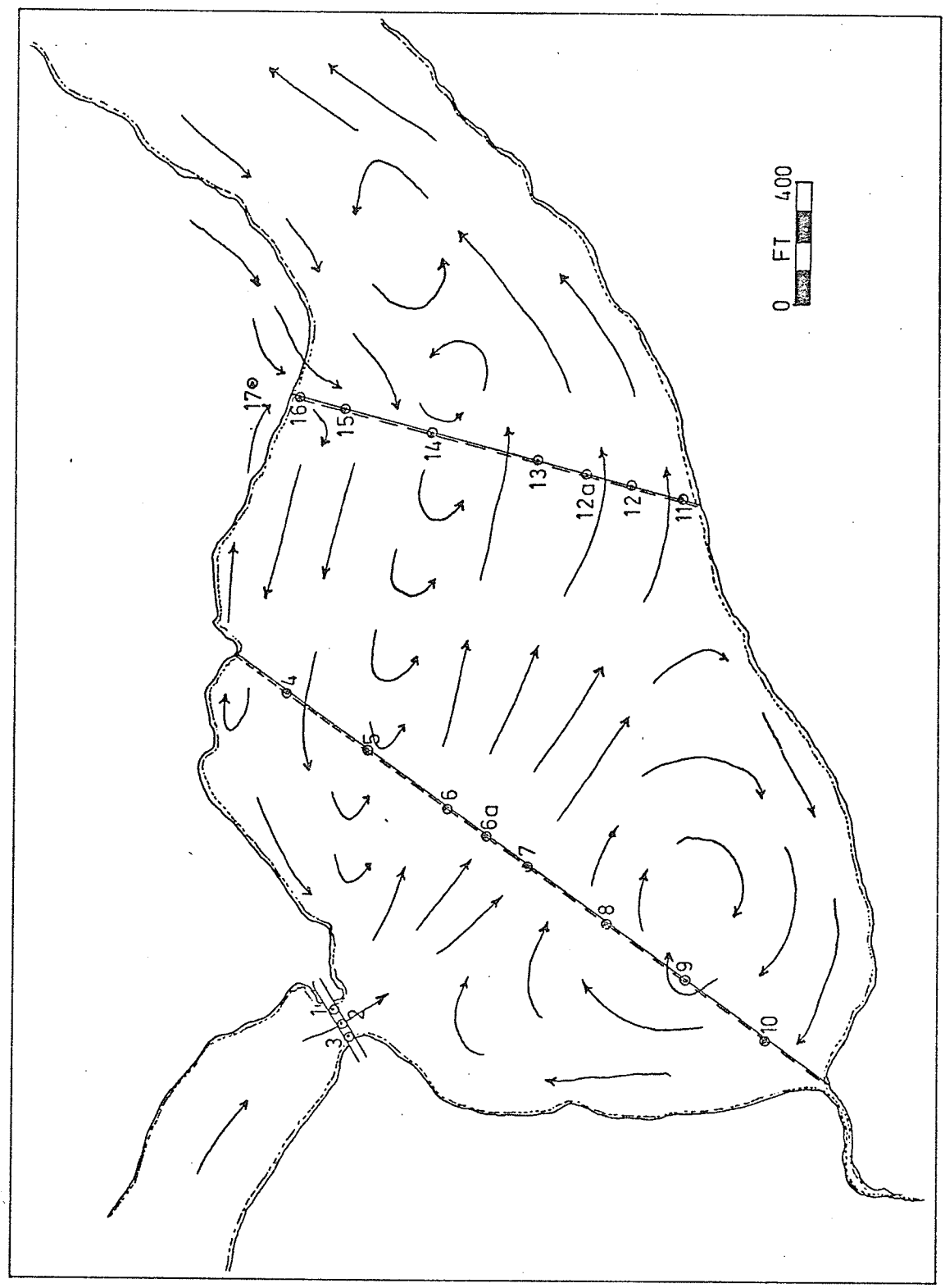

FIGURE D7-2 FLOW PATTERNS Q=35,000 cfs

APPENDIX E

SYNTHETIC RATING CURVES

E1. Synthetic Rating Curve Technique

The following is the procedure to develop synthetic rating curves of trapezoidal overfalls in bedrock rivers.

(1) From a cross-section of the overfall, determine the side-slopes, $\underline{Z}$, and the bottom width, b.

(2) Determine the average side-slope and calculate $\underline{Z}^*$, the horizontal component of the average side-slope when the vertical component is equal to 1.

(3) For a particular head, H, determine b_{ave}, where

$$b_{ave} = H\underline{Z}^* + b$$

(4) Determine the dimensionless ratio H/b_{ave}.

(5) Entering FIGURE E1-1 with this value of H/b_{ave}, determine the discharge constant, $Q/g^{1/2}H^{5/2}$.

(6) Solve for the discharge by

$$Q/g^{1/2}\ H^{5/2} = C$$

$$Q = C\ g^{1/2}\ H^{5/2}$$

(7) Repeat steps (3) through (6) until a sufficient number of relations are available for a variety of expected flows.

(8) After assigning an elevation to the crest of the overfall, the stage-discharge curve can be constructed.

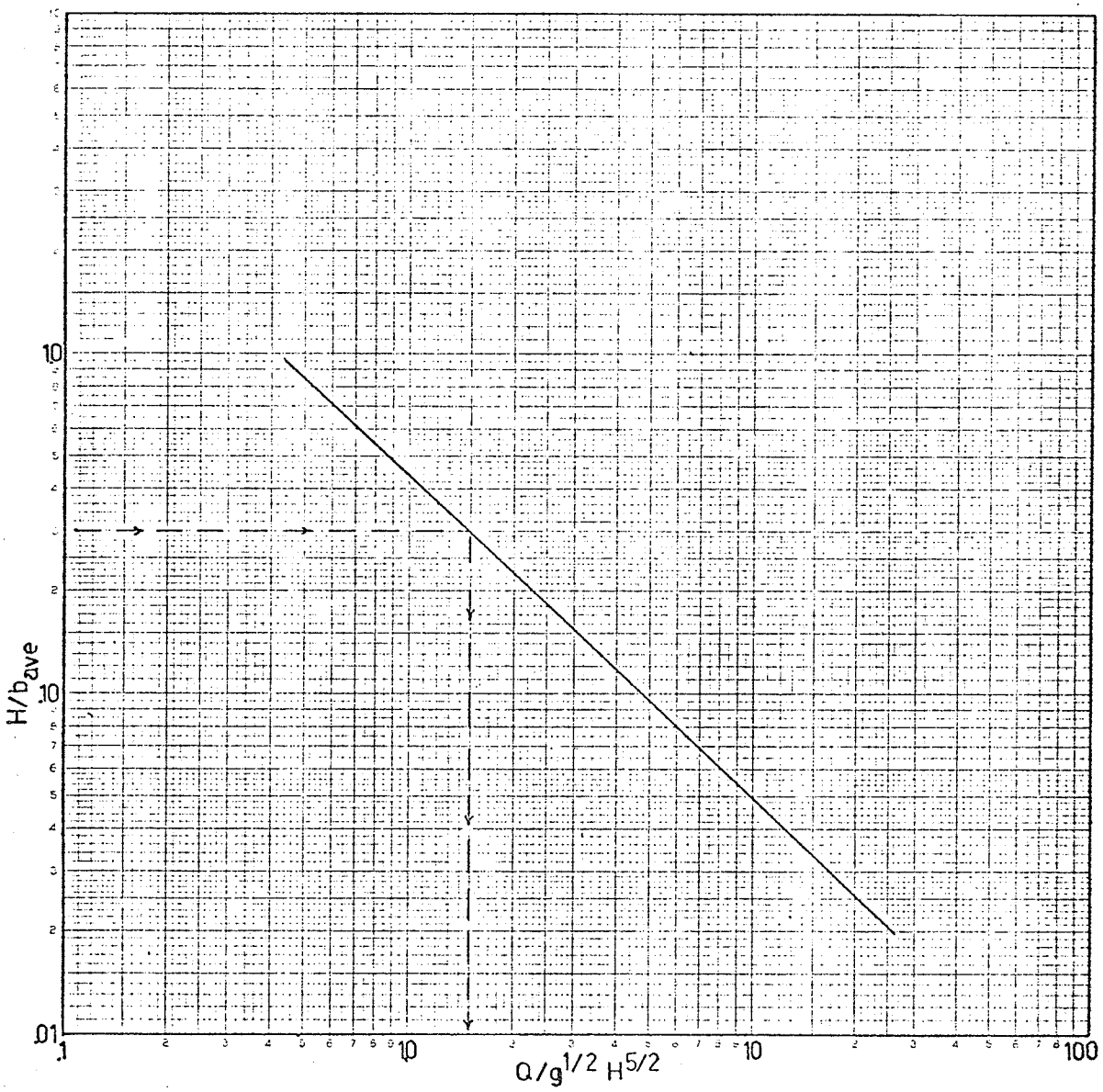

FIGURE E1-1 RATING CURVE DESIGN RELATION

E2 Additional Rating Curve

To further establish the validity of the rating curve technique, overfalls with existing rating curves were analyzed using the developed synthetic rating curve thechnique. Obtaining overfall data complete with rating curve was difficult therefore few sections were analyzed.

Two stations which were studied were Manason Falls and 1st Rapids, both situated on the Burntwood River. (For location map see FIGURE II-1b.) Estimations of overfall sections were made and the synthetic rating curves were established. The resulting stage-discharge relations for the two overfalls are shown in FIGURE E2-1.

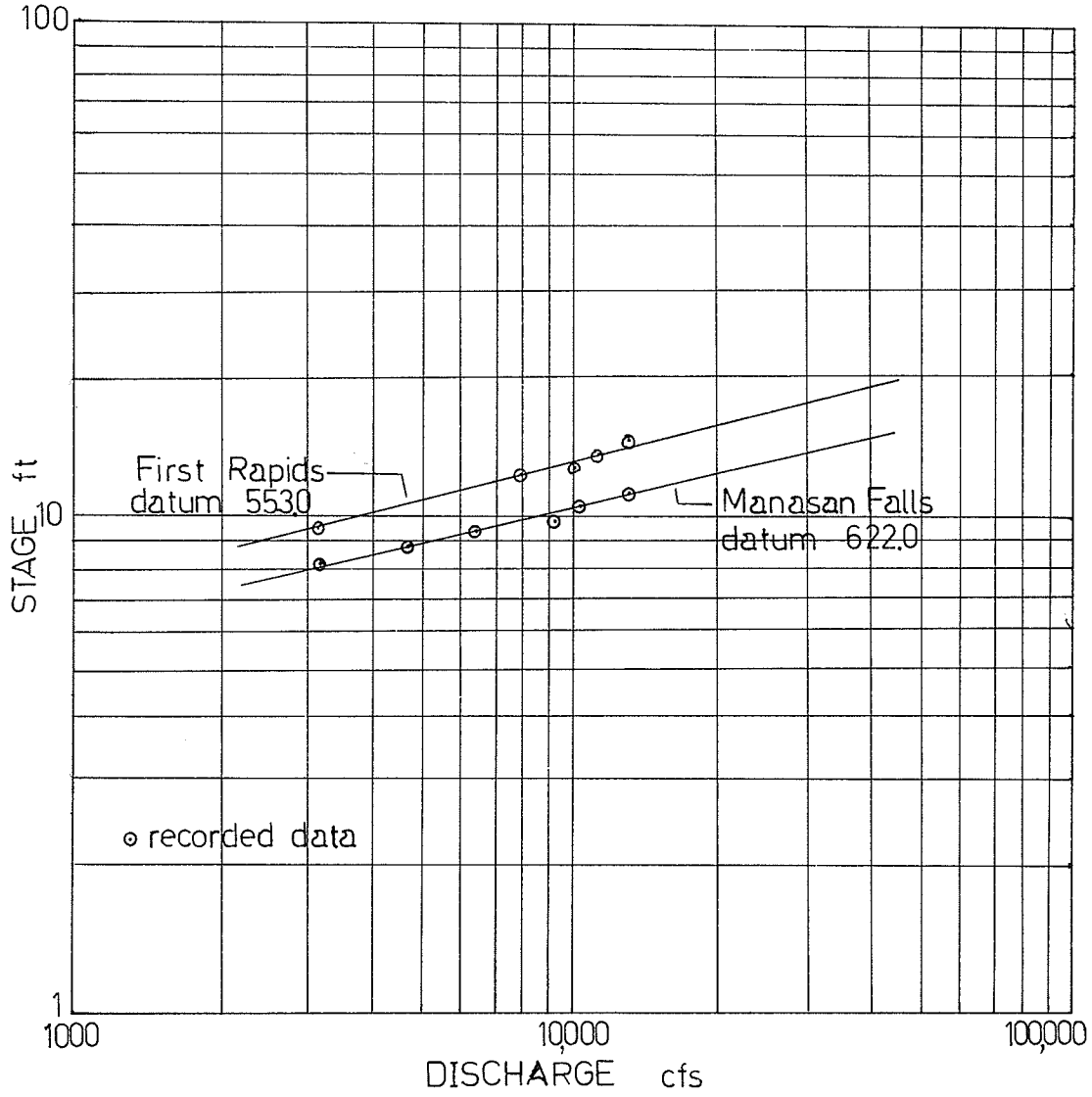

FIGURE E2-1 ADDITIONAL RATING CURVES